



8-2009

Method of Evaluation for Stream Bed Shear Stress and Sediment Transport Capacity in Urbanizing Watershed: Implications for Stream Restoration

William Cantrell
University of Tennessee - Knoxville

Follow this and additional works at: https://trace.tennessee.edu/utk_gradthes



Part of the [Civil and Environmental Engineering Commons](#)

Recommended Citation

Cantrell, William, "Method of Evaluation for Stream Bed Shear Stress and Sediment Transport Capacity in Urbanizing Watershed: Implications for Stream Restoration. " Master's Thesis, University of Tennessee, 2009.

https://trace.tennessee.edu/utk_gradthes/27

This Thesis is brought to you for free and open access by the Graduate School at TRACE: Tennessee Research and Creative Exchange. It has been accepted for inclusion in Masters Theses by an authorized administrator of TRACE: Tennessee Research and Creative Exchange. For more information, please contact trace@utk.edu.

To the Graduate Council:

I am submitting herewith a thesis written by William Cantrell entitled "Method of Evaluation for Stream Bed Shear Stress and Sediment Transport Capacity in Urbanizing Watershed: Implications for Stream Restoration." I have examined the final electronic copy of this thesis for form and content and recommend that it be accepted in partial fulfillment of the requirements for the degree of Master of Science, with a major in Environmental Engineering.

John S. Schwartz, Major Professor

We have read this thesis and recommend its acceptance:

Glenn Tootle, Randall W. Gentry

Accepted for the Council:

Carolyn R. Hodges

Vice Provost and Dean of the Graduate School

(Original signatures are on file with official student records.)

To the Graduate Council:

I am submitting herewith a thesis written by William Cantrell entitled "Method of Evaluation for Stream Bed Shear Stress and Sediment Transport Capacity in Urbanizing Watershed: Implications for Stream Restoration." I have examined the final electronic copy of this thesis for form and content and recommend that it be accepted in partial fulfillment of the requirements for the degree of Master of Science, with a major in Environmental Engineering.

John S. Schwartz

Major Professor

We have read this thesis and
Recommend its acceptance:

Glenn Tootle

Randall W. Gentry

Acceptance for the Council:

Carolyn R. Hodges,

Vice Provost and Dean of the
Graduate School

(Original signatures are on file with official student records)

Method of Evaluation for Stream Bed Shear Stress and Sediment Transport Capacity in
Urbanizing Watershed: Implications for Stream Restoration

A Thesis
Presented for the
Master of Science
Degree
The University of Tennessee, Knoxville

William R. Cantrell
August 2009

Abstract

In the field of stream restoration, use of a one-dimensional flow model with typical Manning's n values for an open channel greatly over-predicts bed shear values. This, in turn, incorrectly predicts the size of the mobile fraction on the bed and if used in a bed-load transport function over-predicts mass movement of the bed material. This study identified 12 sites for which watershed and reach characteristics were compiled, and bed-load sampling was performed. This information was used to produce an empirical relationship between reach pebble count data and an effective Manning's n value that can be used to produce accurate bed-shear values in a one-dimensional flow model. With this tool, simple field activities can provide sufficient information to allow a stream restoration practitioner to accurately predict bed shear values. Relationships between watershed characteristics and reach scale bed characteristics, and bed depositional patchiness and sediment supply were also explored. It was found that Wolman Pebble Count data can be used to predict an effective Manning's n value with sufficient accuracy, while watershed characteristics were not adequate to predict reach scale bed characteristics and bed depositional patchiness was valuable as a threshold indicator but not as a predictive variable.

Acknowledgments

I would like to thank Dr. John Schwartz, my advisor, for his advice and support throughout this process. From the idea for the study, to writing a grant to fund it, to the completion of the thesis, his patience and willingness to answer innumerable questions made it all possible. Thanks also are due to my additional committee members, Dr. Glen Tootle and Dr. Randall Gentry for taking time from their schedules to read and comment on this thesis. Ken Barry and S&ME, Inc. made this project possible through a Business Growth initiative grant from their corporate office. Ken's interest in exploring new practical and empirical methods to improve the practice of stream restoration got this project off the ground. Thanks to Laura DeVilbiss, the primary field and lab assistant on this project put in countless, thankless hours helping gather and process data. Other fellow students, including Keil Neff and Daniel Johnson provided valuable advice from their experiences with similar projects. Larry Roberts and Ken Thomas in the Civil and Environmental Machine Shop were invaluable in acquiring materials and fabricating equipment for this project. My former co-workers at Knox County Stormwater Engineering, Andrew Dodson and Michael Hamrick provided assistance with GIS questions and initial field work. Enormous thanks to my parents, who filled in the gaps financially and with moral support, and without whom I wouldn't have made it to this point.

Table of Contents

Abstract	ii
Acknowledgments	iii
Table of Contents	iv
List of Tables	v
List of Figures	vi
List of Symbols	vii
Chapter 1: Introduction	1
Chapter 2: Methods	5
2.1 Study Design	5
2.2 Study Area	6
2.3 Field Measurements and Sampling Activities	7
2.3.1 Site Setup and Bed Material Classification	7
2.3.2 Bed-load Sampling Method	8
2.3.3 Bed-load Sample Processing	9
2.3.4 Water Surface Measurement at Peak Flow Stage	10
2.4 Geographic Information System Analysis	10
2.4.1 Data Collection	10
2.4.2 GIS Data Processing	11
2.5 Geomorphic Channel Survey Data	11
2.6 HEC-RAS Modeling	12
2.7 Determination of Critical Shear Values	12
2.8 Study Analysis	13
Chapter 3: Results	16
3.1 Watershed Characteristics and Reach-Scale Bed Characteristics	16
3.2 Development of an Empirical Model for n^*	21
3.3 Reach Scale Bed Deposition Patchiness as a Predictive Concept	22
Chapter 4: Discussion	25
4.1 Watershed Characteristics and Reach Scale Bed Characteristics	25
4.2 Development of an Empirical Model for n^*	26
4.3 Reach Scale Bed Deposition Patchiness as a Predictive Concept	28
4.4 Applications to Stream Restoration	28
List of References	30
Appendices	37
Appendix A: Literature Review	38
Appendix B: Site Cross-Sections	50
Appendix C: Site Pebble Counts	63
Appendix D: Bed-load Sample P.S.D.'s	76
Appendix E: Crest Stage Gage and Bed-load Trap Construction/Performance	91
Appendix F: GIS Procedures and Site Watershed Maps	96
Appendix G: Scatterplot Matrices	112
Vita	116

List of Tables

Table 1: Watershed Datasets Acquired from USGS Seamless Site.....	11
Table 2: Results Summary	17
Table 3: Bed-load Sample Kendall τ Correlations.....	18
Table 4: Pebble Count Kendall τ Correlations.....	19
Table 5: Beaver Creek Pebble Count.....	64
Table 6: Cox Creek Pebble Count	65
Table 7: First Creek Pebble Count.....	66
Table 8: Hines Branch Pebble Count.....	67
Table 9: Knob Fork Pebble Count	68
Table 10: Lammie Branch Pebble Count.....	69
Table 11: Meadow Branch Pebble Count	70
Table 12: Mill Branch Pebble Count	71
Table 13: Plumb Creek Pebble Count.....	72
Table 14: Suckstone Creek Pebble Count.....	73
Table 15: Third Creek Pebble Count	74
Table 16: Willow Fork Pebble Count	75
Table 17: Maximum Sampled Particle Size Summary	77
Table 18: 3rd Creek Sample 11/14/2008	78
Table 19: 3rd Creek Sample 12/10/2008	79
Table 20: 3rd Creek Sample 1/7/2009	80
Table 21: Beaver Creek Sample 12/10/2009	81
Table 22: Beaver Creek Sample 1/7/2009	82
Table 23: Willow Fork Sample 12/10/2008.....	83
Table 24: Willow Fork Sample 1/7/2009.....	84
Table 25: Lammie Branch Sample 1/7/2009	85
Table 26: Cox Creek Sample 12/10/2008.....	86
Table 27: Cox Creek Sample 1/7/2009.....	87
Table 28: Cox Creek Sample 1/28/2009.....	88
Table 29: Hines Branch Sample 1/7/2009	89
Table 30: Hines Branch Sample 1/28/2009	90

List of Figures

Figure 1: Research Watersheds.....	6
Figure 2: Assembled Bed-load Sampler	9
Figure 3: Modified Shield's Diagram After Julien (1994).....	13
Figure 4: Relationship Between Average Watershed Slope and Pebble Count d ₅₀	20
Figure 5: Relationship Between Length of Roads in 50-foot Buffer and τ_r	20
Figure 6: Pebble Count d _{max} and n*.....	21
Figure 7: Patchiness vs Shear Ratio.....	23
Figure 8: Stream Power and Sample d _{max}	23
Figure 9: Modeling without and with Bed-load Sampling Data.....	27
Figure 10: Restoration Design Conceptual Framework.....	29
Figure 11: Beaver Creek Cross Sections	51
Figure 12: Cox Creek Cross Sections	52
Figure 13: First Creek Cross Sections	53
Figure 14: Hines Branch Cross Sections	54
Figure 15: Knob Fork Cross Sections.....	55
Figure 16: Lammie Branch Cross Sections	56
Figure 17: Meadow Branch Cross Sections.....	57
Figure 18: Mill Branch Cross Sections.....	58
Figure 19: Plumb Creek Cross Sections	59
Figure 20: Suckstone Creek Cross Sections	60
Figure 21: Third Creek Cross Sections.....	61
Figure 22: Willow Fork Cross Sections.....	62
Figure 23: New Peak Stage (top of photo) on Peak Stage Gage	93
Figure 24: Upper Beaver Creek Watershed Map.....	100
Figure 25: Cox Creek Watershed Map	101
Figure 26: First Creek Watershed Map.....	102
Figure 27: Hines Branch Watershed Map.....	103
Figure 28: Knob Fork Watershed Map	104
Figure 29: Lammie Branch Watershed Map.....	105
Figure 30: Meadow Branch Watershed Map	106
Figure 31: Mill Branch Watershed Map	107
Figure 32: Plumb Creek Watershed Map.....	108
Figure 33: Suckstone Creek Watershed Map.....	109
Figure 34: Third Creek Watershed Map	110
Figure 35: Willow Fork Watershed Map	111
Figure 36: Watershed Characteristics with Pebble Count Data Scatterplot Matrix.....	113
Figure 37: Watershed Characteristics with Bed-load Sample Data Scatterplot Matrix..	114
Figure 38: n* with Pebble Count Data Scatterplot Matrix	115

List of Symbols

d	particle size in mm
d^*	unitless particle size for Julien's Modified Shield's Diagram
d_{\max}	maximum sampled particle size in mm
G	specific gravity of sediment
g	acceleration due to gravity
n^*	effective Manning's n
S	reach slope
τ	bed shear value predicted by HEC-RAS modeling
τ_c	critical shear value from Julien's Modified Shield's Diagram
τ_{*c}	unitless critical shear for Julien's Modified Shield's Diagram
τ_{comp}	shear required to move maximum sampled bed-load particle
τ_{dmax}	shear required to move maximum particle size from Pebble Count
τ_r	shear ratio, defined as $\tau_{\text{dmax}} / \tau_{\text{comp}}$
ν	kinematic viscosity
Ω	stream power

Chapter 1: Introduction

Evaluation of sediment transport supply versus capacity limitation is a central assessment problem in the field of stream restoration. A wide variety of modeling tools are available for these calculations, however many require inputs that are too costly to measure for a given project and/or produce poor predictions using commonly employed models such as HEC-RAS. Success of restoration projects based on stability are critically dependant on selecting default values or measuring input variables for these models. Commonly overlooked during pre-project assessment and design are the uncertainty of model outputs, especially when default values are applied for bed sediment characteristics. Among stream restoration practitioners, there is a growing understanding of the need to sample bed material transport to predict whether systems are sediment transport systems are supply or capacity limited. (Wilcock, 2001; Shields et al, 2003; Bravo-Espinoza, 2003)

In urban watersheds that are typically in geomorphic disequilibrium, understanding the sediment transport conditions is extremely important in completing a successful project. Wolman (1967) suggested a channel evolution model (CEM) that accounts for the effects of urbanization on streams as seen in three distinct phases. In this model, a stream in equilibrium (Stage 1) experiences increased sediment inputs due to construction activities (Stage 2). This would provide excess small sediment, smothering large substrate and leading to channel and bar storage. As the landscape is stabilized and sealed, sediment

input can decrease drastically, possibly to below pre-development levels. This leads to channel enlargement and increase in mean sediment size (Stage 3). During this final stage, others point out that while traditional sediment inputs may be effectively cut off, anthropogenic debris come into play as both fine and coarse sediments (Grable and Harden, 2006). An alternate and more complex six stage CEM was put forth by Simon (1995). Simon's CEM is useful in that it can be used to determine repercussions of current activities, determining the amount of disturbance caused by an event, or in some cases determining the past characteristics of a stream (Simon, 1995). Due to destruction of riparian areas, these sources are generally not subject to filtering by intact riparian zones in urban environments, leading to increased channel inputs (Hook, 2003).

Bed substrate composition is of even greater concern as interest in expanding the regulatory focus of stream restoration to include ecological enhancement as well as hydraulic concerns (Shields et al, 2003). Streams with bed substrates consisting of coarse materials like cobbles and gravels provide necessary benthic habitat for aquatic biota (Buss et al, 2004; Freeman and Schorr, 2004; Williams, 2005). In urban environments where an increase in fine sediment is often encountered, interest lies in determining stable substrate for habitat and size fractions that will be cleared at high flows. The way in which depositional patches that develop in the bed respond to sediment regime conditions and bed-load movement is not yet understood (Buffington and Montgomery, 1999).

Values of shear that will produce conditions of incipient motion are well predicted by the Shield's Diagram; however, modeled predictions of bed shear often exceed observed

values, often by orders of magnitude (Buffington and Montgomery, 1999; Wilcock, 2001). Parker and Klingeman (1982) theorized that bed texture reflect the ratio between stress on the bed (τ) and critical shear stress for the bed material (τ_c). In a typical one-dimensional model such as the Hydrologic Engineering Center River Analysis System (HEC-RAS), the Manning's n value represents all energy loss in the reach. When used as a tool to estimate sediment mobilization for the practitioner, the full Manning's n greatly overestimates bed shear values. This will not only lead to overestimation of the mobile size fraction of the bed, but an over-prediction of transport rate, particularly in exponential rate equations. The Manning-Strickler relationship is a flow resistance partitioning technique that produces an estimate of a Manning's n which represents only the energy dissipated on the bed material based on surficial bed material characteristics. Using this partitioned Manning's n to calculate partitioned flow geometry through Manning's Equation, a more accurate estimate of the bed shear value is produced. A problem of definition is encountered with this procedure however, as the particle size class used to estimate the partitioned Manning's n is not defined, but rather left to professional judgment. (Wilcock, 2006)

The objectives of this study were to explore the efficacy of watershed characteristics in predicting reach-scale bed characteristics, determine the feasibility of developing an empirical n^* value based on bed sediment characteristics, and look at bed depositional patchiness as an indicator of supply or transport limited sediment regime. Watershed metrics, reach bed characteristics, and bed-load data were collected during the extent of this study in order to determine the predictive capability of watershed characteristics on

reach scale bed composition, investigate the development of an effective Manning's n , and look at visually quantifiable bed patchiness as an indicator of bed-load transport and deposition. In the practical realm of hydraulic design for the typical practitioner without the resources for long-term study, a predictive empirical method that makes use of easily obtainable stream geometry and sediment characteristics collected in the short term to accurately predict bed shear would be of great value. The following sections describe processes involved in characterizing research sites, bed-load sampling and processing.

Chapter 2: Methods

2.1 Study Design

Watershed metrics, reach bed characteristics, and bed-load data were collected from November 2008 to March 2009 in order to investigate the development of an effective Manning's n , determine the predictive capability of watershed characteristics on reach scale bed composition, and look at visually quantifiable bed patchiness as an indicator of bed-load transport and deposition. The following sections describe processes involved in characterizing research sites, bed-load sampling and processing, GIS procedures, modeling, and data analysis. ESRI ArcMap software version 9.3 was used to process GIS information. HEC-RAS was used to estimate a Manning's n providing τ values required to move transported sediment and compare with τ_c .

2.2 Study Area

Bedload sampling sites were selected in Ridge and Valley Physiographic Province in an effort to limit extensive differences in sediment yield due to variation in geologic processes (Figure 1). The research watersheds were subwatersheds of Beaver Creek, Third Creek, and First Creek in Knox County, TN; and Suckstone Creek in Union County, TN. Beaver Creek is a high priority watershed in the area with an active watershed association and is the focus of hydrologic remediation activities by the Knox County. Research subwatershed sizes range from just over 1 mi² to almost 12 mi². Two research subwatersheds are “nested,” or completely contained within another, larger research watershed. They were: Cox Creek in the Beaver Creek subwatershed and

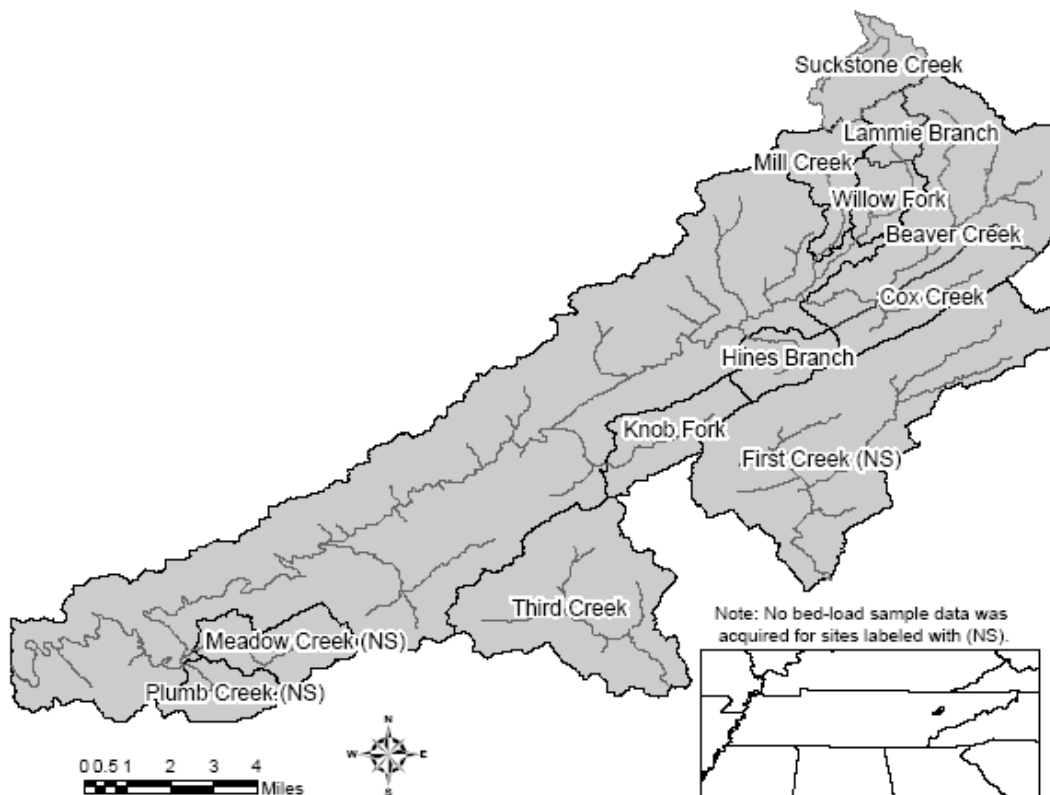


Figure 1: Research Watersheds

Lammie Branch in the Willow Fork subwatershed. GIS analysis helped in the selection of a range of urbanization in the research watersheds, ranging from 1.2% to 27.3%. The research reach in each watershed was selected as having a riffle for bed-load sampling, no knick-points, a length of approximately 150 feet, and easy access from a roadway or parking lot. Reaches display incision from mild to extreme and riparian areas include grass, forested, and asphalt within 50 feet.

2.3 Field Measurements and Sampling Activities

2.3.1 Site Setup and Bed Material Classification

Benchmarks were established at each site using #8 steel rebar. Site datums were set to an assumed elevation of 100 feet at each site. Upstream and downstream channel cross-sections were measured using level surveying techniques with a Nikon AE-7 AutoLevel. Typical spacing was approximately five feet in overbank areas and two feet in the channel. Additionally, any significant changes in slope, along with left and right top of bank and top of channel stations were noted in the field records. Crest stage recorders, a description of which is included in Appendix E were installed at the upstream and downstream extent of the research reach. The actual in-stream length from cross section to cross section was recorded with a surveying tape. A Wolman (1967) pebble count was performed to quantify the bed material in the sampling riffle at each research reach. As part of the pebble count, a semi-qualitative value representing varying deposition patterns in the cross section, referred to as “patchiness”, was recorded. If two modes of bed material were present, the percentage of the bed represented by the coarse mode, gravel or larger, was recorded. For example, if there was one mode of bed material present, the

patchiness percentage value would be 100%. If 85% of the bed was represented by a coarse mode and 15% was represented by a fine mode, a value of 85% was recorded. Pebble count values were classified into 15, 50, 85, and 100th percentiles.

2.3.2 Bed-load Sampling Method

Temporary bed-load sampling devices with capacity to sample throughout the duration of the flow event were modeled after a Bunte's (2004) bedload traps. The final design consisted of 5/16" x 3 1/2" aluminum bar stock frame with an opening measuring 3" x 12"; an interior sampling net with openings sized .05"; and an exterior reinforcing net. Further description of bed-load trap construction is found in Appendix E. Figure 2 shows the assembled sampling device. Before a predicted storm event, the samplers were secured to the bed in a riffle area of each sampled research site reach using #8 rebar driven into the bed. After the peak stage has decreased by at least half, the samplers are removed and returned to the laboratory. Storm events were sampled between 11-14-2008 and 3-28-2009. Error due to sampling a small portion of a cross-section was accepted as a by-product of the process; bed-load sampler use and performance are addressed in Appendix E.



Figure 2: Assembled Bed-load Sampler

2.3.3 Bed-load Sample Processing

Bed-load sampling activities yielded transport and stage information for nine of the twelve selected sites. When samples were removed from the sites, they were brought to the Civil Engineering Geotechnical Laboratory at the University of Tennessee, Knoxville. In order to perform particle size distributions (psd's) on the sediment material, organic material that had accumulated in the traps had to be removed. In this interest, a five gallon container, approximately half-full of water was used. After the samples were removed from the net traps, sediment material was washed from the organic material in the water containers. Organic materials including leaves, stems, nuts, crayfish, and insect larvae were noted among the debris and disposed of according to their nature. Water from the washing vessel was decanted to just above the level of sediment that had accumulated. This remaining material was transferred to a drying pan and was dried in a low temperature oven. After a 24 hour period, the samples were transferred to a high

temperature ignition oven to remove any remaining small organic debris. A dry sieve procedure (ASTM D1921-06) utilizing 10 sieves ranging from 3/8 inch to #200 sieve was performed, providing a psd for each sample recovered. In addition, the largest particle from each sample was individually measured.

2.3.4 Water Surface Measurement at Peak Flow Stage

Crest stage gages similar to the USGS type were employed to measure peak stage from sampled storms. Immediately following a flood, high water marks from displaced cork in the peak stage recorders were marked and dated in permanent marker. Marks at the brackets of the crest stage recorders were checked to ensure no vertical movement of the crest stage recorders took place. Qualitative notes were made regarding evidence of scour or aggradation of the bed surrounding the samplers. Following all sampling activities, peak stage information was surveyed with a level from the benchmarks established for cross section surveying.

2.4 Geographic Information System Analysis.

2.4.1 Data Collection

Latitude and longitude values of sampling sites were identified and collected using a Garmin GPSmap 76 Global Positioning System (GPS). Data layers for GIS analysis were acquired from the US Geological Survey (USGS) Seamless Data Server (seamless.usgs.gov). Elevation data, impervious surface information, and road locations were gathered from this source. Table 2 summarizes the data retrieved from the USGS server.

Table 1: Watershed Datasets Acquired from USGS Seamless Site

USGS Data Sets			
Layer Name	Datum	File Type	Data
NLCD* Impervious	NAD 83	raster	impervious surface
National Elevation Dataset	NAD 83	raster	elevation
BTS [†] Roads	NAD 83	shapefile	roadway locations

*National Land Cover Database

[†]Bureau of Transportation Statistics

2.4.2 GIS Data Processing

The DEM dataset was used to produce many elements in the GIS analysis. From the DEM data and site location data, the watersheds and streams were defined, and average watershed slopes were determined using the Spatial Analyst Toolset. With the watershed defined, an analysis of the impervious layer was analyzed to give a percentage impervious cover in the watershed. Stream and road layers were used to determine the length of roads within 50 feet of the stream above the research sites. An in-depth view of specific GIS analysis processes involved is included as Appendix F.

2.5 Geomorphic Channel Survey Data

Level survey values from the upstream and downstream cross-sections from each 150 ft site were entered in Microsoft Excel and processed to give an elevation relative to the benchmark for each cross sectional station. Cross sections which were recorded from right to left (facing downstream) were re-stationed at this point in accordance with the HEC-RAS input requirements (USACE, 2002).

2.6 HEC-RAS Modeling

Through the HEC-RAS Geometry Data Editor Graphical User Interface (GUI), cross sectional geometry, reach length, and Manning's n values were entered into the HEC-RAS model. Simulations were run with channel Manning's n values ranging from .01 to .035 with a constant bank value of .03. The boundary condition for each reach was defined as normal depth at the downstream cross section for the local slope between cross sections. A flow approximating the water surface level recorded on the crest stage recorder for the sampling event was identified and run at each Manning's n value; flows of the highest stage sampling event were modeled based on peak stage recorder values.

2.7 Determination of Critical Shear Values

Estimated values of bed shear (τ) for each Manning's n value modeled in HEC-RAS were compared with critical shear (τ_c) values from the modified Shield's diagram by Julien (1994) to choose an appropriate Manning's n for each reach based on the maximum sampled particle size (d_{\max}). τ_c values were determined for each classification following the modified Shield's Diagram (Figure 3) by Julien (1994) which allows for direct computation of τ_c , see Figure 3. In this form, the x and y axes of Shield's Diagram are

transformed into unitless values of $d_* = d \left[\frac{G - 1g}{\nu^2} \right]^{1/3}$ and $\tau_{*C} = \frac{\tau_c}{d \rho_s - \gamma_w}$

respectively.

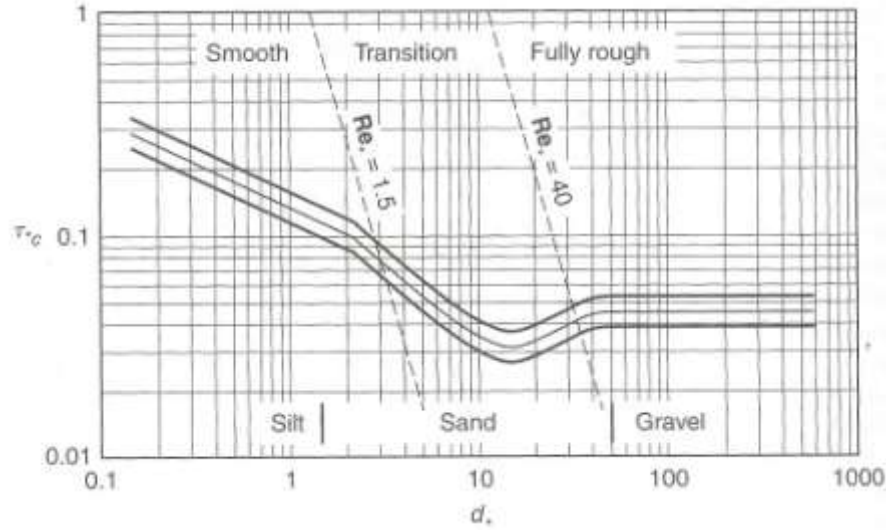


Figure 3: Modified Shield's Diagram After Julien (1994)

In an effort to quantify the availability of sediment to a reach, two additional values were calculated for each sampled site. Shear ratio (τ_r) was defined as $\tau_r = \tau_{d\max} / \tau_{comp}$, where $\tau_{d\max}$ is the shear required to move the maximum particle size found in the pebble count and τ_{comp} is the shear required to move the largest sampled particle from the bed-load sampling. τ_r quantifies the stability of the largest particles in the reach. Additionally, stream power was calculated by $\Omega = \rho g Q S$, where ρ is the density of water, g is the gravitational constant, Q is the discharge estimated from HEC-RAS modeling for n_* , and S is the reach slope.

2.8 Study Analysis

Two analyses were performed to determine the efficacy of watershed characteristics in predicting bed characteristics at the reach scale. These watershed characteristics included percent impervious as a surrogate for urbanization, average watershed slope, and the length of roads within a buffer of 50 ft within the watershed. In the first analysis, all 12

research sites were included in a Kendall's τ correlation of pebble count statistics with the watershed characteristics. The second analysis was similar to the first, but included only the research sites from which bed-load samples were retrieved, with data from the bed-load sampling in place of pebble count data. Bed shear (τ_{bed}) values from the HEC-RAS model and τ_c values from the modified Shield's Diagram (Julien, 1998) were used to determine an effective Manning's n (n^*) for each reach. This n^* value allowed modeling of shear acting on bed particles in an accessible model such as HEC-RAS, which otherwise would produce a shear value that represents all energy dissipated in the reach, greatly overestimating the particle size that will become mobile. This is a logical extension of partitioning channel properties into form and grain effects (Sturm, 2001). The concept of reach-scale bed deposition patchiness was explored as a predictive concept, with particular focus on predicting supply or transport limited bed sediment in a reach. Trends and grouping were visually assessed using shear ratio, stream power, and sampled particle size data from each site.

ArcMap 9.3 was used to process GIS information and HEC-RAS was used to perform one-dimensional hydraulic modeling on the research reaches. SAS's JMP 7.0.1 statistical software package was used to explore correlations related to the first research objective. Matrices were constructed containing relevant data to the first project objective. Multivariate scatter plots and cluster analyses were used to identify significant correlations and characteristic groupings. All scatterplot matrices are included in Appendix F for reference. Regression analysis was used to determine the possibility of predicting an empirical n^* value for the second study objective. For the final study

objective, visualization of groups and patterns through scatterplots was used to identify trends related to bed depositional patches.

Chapter 3: Results

Data gathered for each site in this project yielded cross section information, pebble count, and GIS derived watershed characteristics. Details of these are included in Appendices A, B, and F, respectively. Information from all research objectives is summarized in Table 2, with particle size distributions located in Appendix D. Tables 3 and 4 summarize correlation results between bed-load sample data with watershed characteristics and pebble count data with watershed characteristics, respectively.

3.1 Watershed Characteristics and Reach-Scale Bed Characteristics

Percent impervious area in the watershed had no correlation to any bed sediment size parameters. A positive correlation between average watershed slope and the pebble count d_{50} was noted, confirming the role that watershed slope plays in sediment transport (Figure 4, $P < 0.01$). Interestingly, no correlation was found between reach slope and any bed-load sampling metrics. The length of roads in a 50-foot buffer predicted τ_r well, (Figure 5, $P = .03$). Though two of the metrics showed a correlation with reach scale bed characteristics, they would be most judiciously used as an indicator of trends rather than a predictor of specific values.

Table 2: Results Summary

Watershed	Contributing Watershed Data					Pebble Count Data					Sample/Modeling Data			
	Area (acre)	% Impervious	Avg Watershed Slope (%)	Reach Slope (ft/ft)	Length of Roads in Buffer (ft)	Patchiness (%)	P.C. d ₁₅ (mm)	P.C. d ₅₀ (mm)	P.C. d ₈₅ (mm)	P.C. d _{max} (mm)	Sample d _{max}	Ω (ft lb/s ³)	Shear Ratio	n
Lammie Branch	842.0	1.2	7.58	0.0136	93.8	85%	8	21	45	303	37	956.3525	3.24	0.035
Cox Creek	2363.8	5.5	8.15	0.0129	235.3	95%	10	22	62	122	42	12947.9	1.43	0.020
Mill Branch	1985.3	3.0	7.99	0.0079	212.8	80%	11	22	42	233	42	2395.68	2.86	0.03
Beaver Creek	9597.0	5.4	6.34	0.0063	1199.6	100%	4	6	10	18	18	8819.902	1.00	0.015
First Creek	11950.8	17.7	5.29	0.0061	338.6	90%	6	15	62	225	*	*	*	*
Knob Fork	2163.5	14.9	6.88	0.0050	211.3	80%	4	18	30	195	44	3497.403	2.73	0.025
Suckstone Creek	1889	2.5	6.74	0.0049	1219.2	80%	9	27	78	293	36	1464.985	3.33	0.03
Third Creek	7541.2	27.3	5.54	0.0039	471.8	90%	6	11	19	163	47	13319.38	2.55	0.022
Hines Branch	1408.9	20.9	8.16	0.0032	74.4	95%	9	21	41	143	34	2910.362	3.53	0.025
Meadow Branch	2278.4	12.1	5.79	0.0010	145.7	85%	7	16	27	72	*	*	*	*
Willow Fork	2098.1	1.3	5.2	0.0037	319.9	100%	5	11	19	44	34	1525.293	1.29	0.020
Plumb Creek	1481.8	18.4	6.41	0.0011	63.7	90%	2	11	23	60	*	*	*	*

* no bed-load sample collected

Table 3: Bed-load Sample Kendall τ Correlations

Variable	by Variable	r	p
Sample d50 avg	Area	-0.138	0.702
Sample d50 avg	% Impervious	0.138	0.702
Sample d50 avg	Avg Watershed Slope	0.828	0.022
Sample d50 avg	Reach Slope	0.414	0.251
Sample d50 avg	Length of Roads In Buffer	-0.414	0.251
Sample d85 avg	Area	-0.600	0.142
Sample d85 avg	% Impervious	0.400	0.327
Sample d85 avg	Avg Watershed Slope	0.600	0.142
Sample d85 avg	Reach Slope	0.000	1.000
Sample d85 avg	Length of Roads In Buffer	-0.800	0.050
Sample d85 avg	Sample d50 avg	0.527	0.207
Sample dmax	Area	0.148	0.615
Sample dmax	% Impervious	0.371	0.209
Sample dmax	Avg Watershed Slope	-0.074	0.802
Sample dmax	Reach Slope	0.114	0.673
Sample dmax	Length of Roads In Buffer	0.000	1.000
Sample dmax	Sample d50 avg	0.214	0.559
Sample dmax	Sample d85 avg	0.316	0.449
Shear Ratio	Area	-0.556	0.037
Shear Ratio	% Impervious	0.111	0.677
Shear Ratio	Avg Watershed Slope	0.389	0.144
Shear Ratio	Reach Slope	-0.022	0.929
Shear Ratio	Length of Roads In Buffer	-0.833	0.002
Shear Ratio	Sample d50 avg	0.414	0.251
Shear Ratio	Sample d85 avg	0.800	0.050
Shear Ratio	Sample dmax	-0.057	0.833

Table 4: Pebble Count Kendall τ Correlations

Variable	by Variable	r	p
PC d50	Area	-0.305	0.205
PC d50	% Impervious	-0.191	0.428
PC d50	Avg Watershed Slope	0.610	0.011
PC d50	Reach Slope	0.224	0.346
PC d50	Length of Roads In Buffer	-0.305	0.205
PC dmax	Area	-0.164	0.484
PC dmax	% Impervious	-0.018	0.938
PC dmax	Avg Watershed Slope	0.200	0.392
PC dmax	Reach Slope	0.418	0.073
PC dmax	Length of Roads In Buffer	-0.127	0.586
PC dmax	PC d50	0.552	0.015
Shear Ratio	Area	-0.556	0.037
Shear Ratio	% Impervious	0.111	0.677
Shear Ratio	Avg Watershed Slope	0.389	0.144
Shear Ratio	Reach Slope	-0.022	0.929
Shear Ratio	Length of Roads In Buffer	-0.833	0.002
Shear Ratio	PC d50	0.506	0.046
Shear Ratio	PC dmax	0.556	0.025

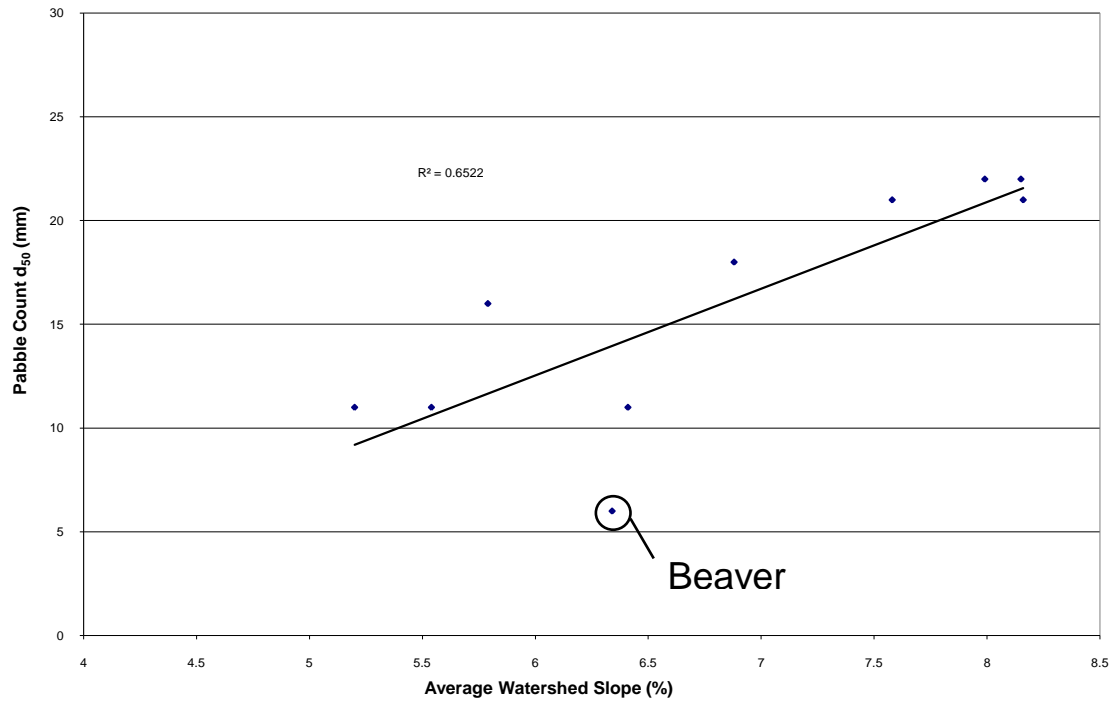


Figure 4: Relationship Between Average Watershed Slope and Pebble Count d_{50}

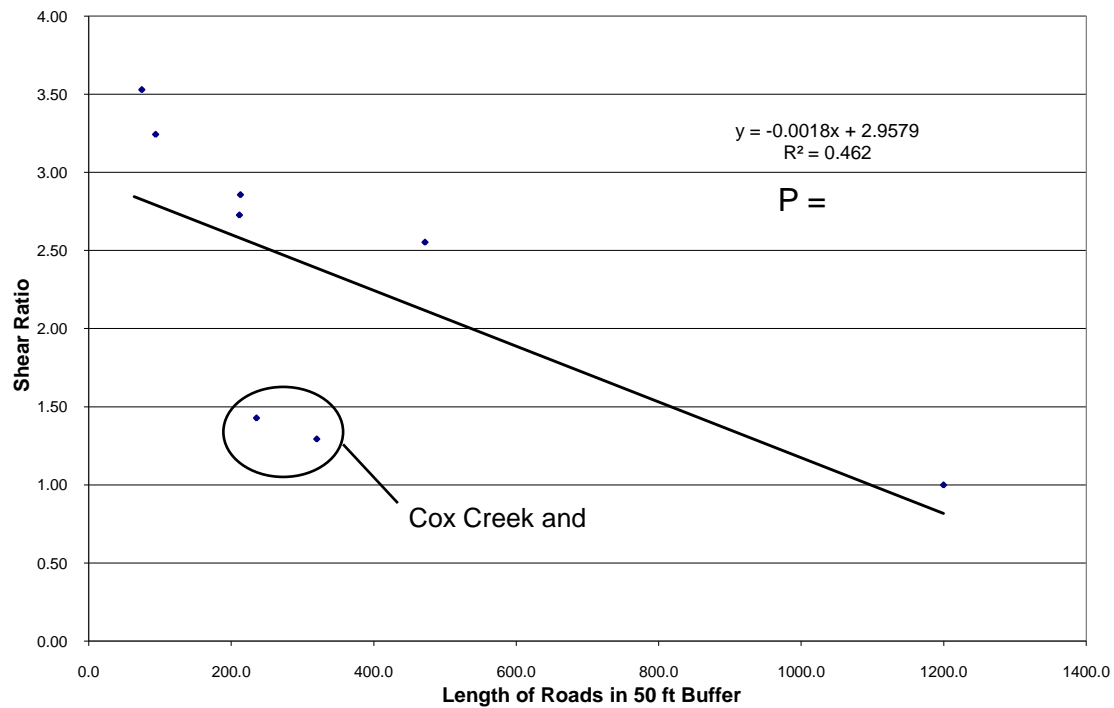


Figure 5: Relationship Between Length of Roads in 50-foot Buffer and τ_r

3.2 Development of an Empirical Model for n^*

In an effort to define an empirical relationship between bed composition and n^* , correlations were explored between each sites' pebble count d_{15} , d_{50} , d_{85} , and d_{\max} and the n^* value determined for each reach (Table 2). A strong linear correlation was identified between the maximum particle size (d_{\max}) identified in the reach and n^* , as seen in Figure 6. No significant correlations were observed with the remaining three pebble count metrics.

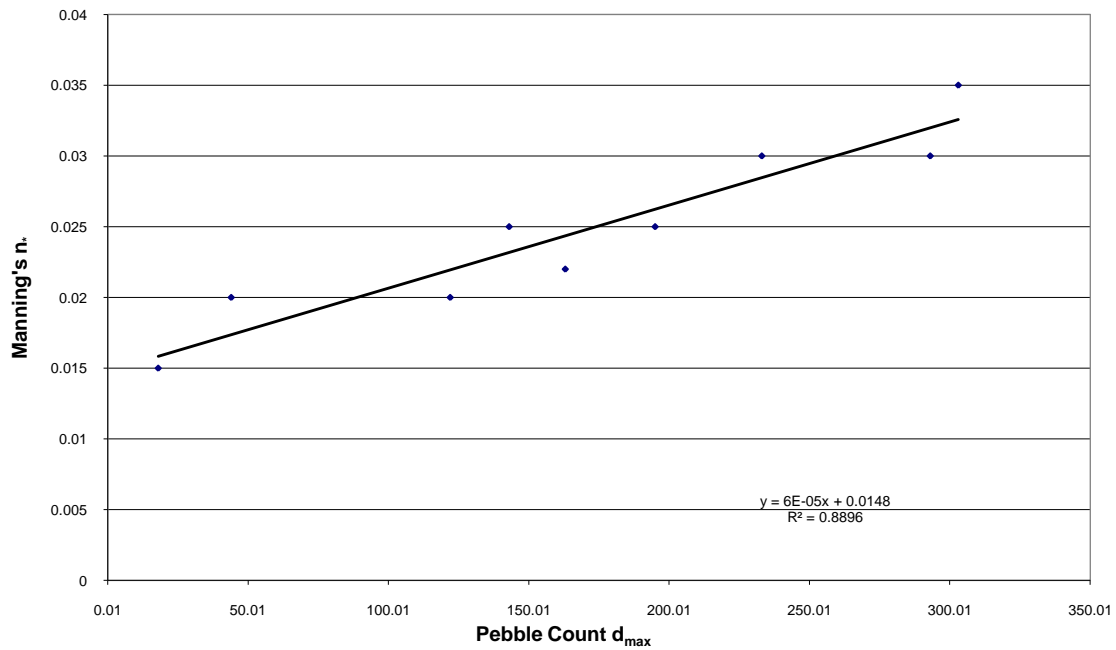


Figure 6: Pebble Count d_{\max} and n^*

3.3 Reach Scale Bed Deposition Patchiness as a Predictive Concept

In comparing τ_r and patchiness, the potentially supply-limited sites appeared in a group. Cox Creek, at 95% patchiness, appeared to be in a transition zone while Beaver Creek and Willow Fork, at 100%, are clearly disconnected from the other sites (Figure 7). All sites with a patchiness value $\leq 90\%$ have τ_r values > 2.50 . No correlation was observed between τ_r or Ω and watershed scale characteristics (Table 2). For the purpose of this study, $\tau_r < 1.5$ was assumed to indicate a potentially supply-limited sediment regime since shear values near incipient motion for the largest observed bed material were approached. This produces a population of Beaver Creek, Cox Creek, and Willow Fork as candidates for supply-limited reaches (Figure 7). A comparison was made between the bed-load sample d_{\max} and Ω in an effort to determine if Ω trends can be applied to comparatively identify true supply-limited reaches (Figure 8). Interestingly, Beaver Creek appears as the outlier in Figure 4, while Cox Creek and Willow Fork appear as outliers in Figure 5.

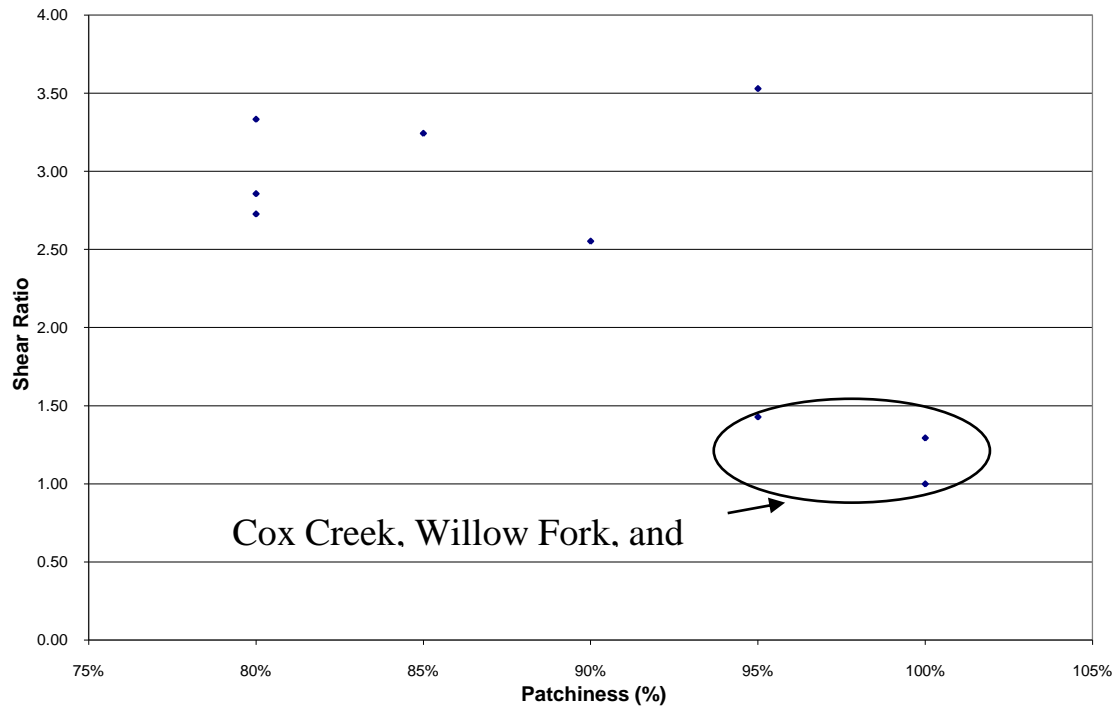


Figure 7: Patchiness vs Shear Ratio

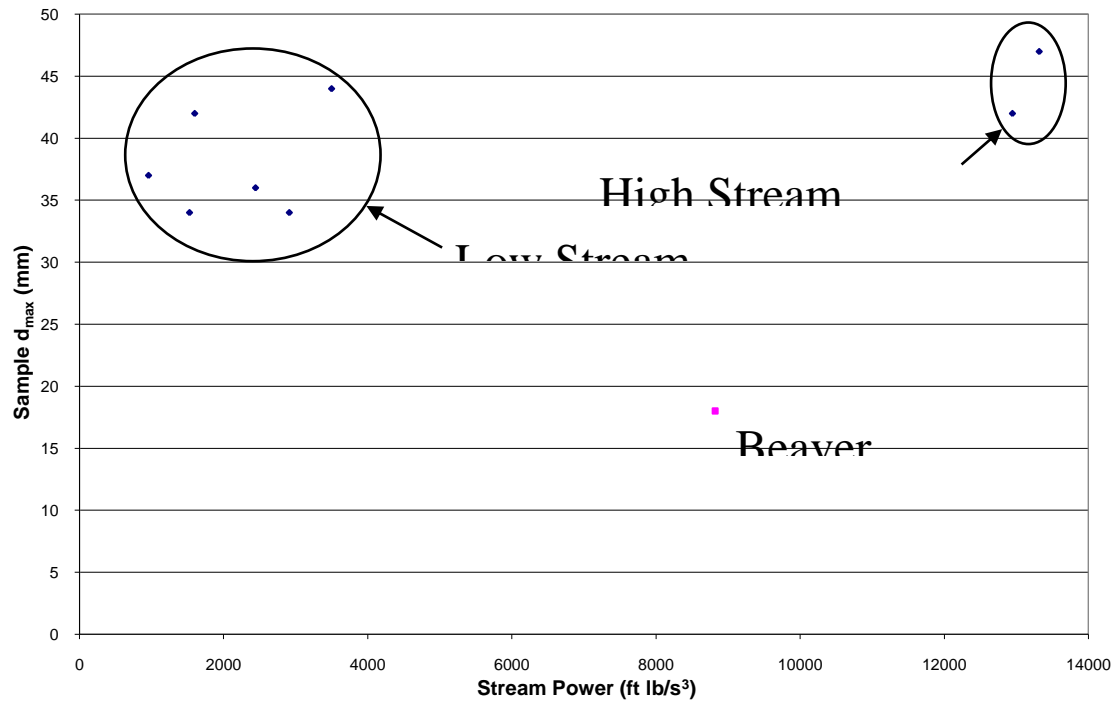


Figure 8: Stream Power and Sample d_{max}

In visualizing Ω 's relationship to sample d_{\max} , it was observed that Beaver Creek was the only low τ_r site to lie significantly apart from the sample d_{\max} values of both low and high stream power groups. Cox Creek lies in the high stream power group, and Willow Fork lies in the low stream power group. That the high and low stream power groups include sites with both high and low τ_r values suggest that the low τ_r sites that fall within the groups are in regime for their discharge and sediment supply characteristics. This suggests that Beaver Creek is the only true supply-limited stream in the population of sampled sites. Though this comparative analysis was useful in this study to differentiate potential supply-limited sites from true supply-limited sites, a predictive method using Ω was not identified. There were no significant correlations involving pebble count data and stream power that would predict a site falling into the groups identified from bed-load sampling. The grouping that is implied in comparing Ω and sample d_{50} becomes less clear when considering the relationship between Ω and τ_r directly.

Chapter 4: Discussion

Increasing the accuracy of inputs for a stream restoration design should improve the viability of the designs from both a structural and biological perspective. Broad watershed characteristics are not sufficient predictors of reach scale channel characteristics. Reach-scale depositional patchiness, as a visually identifiable surrogate for shear variance in a reach may be integrated into a channel stability index or to indicate reaches of concern for restoration activities. Identification of easily gathered channel characteristics that can help improve input for restoration design and can be applied in an economically viable way for practitioners.

4.1 Watershed Characteristics and Reach Scale Bed Characteristics

The generally poor correlations between watershed characteristics and reach-scale bed characteristics indicate that a snapshot view of watershed characteristics is insufficient to predict specific reach conditions. A more effective approach may be to look at time series land use information that could be related to Simon's CEM to track effects on the channel as they migrate downstream and progress through time (Langendoen and Alonso, 2008). That the length of roads in a 50-foot buffer predicted τ_r suggests that hydrologic connectivity or proximity of impervious surfaces might be a better indicator of reach scale conditions. Though two of the metrics showed a correlation with reach-scale channel characteristics, they would be most judiciously used as an indicator of trends rather than a predictor of specific values. Comparison between basins might aid in

identifying target watersheds for further investigation but was beyond the scope of this study.

4.2 Development of an Empirical Model for n^*

The strong correlation observed between the maximum particle size identified in a reach and the n^* value determined through modeling indicates that an empirical method for determining an n^* value from bed composition metrics is possible to develop. This, in conjunction with a one-dimensional flow model, will accurately predict values of bed shear. Instead of estimating a value for Manning's n from channel and bed characteristics where shear values are greatly overestimated, this technique would give a solid base from which to move through the modeling process (Figure 9).

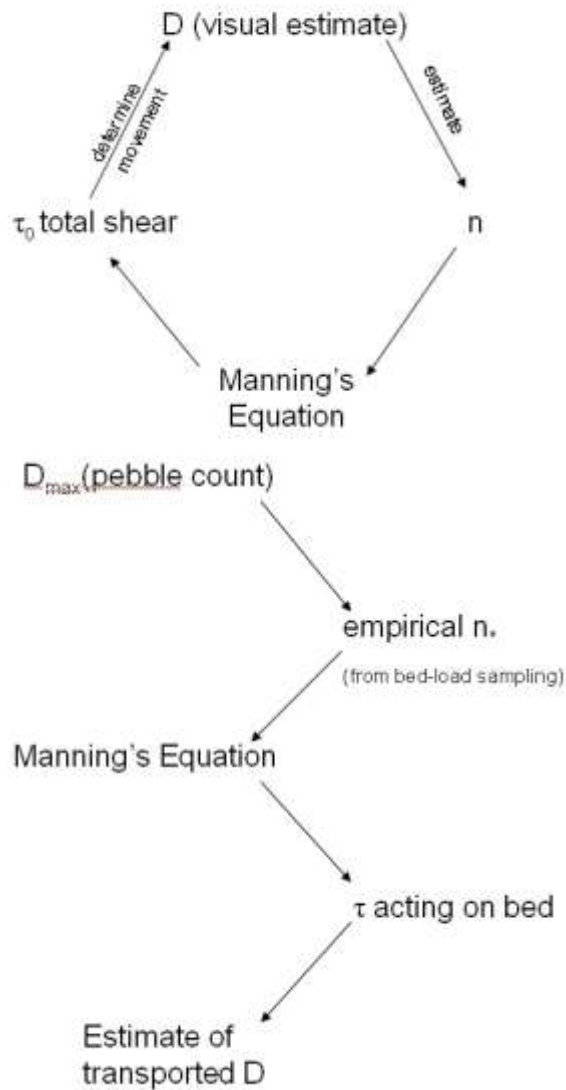


Figure 9: Modeling without and with Bed-load Sampling Data

That the significant correlation is with the pebble count d_{\max} particle size in the reach suggests that these are the particles dominating the turbulent structures near the bed that initiate movement of bed material. As a practical and simple tool for the stream restoration practitioner, an accurate estimation of the mobile fraction of bed material in a reach can help in designing stable portion of the bed and a portion that will become mobile, allowing design of heterogeneous bed material suitable as benthic and spawning

habitat (Wilcock, 2001). From a modeling standpoint, the observed relationship gives an empirical basis for choosing a value for n^* to determine approximate values for particles to become mobile during bankfull flow events. Though the relationship determined in the Ridge and Valley physiographic province may have limited geographic and geologic applicability it suggests that the possibility of developing similar relationships in other physiographic provinces is also possible.

4.3 Reach Scale Bed Deposition Patchiness as a Predictive Concept

An interesting relationship is seen when looking at stream order and τ_r . All first order watersheds in the study have a τ_r value greater than 2.5, classifying them as transport limited; the two potentially supply limited sites were the second order watersheds in the study; while the only conclusively supply limited stream in the study was a third order watershed. Previous observations (Ferguson et al, 1996) have noted rapid fining of bed sediment in the downstream direction. In a channel that still has high stream power, this could lead to a supply limited sediment regime. As a concept, reach-scale depositional patchiness needs methodological refinement. However, as a quick indicator of sites that may be supply limited or ecologically impaired, or as an additional metric in a channel assessment protocol, it may be effective.

4.4 Applications to Stream Restoration

As biological recovery becomes a recognized goal of stream restoration and potentially a part of regulatory assessment of project success, clearly defined goals along with techniques to achieve these goals become necessary (Shields et al, 2003; Palmer et al, 2005; Bernhardt and Palmer, 2007). The results of this study have been incorporated into

a decision chart to provide a framework for the restoration design process (Figure 10). These results are used in conjunction with Williams' (2005) findings showing a correlation between bed substrate characteristics with Rapid Bioassessment Protocol III (RBP III) scores using benthic macroinvertebrates and Dworak's (2005) hydraulic modeling. Using findings from these studies with a conceptual framework similar to that outlined below, it would support design of stream restoration projects, clearly defining biological and morphological goals.

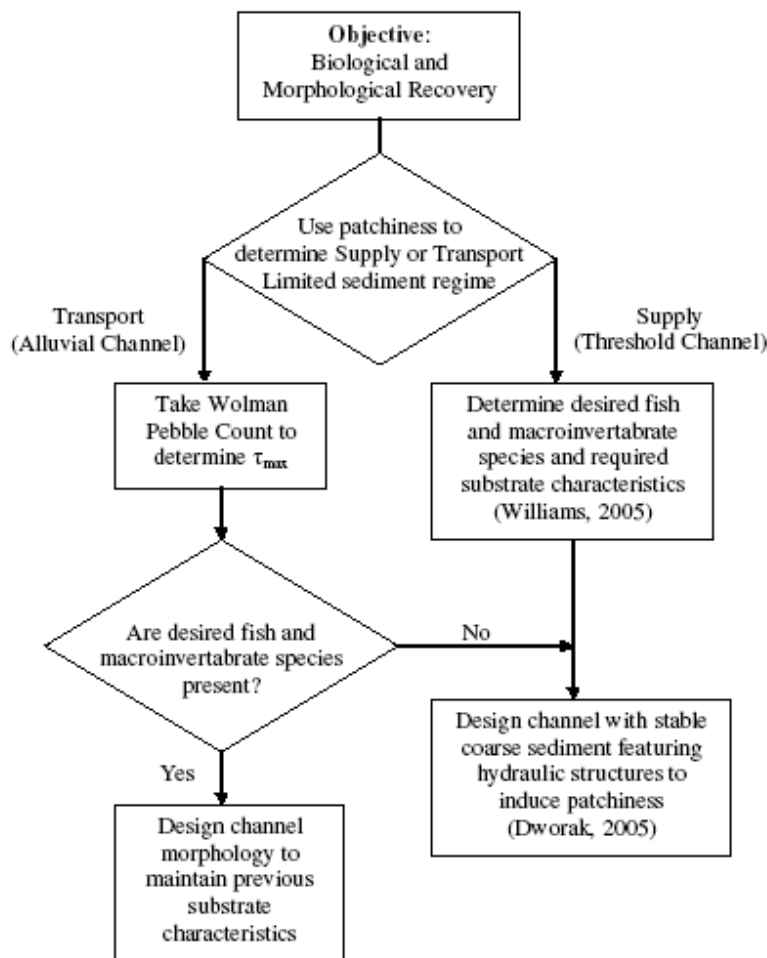


Figure 10: Restoration Design Conceptual Framework

Though watershed metrics, as studied, had no practical predictive ability as applied to local reach-scale bed characteristics, the concept of an empirical n^* value and using bed depositional patchiness to assess supply or transport limited sediment regimes revealed are of practical importance to the stream restoration practitioner. The ability to predict and design for sediment characteristics at a site with easily gathered field data has been lacking (Wilcock, 2001). Knowing bed-shear values, sediment regime characteristics, and being able to integrate these with clearly stated biological requirements is invaluable in the field of stream restoration.

List of References

- Arnold, C.L., P.J. Boison, and P.C. Patton. (1982) Sawmill Brook: an example of rapid geomorphic change related to urbanization. *Journal of Geology*. 90:2, 155-166.
- Arnold Jr., C.L. and J.C. Gibbons. (1996) Impervious surface coverage: the emergence of a key environmental indicator. *Journal of the American Planning Association*. 62:2, 243-258.
- Bagnold, R.A. (1977) Bed-load transport in natural rivers. *Water Resources Research*. 13:2, 303-312.
- Bathurst, J.C. (2007) Effect of coarse surface layer on bed-load transport. *Journal of Hydraulic Engineering*. 133:11, 1192-1205.
- Beighley, R.E. and G.E. Moglen. (2002) Trend assessment in rainfall-runoff behavior in urbanizing watersheds. *Journal of Hydrologic Engineering*. 7:1, 27-34.
- Bernhardt, E.S. and M.A. Palmer. (2007) Restoring streams in an urbanizing world. *Freshwater Biology*. 52, 738-751.
- Bledsoe, B.P. and C.C. Watson. (2001) Effects of urbanization on channel instability. *Journal of the American Water Resources Association*. 37:2, 255-270.
- Booth, D.B. (1990) Stream channel incision following drainage basin urbanization. *Journal of the American Water Resources Association*. 26:3, 407-417.
- Booth, D.B. and Jackson, C.R. (2007) Urbanization of aquatic systems – degradation thresholds, stormwater detection, and the limits of mitigation. *Journal of the American Water Resources Association*, 33. 1077-1090.

- Bravo-Espinoza, M.; W.R. Osterkamp; and V.L. Lopes. (2003) Bedload transport in alluvial channels. *Journal of Hydraulic Engineering*. 129:10, 783-795.
- Buffington, J.M. and D.R. Montgomery. (1997) A systematic analysis of eight decades of incipient motion studies, with special reference to gravel-bedded rivers. *Water Resources Research*. 22:8, 1993-2029.
- Buffington, J.M. and D.R. Montgomery. (1999) Effects of hydraulic roughness on surface textures of gravel-bed rivers. *Water Resources Research*. 35:11, 3507-3521.
- Buffington, J.M. and D.R. Montgomery. (1999) Effects of sediment supply on surface textures of gravel-bed rivers. *Water Resources Research*. 35:11, 3523-3530.
- Bunte, K.; S.R. Abt; J.P. Potyondy; and S.E. Ryan. (2004) Measurement of coarse gravel and cobble transport using portable bedload traps. *Journal of Hydraulic Engineering*. 130:9, 879-893.
- Bunte, K.; S.R. Abt; J.P. Potyondy; and K.W. Swingle. (2008) A comparison of coarse bedload transport measured with bedload traps and helley-smith samplers. *Geodinamica Acta*. 21:1-2, 53-66.
- Buss, D.F.; D.F. Baptista; J.L. Nessimian; and M. Egler. (2004) Substrate specificity , environmental degradation and disturbances structuring macroinvertebrate assemblages in neotropical streams. *Hydrobiologica*. 518, 179-188.
- Carter, J.; P.N. Owens; D.E. Walling; G.J.L. Leeks. (2003) Fingerprinting Suspended Sediment Sources in a Large Urban River System. *Science of the Total Environment*. 314:16, 513-534.
- Chin, A. and K.J. Gregory. (2005) Managing urban river channel adjustments. *Geomorphology*. 69, 28-45.
- Curran, J.C. and P.R. Wilcock. (2005) Effect of sand supply on transport rates in a gravel-bed channel. *Journal of Hydraulic Engineering*. 131:11, 961-967.
- Daniel, T.C., P.E. McGuire, D. Stoffel, and B. Miller. (1979) Sediment and nutrient yield from residential construction sites. *Journal of Environmental Quality*. 8:3, 304-308.
- Dawdy, D.R. Knowledge of sedimentation in urban environments. *Journal of the Hydraulics Division, ASCE*. 6, 235-245.

- Dworak, F. (2005) Characterizing turbulence structure along woody vegetated banks in incised channels: implications for stream restoration. Thesis, University of Tennessee, Knoxville.
- Finkenbine, J.K., J.W. Atwater, and D.S. Mavinic. (2000) Stream health after urbanization. *Journal of the American Water Resources Association*. 36:5, 1149-1159.
- Ferguson, R., T. Hoey, S. Wathen, and A. Werritty. Field evidence for rapid downstream fining of river gravels through selective transport. *Geology*. 24:2, 179-182.
- Freeman, P.L. and M.S. Schorr (2004) Influence of watershed urbanization on fine sediment and macroinvertebrate assemblage characteristics in Tennessee Ridge and Valley streams. *Journal of Freshwater Ecology*. 19:3, 353-362.
- Galay, V.J. (1983) Causes of river bed degradation. *Water Resources Research*. 19:5, 1057-1090.
- Garcia, M. and G. Parker. (1991) Entrainment of bed sediment into suspension. *Journal of Hydraulic Engineering*. 117:4, 414-435.
- Grable, J.L. and C.P. Harden. (2006) Geomorphic response of an appalachian valley and ridge stream to urbanization. *Earth Surface Processes and Landforms*. 31, 1707-1720.
- Graf, W.L. The impact of suburbanization on fluvial geomorphology. *Water Resources Research*. 11:5, 690-692.
- Hammer, T.R. (1972) Stream channel enlargement due to urbanization. *Water Resources Research*. 8:6, 1530-1540.
- Haschenburger, J.K. and P.R. Wilcock. (2003) Partial transport in a natural gravel bed channel. *Water Resources Research*. 39:1, 1020-1029.
- Henshaw, P.C. and D.B. Booth. Natural restabilization of stream channels in urban watersheds. *Journal of the American Water Resources Association*. 36:6, 1219-1236.
- Hollis, G.E. (1975) The effects of urbanization on floods of different recurrence intervals. *WaterResources Research*. 11, 431-435.
- Hook, P.B. (2003) Sediment retention in rangeland riparian buffers. *Journal of Environmental Quality*. 32:2, 1130-1137.

- Johnson, D. (2008) The application of a two-dimensional sediment transport model in a cumberland plateau mountainous stream reach with complex morphology and coarse substrate. Thesis, University of Tennessee, Knoxville.
- Klein, R.D. (1979) Urbanization and stream quality impairment. *Water Resources Bulletin*. 15:4, 948-963.
- Knighton, D. (1998) *Fluvial forms and processes*. Arnold Publishing, London.
- Lane, E.W. (1955) The importance of fluvial morphology in hydraulic engineering. *Proceedings of the American Society of Civil Engineers*. 84, 1-17.
- Langendoen, E.J. and C.V. Alonso. (2008) Modeling the evolution of incised streams: I. model formulation and validation of flow and streambed evolution components. *Journal of Hydraulic Engineering*. 134:6, 749-762.
- Leopold, L.B. (1968) *Hydrology for urban land planning – a guidebook on the hydrologic effects of urban land Use*. US Geological Survey Professional Paper 252. US Government Printing Office: Washington, DC.
- Leopold, L.B. and W.W. Emmett. (1976) Bedload measurements, East Fork River, Wyoming. *Proceedings of the National Academy of Sciences, USA*. 73:4, 1000-1004.
- Leopold, L.B. and W.W. Emmett. (1977) 1976 Bedload measurements, East Fork River, Wyoming. *Proceedings of the National Academy of Sciences, USA*. 74:7, 2644-2648.
- Nelson, E.J. and D.B. Booth. (2002) Sediment sources in an urbanizing, mixed land-use watershed. *Journal of Hydrology*. 264, 52-68.
- Palmer, E.A., E.S. Bernhardt, J.D. Allan, P.S. Lake, G. Alexander, S. Brooks, J. Carr, S. Clayton, C.N. Dahm, J. Follstad Shah, D.L. Galat, S.G. Loss, P. Goodwin, D.D. Hart, B. Hassett, R. Jenkinson, G.M. Kondolf, R. Lave, J.L. Meyer, T.K. O'Donnell, L. Pagano, and E. Sudduth. (2005) Standards for ecologically successful river restoration. *Journal of Applied Ecology*. 42, 208-217.
- Parker, G. and P.C. Klingeman. (1982) On why gravel bed streams are paved. *Water Resources Research*. 18, 1409-1423.
- Paul, M.J. and J.L. Meyer. (2001) Streams in the urban landscape. *Annual Review of Ecology and Systematics*. 32, 333-365.

- Pizzuto, J.E., W.C. Hession, and M. McBride. (2000) Comparing gravel-bed rivers in paired urban and rural catchments of southeastern pennsylvania. *Geology*. 28:1, 79-82.
- Rhoads, B.L., D. Wilson, M. Urban, and E.E. Herricks. (1999) Interaction between scientists and nonscientists in community-based watershed mangagement: emergence of the concept of stream naturalization. *Environmental Management*. 24:3, 297-308.
- Riley, A.L. (1998) Restoring streams in cities: a guide for planners, policymakers, and citizens. Island Press, Washington D.C.
- Robinson, A.M. (1976) The effects of urbanization on stream channel morphology. *Proceedings: International Symposium on Urban Hydrology, Hydraulics and Sediment Control*. University of Kentucky, Lexington, KY. 65-74.
- Ryan, S.E.; K.Bunte; and J.P. Potyondy. (2005) Breakout session 2: bedload transport measurement, data needs, uncertainty, and new technologies. *Proceedings of the Federal Interagency Sediment Monitoring Instrument and Analysis Research Workshop*, September 9-11, 2003, Flagstaff, AZ. US Geological Survey Circular 1276, 16-28.
- Sambrook Smith, G.H. and R.L. Ferguson. The gravel-sand transition along river channels. *Journal of Sedimentary Research*. A65:2, 423-430.
- Schwartz, J.S. and E.E. Herricks. Evaluation of pool-riffle naturalization structures on habitat complexity and the fish community in an urban Illinois stream. *River Research and Applications*. 23, 451-466.
- Shields Jr., F.D., R.R. Copeland, P.C. Klingeman, M.W. Doyle, and A.Simon. (2003) Design for stream restoration. *Journal of Hydraulic Engineering*. 129:8, 575-584.
- Simon, A. (1995) Adjustment and recovery of unstable alluvial channels: identification and approaches for engineering management. *Earth Surface Processes and Landforms*. 20. 611-628.
- Simon, A., A. Curini, S.E. Darby, and E.J. Langendoen. (2000) Bank and near-bank processes in an incised channel. *Geomorphology*. 35, 193-217.
- Simon, A., Langendoen, E.J., Bingner, R.L., Wells, R., Yuan, Y. and Alonso, C.V. (2004) Suspended-sediment transport and bed-material characteristics of shades creek, Alabama and ecoregion 67: developing water-quality criteria for suspended and bed-material sediment. *National Sedimentation Laboratory Report No. 43*, 150 p.

- Solo-Gabrielle, H.M. and F.E. Perkins. (1997) Streamflow and suspended sediment transport in an urban environment. *Journal of Hydraulic Engineering*. 123:9, 807-811.
- Song, T., Y.M. Chiew, and C.O. Chin. (1998) Effect of bed-load movement on flow friction factor. *Journal of Hydraulic Engineering*. 124:2, 165-175.
- Trimble, S.W. (1995) Catchment sediment budgets and change. *Changing River Channels*: A. Gurnell and G. Petts eds. John Wiley & Sons, Chichester. 1-23.
- USACoE (2002) HEC-RAS River Analysis System, User's Manual, Version 3.2, US Army Corps of Engineers; Hydrologic Engineering Center; Davis, California.
- Walsh, C.J.; Roy, A.H.; Feminella, J.W.; Cottingham, P.D.; Groffman, P.M.; Morgan, R.P. (2005) The urban stream syndrome: current knowledge and the search for a cure. *Journal of the North American Benthological Society*. 24:3. 706-723.
- Wiberg, P.L. and J. Dungan Smith. (1989) Model for calculating bed load transport of sediment. *Journal of Hydraulic Engineering*. 115:1, 101-123.
- Wilcock, P.R. (1997) The components of fractional transport rate. *Water Resources Research*. 33:1, 247-258.
- Wilcock, P.R. (1998) Two-fraction model of initial sediment motion in gravel-bed rivers. *Science*. 280:4, 410-412.
- Wilcock, P.R. (2001) Toward a practical method for estimating sediment-transport rates in gravel-bed rivers. *Earth Surface Processes and Landforms*. 26, 1395-1408.
- Wilcock, P.R. and J.C. Crowe. (2003) Surface based transport model for mixed-size sediment. *Journal of Hydraulic Engineering*. 129:2, 120-128.
- Williams, K. (2005) Linking channel stability and bed sediment characteristics to biological integrity in Tennessee Ridge and Valley streams. Thesis, University of Tennessee, Knoxville.
- Wolman, M.G. (1967) A cycle of sedimentation and erosion in urban river channels. *Geografiska Annaler. Series A, Physical Geography*. 49:2/4. 385-395.
- Wolman, M.G. and A.P. Schick. Effects of construction on fluvial sediment, urban and suburban areas of Maryland. *Water Resources Research*. 3:2, 451-464.

Appendices

Appendix A: Literature Review

Urbanization in a watershed begins a chain reaction of effects in the water resources of that watershed (Bledsoe and Watson, 2001; Booth and Jackson, 1997; Walsh et al., 2005). Hydrologic changes lead to changes in sediment flux which in turn lead to changes in form and function of the streams from both a structural and biological perspective (Simon, 1995; Schwartz and Herricks, 2007). As infiltration and storage capacities are altered due to construction activities including clearing and grubbing, paving, and building construction; hydrograph values and shapes change, with peaks and durations increasing (Hollis, 1975; Leopold, 1968). Delivery paths to the streams are concurrently altered by use of storm-water collection and distribution infrastructure which delivers high volumes to the stream with a low time of concentration (Booth and Jackson, 1997). Due to sediment transport's link to storm runoff and discrete inputs of sediment (as in bank failures), these effects in the watershed can be separated both spatially and temporally from the source of disturbance (Gregory, 1977).

Wolman (1967) suggested a channel evolution model that accounts for the effects of urbanization on streams as seen in three distinct phases. First, uncontrolled erosion during construction activities, early erosion in the channel, and late erosion in the channel. In this model, a stream in equilibrium (Stage 1) experiences increased sediment inputs due to construction activities (Stage 2). This would provide excess small sediment, smothering large substrate and leading to channel and bar storage. As the landscape is stabilized and sealed, sediment input can decrease drastically, possibly to below pre-development levels. This leads to channel enlargement and increase in mean sediment size (Stage 3). During this final stage, others point out that while traditional sediment

inputs may be effectively cut off, anthropogenic debris come into play as both fine and coarse sediments (Grable and Harden, 2006). An alternate and more complex six stage CEM was put forth by Simon in 1995. Simon's CEM is useful in that it can be used to determine repercussions of current activities, determining the amount of disturbance caused by an event, or in some cases determining the past characteristics of a stream (Simon 1995). Due to destruction of riparian areas, sources for these and other sources are generally not subject to filtering by intact riparian zones in these urban environments, leading to increased channel inputs (Hook, 2003).

Phase 2, as defined by Wolman, seems to be focused on sediment load, but there also appears to be a hydrologic/hydraulic component that plays a part in it. The same activities that compact and seal in traditional sediment inputs also prevent infiltration in urbanizing areas. Increases in flood frequencies and in peak flood flows reflect this basic hydrologic change. This increase in hydraulic conveyance requirements would predict channel enlargement even with a constant sediment load (Lane, 1955; Galay, 1983). Lane's model of channel dynamics actually matches well with Wolman's Channel Evolution Model. This may be exacerbated by the concurrent constriction of sediment input into the system. Over a seven year period, significant widening and incision of streams with urbanized but constant land use is apparent from visual inspection (Wolman, 1967).

Changes in channel sinuosity can also lead to similar widening and incising activity. A study of change in stream power due to changes in watershed hydrology indicated that channel straightening or braiding are possible outcomes of increased stream power

(Bledsoe and Watson, 2001). Though not as common under current regulatory practices, deliberate channelization and straightening may also occur as part of the urbanization of an area. Though often a remnant of agricultural practices in the watershed, this type of channel alteration can have severe effects on channel morphology. In the first case, this adjustment may be morphological action by the stream to balance incoming sediment load with the dominant flow in the channel and the physical channel characteristics, per Lane's Law. In the second case, this straightening effectively provides an increase in channel slope, increasing unit energy and encouraging downcutting as the sediment load in a reach balances with the new stream power profile.

In predicting changes in watershed hydrology, a common metric is the percent impermeable surface over the area. While good correlation with runoff increases exists with this method, consideration of connectivity of these areas to each other and to the stream have a strong impact on the timing and intensity of these peak flows. Two methods of quantifying this distinction are presented by Booth and Jackson. From above, the former situation would be classified as a "total impervious area" method (TIA). This method ignores unsealed areas where compaction has prevented normal infiltration rates as well as the effects of hydrologic connectivity between pervious and impervious areas. An "effective impervious area" (EIA) method takes into account hydrologic separation of impervious areas by increasing or decreasing the value calculated for TIA. This relationship must be calibrated experimentally for a specific application. (Booth and Jackson, 1997) An analysis of development activities related to increases in peak runoff revealed that a threshold for significant flow change occurs at approximately 5% removal

of forest cover. The next best indicator is the percentage of development that is composed of less than .1 ha lots. Research also indicates that significant differences in predicted runoff are not indicated using variable source area versus hortonian runoff modelling. (Valeo and Moin, 2001)

These changes in hydrology are accompanied by incidental changes in sediment supply. In fact, construction has been observed to increase the sediment yield in watersheds by orders of magnitude over undisturbed and even agricultural watersheds (Wolman and Schick, 1967; Daniel et al, 1979). It has more recently been noted that new sources of sediment that are difficult to quantify in both mass and composition are introduced post-development, including slope instability, bank failure due to undercutting, anthropogenic debris, and roadway erosion (Grable and Harden, 2006; Nelson and Booth, 2001). Fining of bed sediment toward sand due to changes in sediment sources has also been noted in urbanized portions of watersheds (Simon et al., 2004). Valley slope, as an important contributor to selective downstream fining, can exacerbate sediment transport changes initiated by urbanization (Ferguson et al, 1996; Hammer, 1972, Sambrook Smith and Ferguson, 1995).

Changes both in hydrologic conditions and sediment supply in turn affect channel stability. Higher flow rates with lower upstream sediment loads tend to lead to widening, incision, or a combination of the two (Hammer, 1972; Booth, 1990; Arnold et al, 1982, Langendoen and Alonso, 2008). Even without changes in sediment supply, the increased hydraulic conveyance requirements would predict channel enlargement (Lane, 1955;

Galay, 1983). Incision can increase transport of fine sediment downstream through both in-channel erosion and by isolating the channel from its floodplain (Allmendinger et al, 2007; Hook, 2003). Separate from hydrologic changes, other effects on the channel are felt. Riparian areas are often removed during urbanization activities, removing a valuable habitat resource as well as a sediment filtering feature (Hook, 2003). Simon (1995) identified six stages of channel evolution in a disturbed watershed; the primary features of the post-disturbance channel being downcutting and widening. As channel area has been sufficiently increased, aggradation takes place, leading to restabilization. Effective restabilization has been noted to take place in the time frame of decades with constant land use in the watershed (Henshaw and Booth, 2000; Trimble, 1995).

An alternate and more complex six stage CEM was put forth by Andrew Simon in 1995. Simon's CEM is useful in that it can be used to determine repercussions of current activities, determining the amount of disturbance caused by an event, or in some cases determining the past characteristics of a stream. Stage I is the pre-disturbance stage and is characterized by a channel in dynamic equilibrium (more discussion to follow), with the typical erosion on the outside of bends balanced by bar accretion on the inside of curves. Banks are typically stable in this stage while slight increases in overall longitudinal relief are possible. The constructed phase, number II, features the removal of riparian vegetation, channelization, urbanization, or any disturbance to the channel. This includes the beginning of changes in bed height and channel geometry. Stage III marks the beginning of notable change in the channel's geometry. Banks grow both taller and steeper due to general incision in the channel, with undercutting at the base becoming evident.

Remaining vegetation near the bank may become either unstable due to undercutting or move toward the channel in competition for light. The channel becomes disconnected from its historical floodplain. In Stage IV, the threshold stage, mass bank failures begin, widening the stream and reducing bank angles. Due to this widening, the water height in the stream drops well below the top of the bank and any vegetation near the bank is introduced into the stream. The aggradation stage, Stage V, represents the beginning of the redevelopment of the stream. Bed height rises, redevelopment of alternate bar structure occurs, and imbrication of material now found on the bottom of the bank begins. If possible, reestablishment of riparian cover may now begin and possibly the formation of a terrace structure in the former floodplain. Restabilization begins in Stage VI as the water line again becomes higher in relation to the top of bank, bank angles become much lower, and alternate bar patterns become well established. Bank stability returns as the bank develops a convex shape and angles are further reduced. (Simon, 1995)

Though a useful conceptual model, Simon's approach assumes the possibility of return to a stable equilibrium with positive feedback. In an urban environment, there may also be issues related to the definition of a "stable" channel. In a natural setting, this would have a straightforward and generally accepted connotation. However, with constraints imposed on urbanized channels, particularly those wholly confined by man made structures, stability takes on a meaning where channel geometry stays relatively constant and does not encroach on surrounding infrastructure elements (Henshaw and Booth, 2000).

Stream restoration efforts are increasingly focused on these urbanizing areas (Riley, 1998). The traditional method of using an undisturbed reference reach translates poorly to these urbanized watersheds, leading to a design with no or poorly suited empirical basis (Pizzuto et al, 2000). Actions not traditionally thought of as stream restoration such as stormwater management, hydrologic remediation, and riparian replantings are now considered to be stream restoration activities in many urban areas (Bernhardt and Palmer, 2007). With more traditional stream restoration practices such as channel stabilization or ecological rehabilitation, goals are often ambiguously stated due to a lack of appropriate monitoring protocols (Montgomery and MacDonald, 2002; Schwartz et al, ?). It is becoming evident that geomorphic stability and ecologic recovery must be synthesized early in the design process as accomplishment of one of these goals does not imply the success of the other (Henshaw and Booth, 2000; Booth and Jackson 1997). Even with more site specific design protocols, input from community stakeholders along with engineering and scientific perspectives must be balanced in a way that is acceptable to all parties in order to be fully and successfully implemented (Rhoads et al., 1999). As new information on the effects of urbanization is compiled, a more complete understanding of natural versus anthropogenic influence is developed. A better understanding of this interaction allows for incorporation of natural processes in stream restoration practice (citation).

This also brings into question different possible states of dynamic equilibrium. A river channel is never at a point that could be identified as static equilibrium. However, the concept of a healthy dynamic equilibrium explains a channel's ability to recover from

disturbance within a threshold. Conceptually visualized as a ball between two hills, a channel in this state can be pushed from equilibrium by, for example, an increase in sediment load and the channel width and slope will be adjusted in a way with the dominant discharge that any significant change in profile will be readjusted. The converse of this, an unstable equilibrium, can be visualized as a ball balanced on a hill, with any push from the state of equilibrium inducing negative feedback and a fall to a new state of equilibrium. (Knighton, 1998)

While a watershed's EIA is used as a general predictor of impacts, the conditions that indicate a channel's ability to respond to these changes, much less to rebound are best viewed on a case by case basis. Though typical periods of restabilization range from 10 to 20 years, in some cases 30 or more years pass with no indication of a return to stability. An important confounding factor is the geology of the area, particularly that which is immediately underlying the channel bottom and the condition of the soil in the banks. With a relatively resilient subgrade, significant watershed changes may only slightly disturb the channel, resulting in a shorter or at least finite period of re-adjustment. It is also noted that though not all extremely urbanized (90-95% impervious) streams fail to restabilize, though all unstabilized encountered streams did fall into this category. A common feature of these streams is destruction of bedload source outside of slaking bedrock or anthropogenic debris. Fine sediment inputs continue due to bank failure as well as degradation of manmade infrastructure elements. Streams in this condition also typically feature significant reaches of total hydraulic and geologic confinement (ie. box

culverts) which may play a role in hindering a return to an equilibrium state. (Henshaw and Booth, 2000; Grable and Harden, 2006)

With a general understanding of the processes initiating change in sediment and hydraulic flow rates, morphological implications of this change of inputs, and potential for natural recovery, the next logical step is to investigate possible mitigation techniques. Though stream restoration is part of the common vernacular as a catch-all for channel restructuring, formal distinctions are presented by Rhoades et al, 1999. Stream naturalization is likely the most pertinent in an urban setting. In this case, the stream has been modified by its surroundings to the point that return to a pre-disturbance state is impossible. In comparison with stream restoration, which reverts the stream structurally and ecologically to a pristine state, and stream rehabilitation, which reinstalls as much of the structural and ecological function as possible, the conditions defining stream naturalization are defined by stakeholders affected by the condition of the stream. A compromise is reached between land owners, business owners, and members of the scientific community taking into account the scientific/engineering perspective as well as the value system of the community at large. In this approach, interaction between these groups is key in successfully implementing an approach to stream improvement. (Rhoades et al, 1999)

There are several general categories under which most all reconstruction activities fall when performing mitigation activities. Bank stabilization includes the use of bio-engineered products, inorganic materials such as rip-rap, and the use of geotextiles to stabilize the

bank as vegetation is established. Typically bank geometry is altered to a more stable state immediately previous to the application of the treatment. Channel reconfiguration and grade control encompasses two fairly distinct classes of alteration. The channel reconfiguration part generally refers to readjustment of the planform to accommodate the dominant discharge and sediment loads within the valley gradient. Grade control, on the other hand involves control of the longitudinal profile of the stream. This is typically accomplished by establishing nickpoints at specific locations and elevations to control downcutting and headcutting of the stream. Often in an urban setting, the most effective activity is riparian replanting and management. When space is limited or land-owner cooperation is minimal, eradication of invasive species and establishment of a healthy riparian zone is effective as a buffer zone as well as controlling sun exposure to the channel, thus controlling water temperature (Bernhardt and Palmer, 2007).

Sediment transport measurements in urbanizing watersheds have thus far focused on suspended sediment concentrations and bed-load studies have focused primarily on non-urbanized watersheds (Solo-Gabrielle and Perkins, 1997; Carter et al, 2003; Bunte et al, 2004; Leopold and Emmett, 1976). Robinson (1976) actually found that bed material (by d_{84}) in urban watersheds could be up to four times greater than in paired rural watersheds, though movement of the particles was not addressed. Bed-load transport data can vary widely, even over similar flow rates in the same channel, showing greater rates for some smaller discharges and similar seemingly unpredictable behavior (Leopold and Emmett, 1977). A search for a standardized bed-load sampling method is currently under

discussion with many methods from direct sampling to remote sensing are being evaluated (Ryan et al, 2005).

With a basic understanding of the processes affecting channels in urbanizing watersheds, the potential for further research in this area becomes clear quickly. Accurate predictive models may be elusive due to the extensive variables affecting changes in these channels, but further investigation may provide an insight as to what currently overlooked variables are pertinent in predicting natural restabilization or alternative methods of stabilizing these channels. Methods of predicting anthropogenic sediment, prediction of bed-load sediment cutoff by percent impervious, and a more accurate and simple method of approximating routing between impervious areas without extensive modelling are just a few areas of research which could provide valuable insight on the process side of erosion and sedimentation in streams located in urban or urbanizing watersheds.

Appendix B: Site Cross-Sections

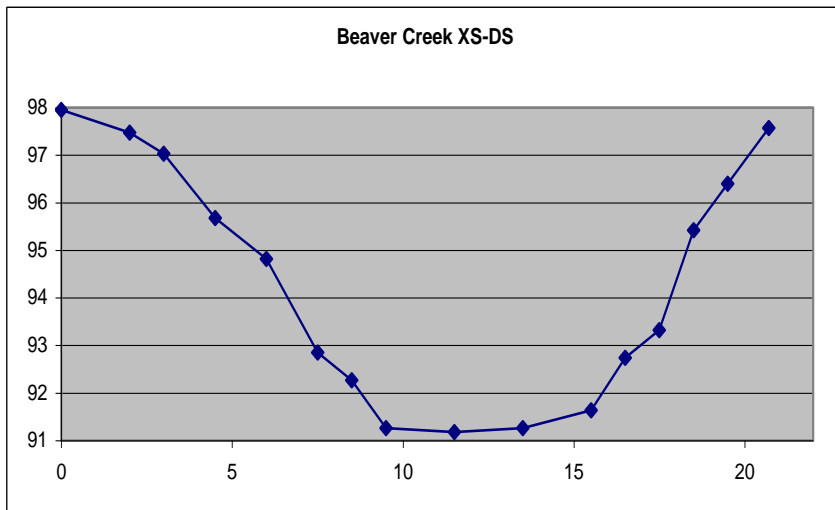
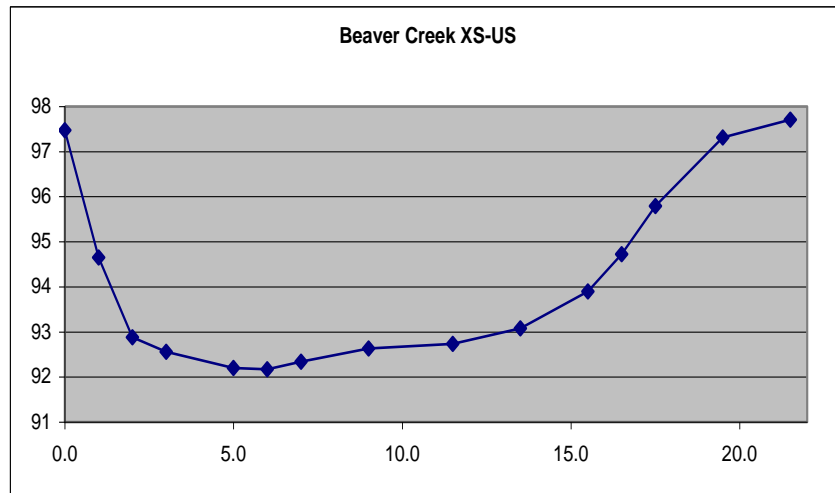


Figure 11: Beaver Creek Cross Sections

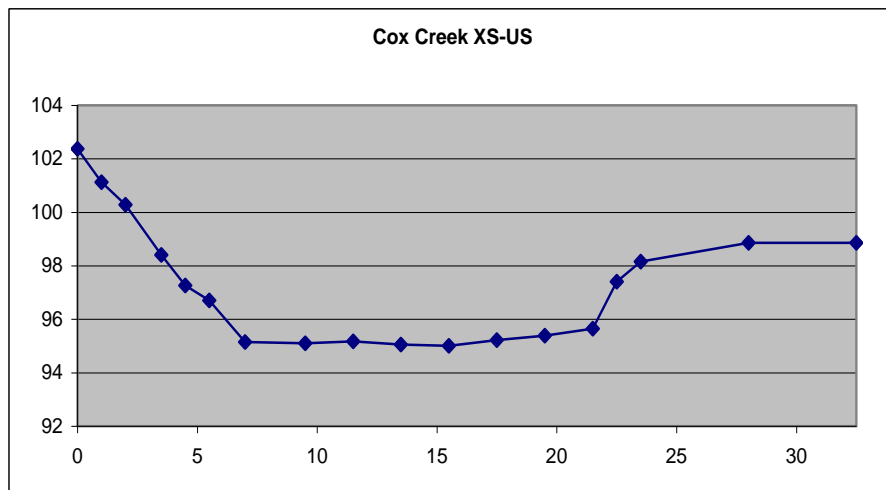
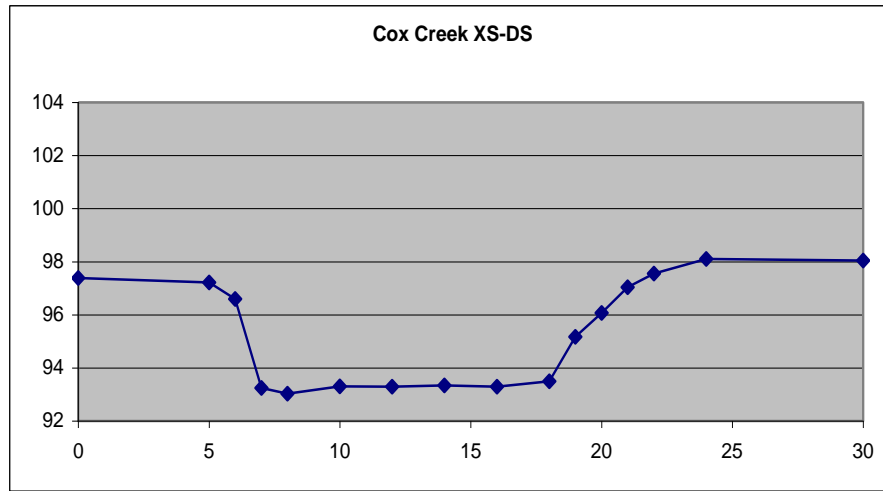


Figure 12: Cox Creek Cross Sections

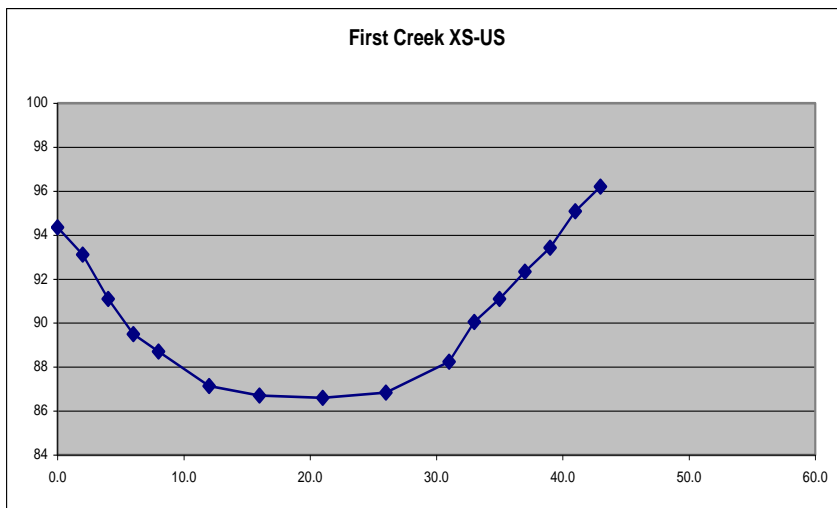
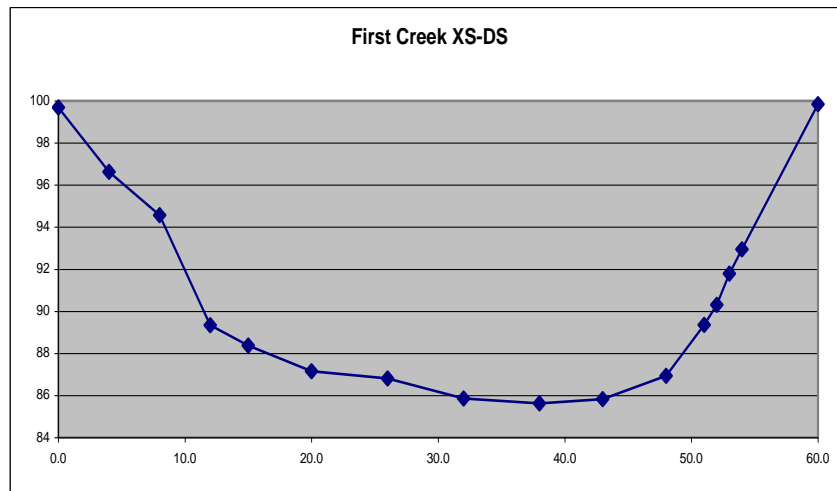


Figure 13: First Creek Cross Sections

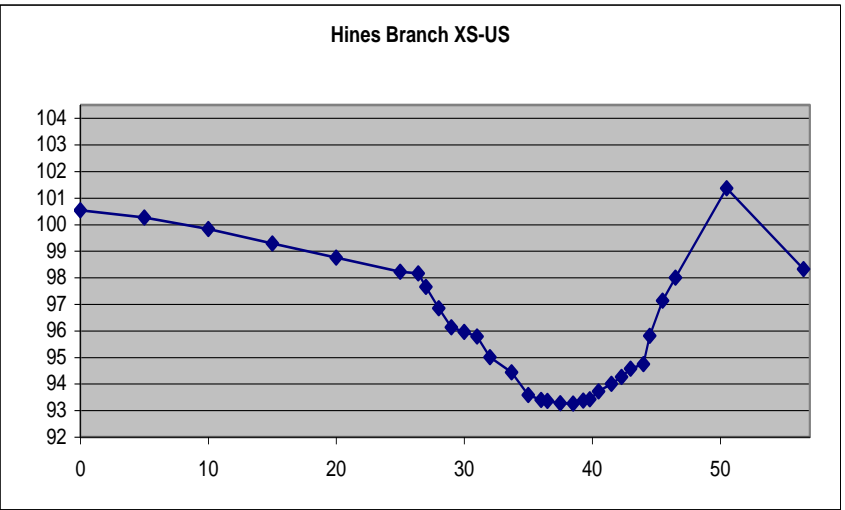
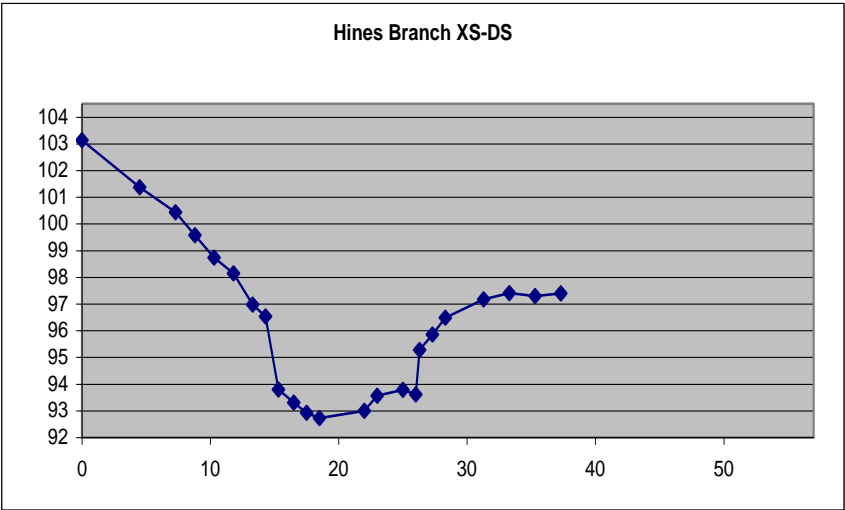


Figure 14: Hines Branch Cross Sections

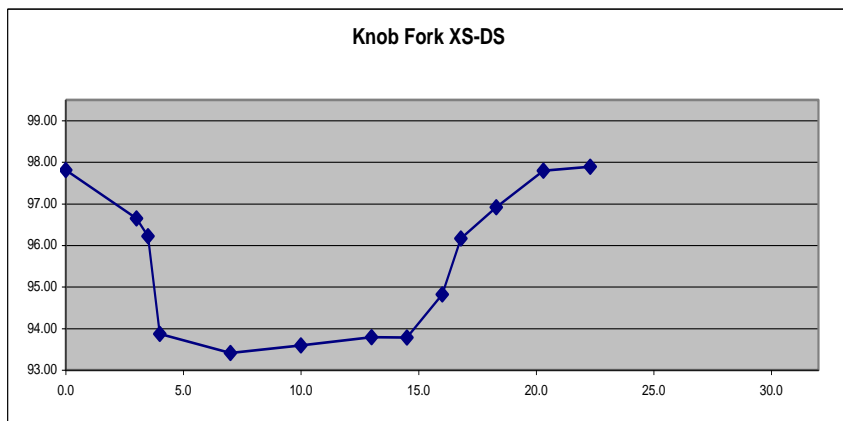
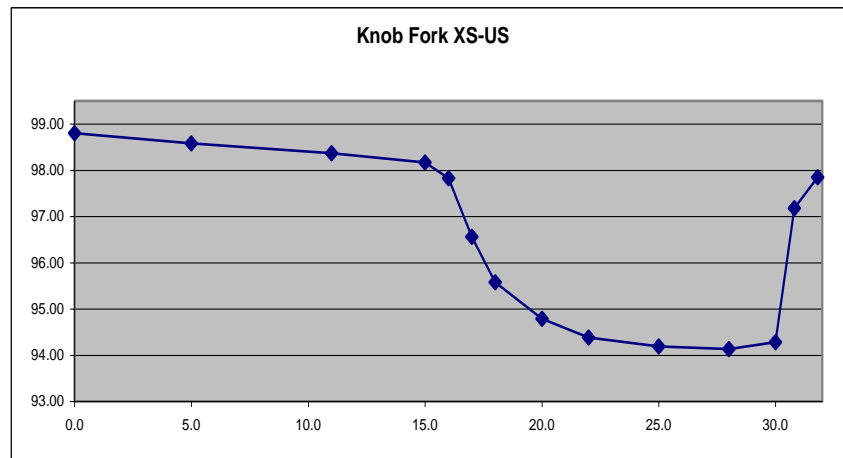


Figure 15: Knob Fork Cross Sections

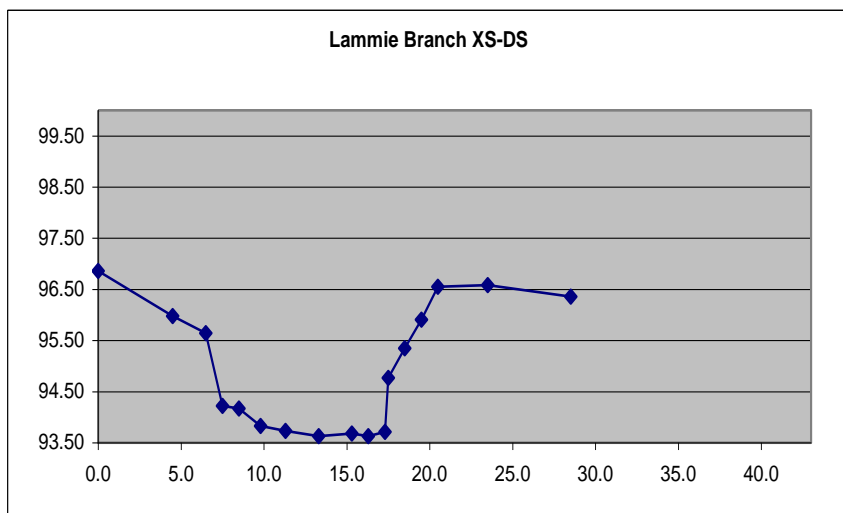
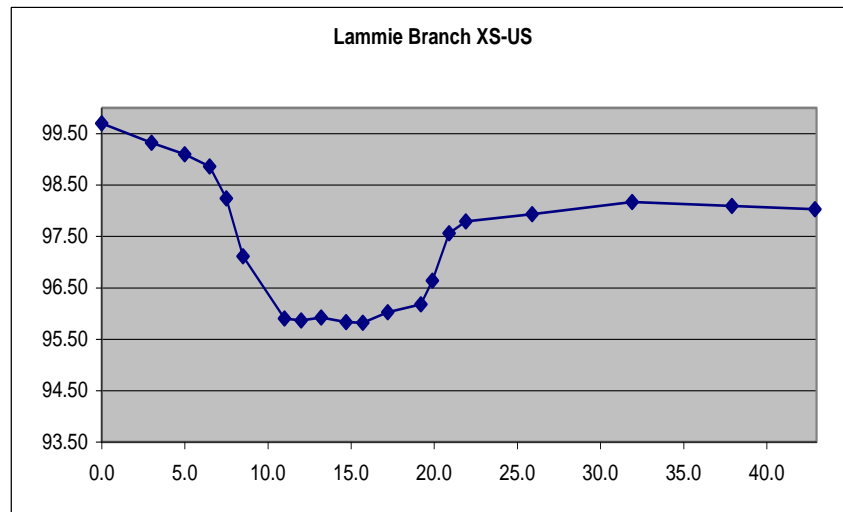


Figure 16: Lammie Branch Cross Sections

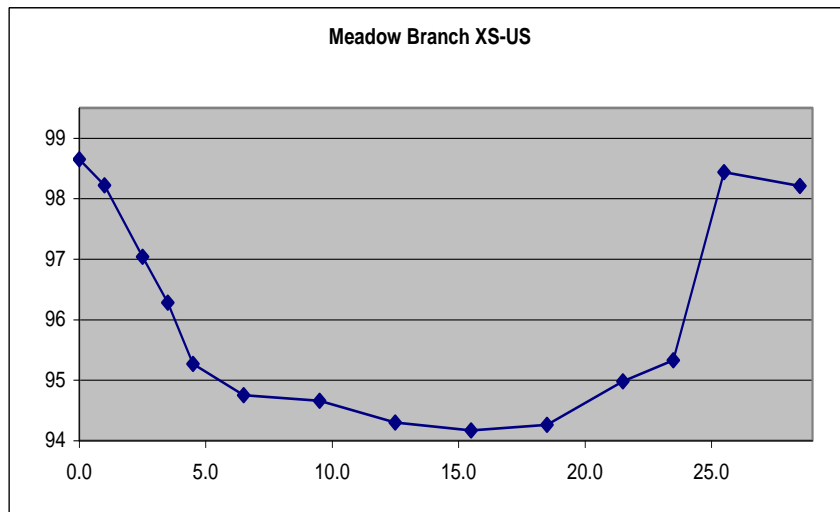
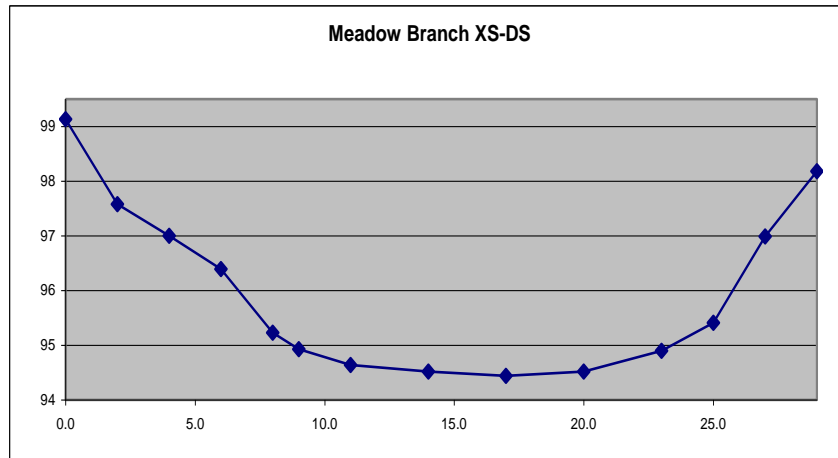


Figure 17: Meadow Branch Cross Sections

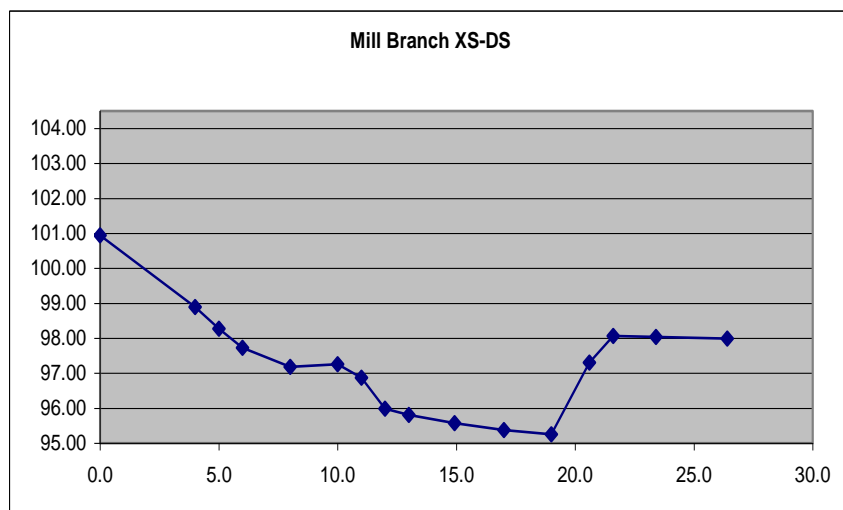
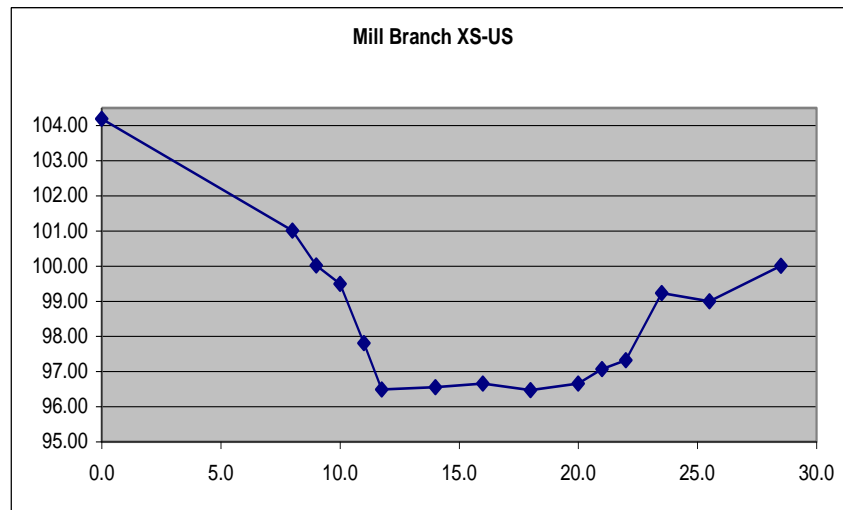


Figure 18: Mill Branch Cross Sections

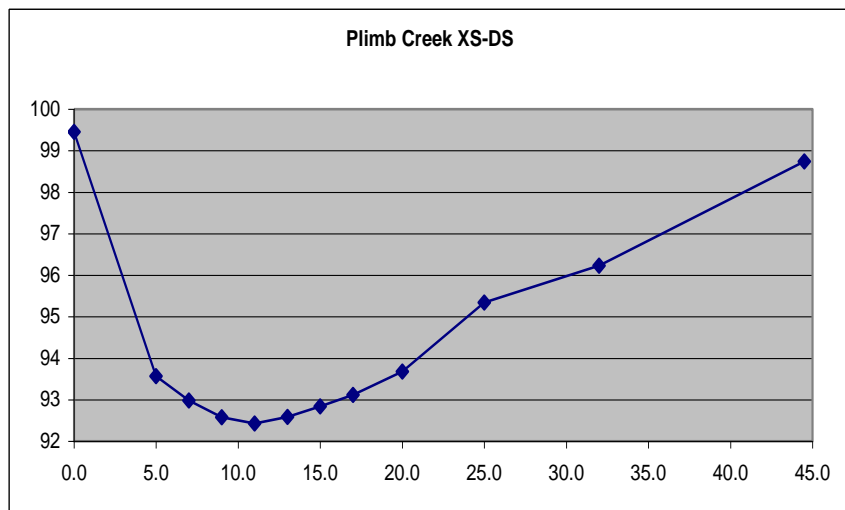
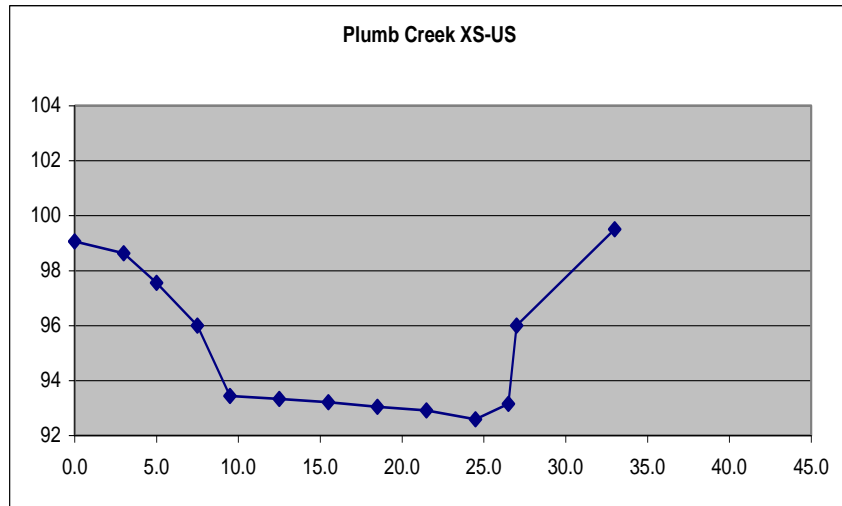


Figure 19: Plumb Creek Cross Sections

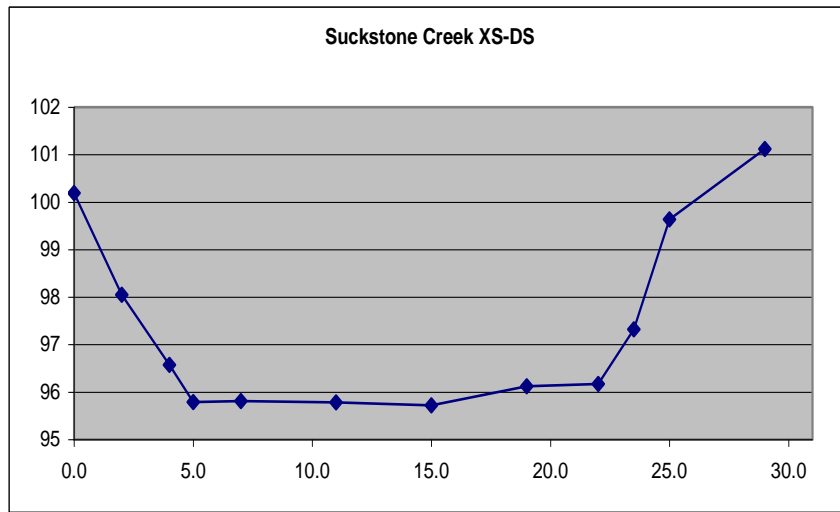
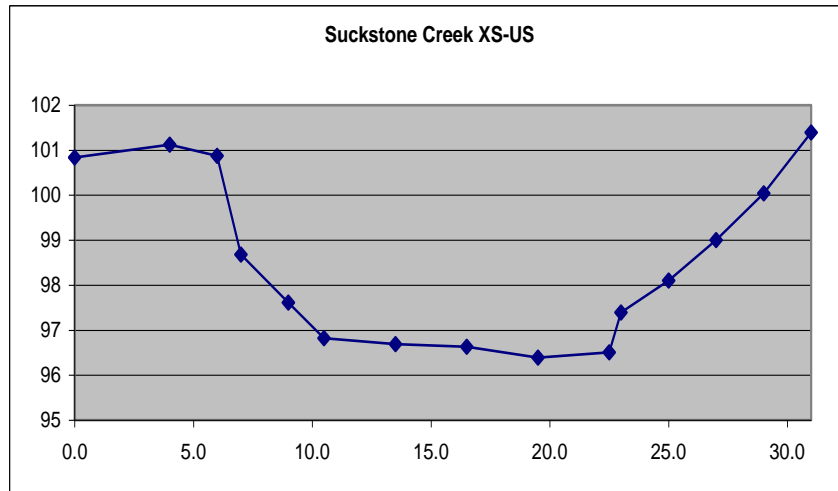


Figure 20: Suckstone Creek Cross Sections

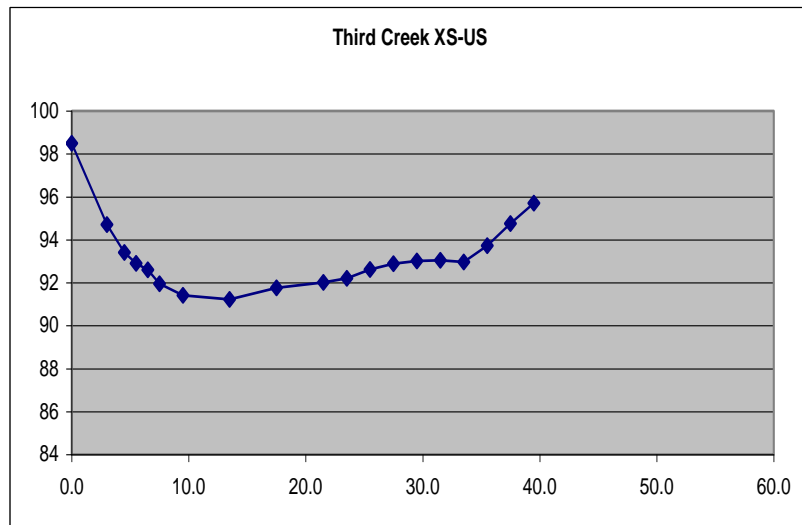
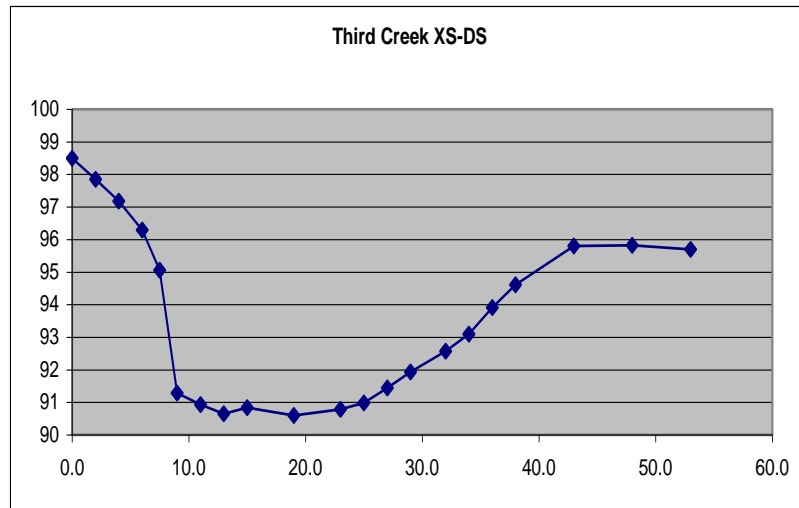


Figure 21: Third Creek Cross Sections

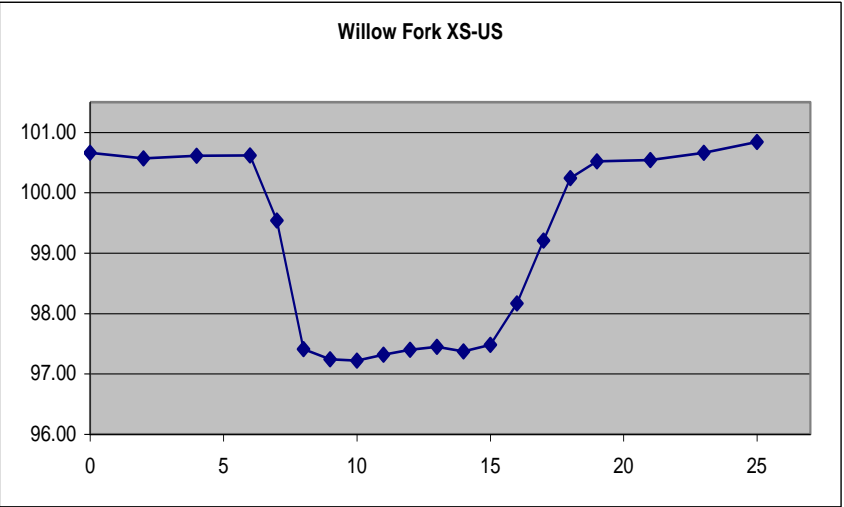
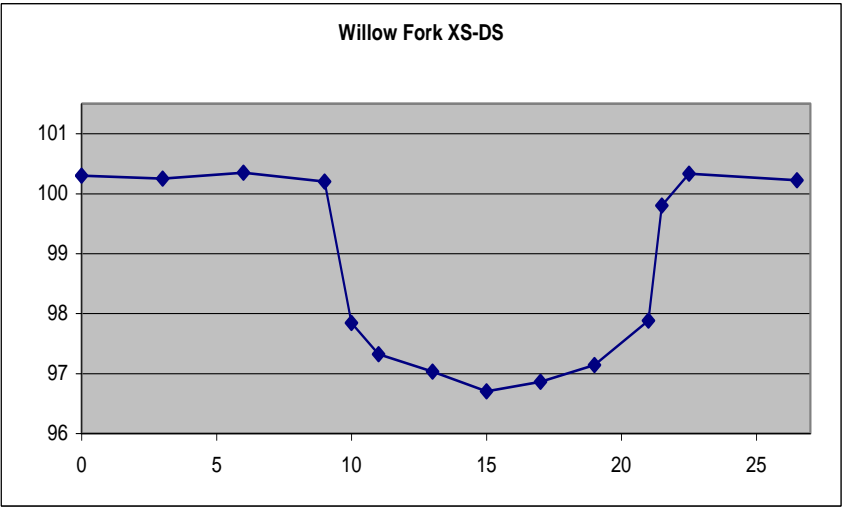


Figure 22: Willow Fork Cross Sections

Appendix C: Site Pebble Counts

Table 5: Beaver Creek Pebble Count

Pebble Count (mm)				
1	4	6	7	10
2	4	6	7	10
3	4	6	8	10
3	5	6	8	10
3	5	6	8	10
3	5	6	8	10
3	5	6	8	11
3	5	6	9	11
3	5	6	9	11
3	5	6	9	11
3	5	6	9	11
3	5	6	9	11
3	5	7	9	11
4	5	7	9	12
4	5	7	9	13
4	6	7	10	13
4	6	7	10	13
4	6	7	10	14
4	6	7	10	16
4	6	7	10	18

patchiness:	100%	$\tau_{\text{competence}}$
$d_{15} =$	4	0.058
$d_{35} =$	5	0.083
$d_{50} =$	6	0.103
$d_{85} =$	10	0.182
$d_{\text{max}} =$	18	0.328

Table 6: Cox Creek Pebble Count

Pebble Count (mm)				
3	12	17	27	46
3	12	17	27	48
3	13	19	27	57
4	13	19	28	62
5	13	19	29	64
6	14	20	30	66
6	14	21	31	69
6	14	21	31	73
7	14	21	31	73
7	14	22	33	73
8	15	22	34	81
8	15	23	35	87
9	16	23	37	87
9	16	23	38	92
9	16	23	39	94
10	16	24	41	97
10	17	26	41	98
10	17	26	41	109
11	17	27	44	121
11	17	27	45	122

patchiness:	95%	$\tau_{\text{competence}}$
$d_{15} =$	9	0.164
$d_{35} =$	16	0.292
$d_{50} =$	22	0.401
$d_{85} =$	64	1.167
$d_{\text{max}} =$	122	2.189

Table 7: First Creek Pebble Count

Pebble Count (mm)				
2	6	11	21	51
4	6	11	21	55
4	7	11	22	56
4	7	12	22	60
4	7	13	23	62
4	7	14	23	63
5	7	14	23	66
5	7	14	24	66
5	8	15	26	71
5	8	15	28	73
5	8	15	30	73
5	9	15	30	93
5	9	16	31	94
6	9	17	41	103
6	9	18	44	108
6	10	19	44	136
6	10	19	45	150
6	10	20	45	163
6	10	20	45	186
6	11	21	47	225

patchiness:	90%	$\tau_{\text{competence}}$
$d_{15} =$	6	0.103
$d_{35} =$	9	0.164
$d_{50} =$	15	0.274
$d_{85} =$	62	1.131
$d_{\text{max}} =$	225	2.189

Table 8: Hines Branch Pebble Count

Pebble Count (mm)				
3	11	18	26	38
4	11	19	27	38
5	11	19	27	39
6	12	19	27	41
7	12	20	27	42
7	12	20	28	42
7	12	21	28	43
7	13	21	28	43
8	13	21	29	44
8	14	21	29	49
8	14	23	33	50
9	14	23	34	61
9	15	23	34	66
9	16	23	34	68
9	16	24	35	69
9	16	24	36	72
10	17	26	37	82
10	17	26	38	99
10	17	26	38	132
11	18	26	38	143

patchiness:	95%	$\tau_{\text{competence}}$
$d_{15} =$	9	0.164169
$d_{35} =$	16	0.291855
$d_{50} =$	21	0.38306
$d_{85} =$	42	0.76612
$d_{\text{max}} =$	143	2.188913

Table 9: Knob Fork Pebble Count

Pebble Count (mm)				
1	5	15	21	28
1	5	15	22	28
2	6	15	22	29
2	6	17	22	30
2	6	17	22	32
2	6	17	23	34
2	7	18	23	35
2	7	18	24	35
3	8	18	24	37
3	8	18	24	38
3	9	19	24	39
3	9	19	24	39
3	10	19	25	41
4	10	19	25	45
4	11	19	26	54
4	12	19	26	55
5	13	20	27	57
5	13	21	27	94
5	14	21	27	182
5	14	21	28	195

patchiness:	80%	$\tau_{\text{competence}}$
$d_{15} =$	4	0.058
$d_{35} =$	11	0.201
$d_{50} =$	18	0.328
$d_{85} =$	32	0.584
$d_{\text{max}} =$	195	2.189

Table 10: Lammie Branch Pebble Count

Pebble Count (mm)				
2	9	17	25	44
2	10	18	27	44
4	11	18	28	45
5	11	19	29	45
6	11	19	30	46
6	11	20	30	47
6	12	20	31	48
6	12	21	32	49
7	12	21	32	51
7	12	21	33	56
7	13	22	33	56
7	14	22	34	57
8	14	23	34	60
8	14	23	35	61
8	14	23	37	61
8	15	23	40	75
8	15	23	42	81
9	16	24	42	88
9	16	24	43	92
9	17	25	43	303

patchiness:	85%	$\tau_{\text{competence}}$
$d_{15} =$	8	0.146
$d_{35} =$	14	0.255
$d_{50} =$	21	0.383
$d_{85} =$	46	0.839
$d_{\text{max}} =$	303	2.189

Table 11: Meadow Branch Pebble Count

Pebble Count (mm)				
3	8	13	18	26
3	8	13	18	26
4	9	13	18	27
5	9	14	19	27
5	9	14	19	27
5	9	16	20	28
5	9	16	20	28
6	10	16	20	30
6	10	16	21	31
6	10	16	22	33
6	10	17	22	34
6	11	17	22	34
6	11	17	22	35
7	11	18	22	36
7	11	18	22	36
7	11	18	23	40
7	11	18	24	46
8	11	18	25	47
8	12	18	25	51
8	12	18	26	72

patchiness:	85%	$\tau_{\text{competence}}$
$d_{15} =$	7	0.128
$d_{35} =$	11	0.201
$d_{50} =$	16	0.292
$d_{85} =$	27	0.493
$d_{\text{max}} =$	72	1.313

Table 12: Mill Branch Pebble Count

Pebble Count (mm)				
4	12	18	28	39
4	12	19	28	39
5	12	19	28	39
6	12	20	29	42
6	13	20	29	43
7	13	20	29	45
7	14	21	29	45
7	14	21	30	45
8	14	22	31	47
9	15	22	31	48
9	15	22	31	48
9	16	23	31	54
9	16	23	31	58
10	16	24	33	68
10	17	24	33	81
11	17	24	33	87
11	17	25	35	113
11	18	26	35	145
12	18	27	35	167
12	18	28	36	233

patchiness:	80%	$\tau_{\text{competence}}$
$d_{15} =$	10	0.182
$d_{35} =$	17	0.310
$d_{50} =$	22	0.401
$d_{85} =$	43	0.784
$d_{\text{max}} =$	233	2.189

Table 13: Plumb Creek Pebble Count

Pebble Count (mm)				
1	3	8	14	19
1	3	9	14	21
1	3	9	14	21
1	4	9	14	23
1	4	9	14	23
1	4	10	14	23
1	4	11	14	24
1	4	11	15	25
2	4	11	15	26
2	4	11	15	26
2	4	12	15	27
2	5	12	16	28
2	5	12	16	29
2	5	12	16	30
2	5	12	17	30
3	6	12	18	31
3	6	13	18	35
3	6	13	18	36
3	6	13	18	41
3	7	13	19	60

patchiness:	90%	$\tau_{\text{competence}}$
$d_{15} =$	2	0.024
$d_{35} =$	5	0.083
$d_{50} =$	11	0.201
$d_{85} =$	23	0.420
$d_{\text{max}} =$	60	1.094

Table 14: Suckstone Creek Pebble Count

Pebble Count (mm)				
2	11	23	36	72
3	12	24	38	72
3	12	25	38	75
4	14	25	39	78
6	14	25	43	81
6	14	26	49	84
6	15	26	49	86
6	15	26	51	89
7	16	26	51	93
7	16	27	55	95
7	17	28	55	97
8	18	28	56	118
8	19	28	56	123
8	19	28	57	126
8	20	32	65	159
9	20	32	67	169
10	20	33	68	173
10	21	35	68	176
11	23	35	70	220
11	23	36	71	293

patchiness:	80%	$\tau_{\text{competence}}$
$d_{15} =$	8	0.145928
$d_{35} =$	20	0.364819
$d_{50} =$	27	0.492506
$d_{85} =$	81	1.477517
$d_{\text{max}} =$	293	2.188913

Table 15: Third Creek Pebble Count

Pebble Count (mm)				
4	7	9	12	17
4	7	9	12	18
4	7	9	12	18
4	7	9	13	19
4	7	9	14	19
5	7	10	14	20
5	7	10	14	20
5	7	10	14	20
5	8	10	14	20
5	8	11	14	20
5	8	11	15	22
6	8	11	15	22
6	8	11	15	23
6	8	11	16	24
6	8	11	16	25
6	8	12	16	27
6	8	12	16	29
6	8	12	16	36
6	9	12	17	123
7	9	12	17	163

patchiness:	90%	$\tau_{\text{competence}}$
$d_{15} =$	6	0.103
$d_{35} =$	8	0.146
$d_{50} =$	11	0.201
$d_{85} =$	19	0.347
$d_{\text{max}} =$	163	2.189

Table 16: Willow Fork Pebble Count

Pebble Count (mm)				
2	6	10	14	18
2	6	10	14	18
3	7	10	14	19
3	7	10	14	19
3	7	11	14	19
3	7	11	14	19
4	7	11	14	21
4	7	11	14	22
4	7	11	14	22
4	7	11	15	22
4	8	12	15	22
4	8	12	15	23
5	8	12	16	23
5	9	12	16	25
5	9	12	16	26
5	9	12	17	27
5	9	13	17	28
5	9	13	17	35
6	9	13	18	39
6	9	14	18	44

patchiness:	100%	$\tau_{\text{competence}}$
$d_{15} =$	5	0.083
$d_{35} =$	9	0.164
$d_{50} =$	11	0.201
$d_{85} =$	19	0.347
$d_{\text{max}} =$	44	0.803

Appendix D: Bed-load Sample P.S.D.'s

Table 17: Maximum Sampled Particle Size Summary

Site Location	Storm Date	d _{max} (mm)
3rd Creek	11/14/2008	39
3rd Creek	12/10/2008	22
Beaver Creek	12/10/2008	18
Willow Fork	12/10/2008	17
Cox Creek	12/10/2008	34
3rd Creek	1/7/2009	47
Beaver Creek	1/7/2009	10
Willow Fork	1/7/2009	34
Lammie Branch	1/7/2009	37
Cox Creek	1/7/2009	27
Hines Branch	1/7/2009	37
Cox Creek	1/28/2009	42
Hines Branch	1/28/2009	22
Meadow Branch	3/28/2009	24
Cox Creek	3/28/2009	25
Mill Branch	3/28/2009	42
Suckstone Creek	3/28/2009	36
Knob Fork	3/28/2009	44

Table 18: 3rd Creek Sample 11/14/2008

Sample Location 3rd Creek
 Storm Date 11/14/2008
 Total Sample Mass 1896.6

ASTM Sieve #	Sieve Opening (mm)	Sieve Mass (g)	Sieve and Soil Mass (g)	Mass Retained (g)	Percent Retained	Cumm. % Retained	Percent Passing
4	4.75	526.4	684.2	157.8	8.320152	8.320152	91.67985
10	2	561.8	704.9	143.1	7.545081	15.86523	84.13477
16	1.18	428.3	628.6	200.3	10.561	26.42624	73.57376
20	0.85	413.2	790.3	377.1	19.88295	46.30918	53.69082
30	0.6	577.8	1047.7	469.9	24.77591	71.0851	28.9149
40	0.425	575.3	890.3	315	16.60867	87.69377	12.30623
50	0.3	448.9	570.7	121.8	6.422018	94.11579	5.884214
100	0.15	341.8	413.2	71.4	3.764631	97.88042	2.119582
200	0.075	334.1	357.1	23	1.212696	99.09311	0.906886
pan		412.7	429.9	17.2	0.906886	100	0

Σ

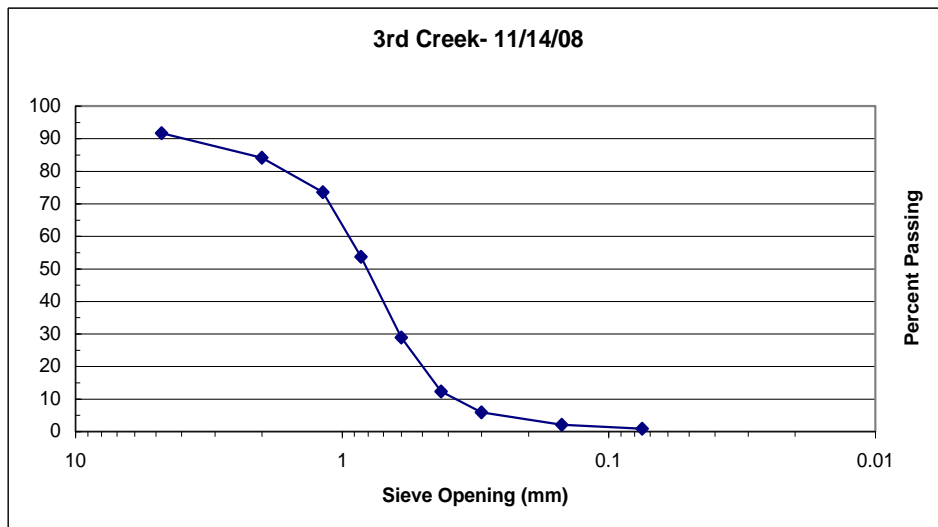


Table 19: 3rd Creek Sample 12/10/2008

Sample Location 3rd Creek
 Storm Date 12/10/2008
 Total Sample Mass 1055.9

ASTM Sieve #	Sieve Opening (mm)	Sieve Mass (g)	Sieve and Soil Mass (g)	Mass Retained (g)	Percent Retained	Cumm. % Retained	Percent Passing
4	4.75	526.4	587.9	61.5	5.824415	5.824415	94.17558
10	2	561.8	668	106.2	10.05777	15.88219	84.11781
16	1.18	428.3	544	115.7	10.95748	26.83966	73.16034
20	0.85	413.2	520.5	107.3	10.16195	37.00161	62.99839
30	0.6	578	703.9	125.9	11.92348	48.92509	51.07491
40	0.425	575.3	722.4	147.1	13.93124	62.85633	37.14367
50	0.3	448.8	573	124.2	11.76248	74.61881	25.38119
100	0.15	341.5	519.1	177.6	16.81977	91.43858	8.561417
200	0.075	334	393.7	59.7	5.653945	97.09253	2.907472
pan		412.7	443.4	30.7	2.907472	100	0

Σ

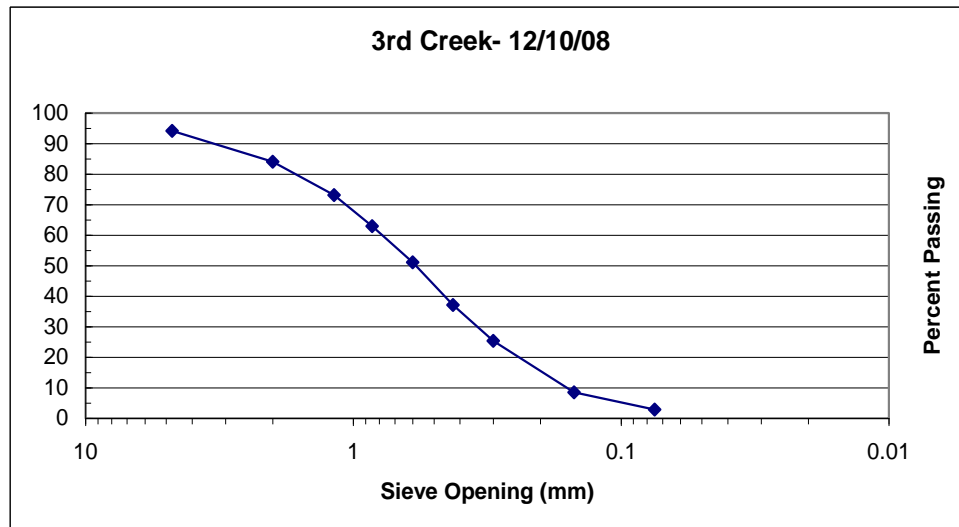


Table 20: 3rd Creek Sample 1/7/2009

Sample Location 3rd Creek
Storm Date 1/7/2009
Trap Type wrc
Total Sample Mass 2017.1

ASTM Sieve #	Sieve Opening (mm)	Sieve Mass (g)	Sieve and Soil Mass (g)	Mass Retained (g)	Percent Retained	Cumm. % Retained	Percent Passing
3/8"	9.75	813.8	888.9	75.1	3.723167	3.723167	96.27683
4	4.75	526.2	649.8	123.6	6.127609	9.850776	90.14922
10	2	561.8	694.4	132.6	6.573794	16.42457	83.57543
16	1.18	428.4	507.1	78.7	3.901641	20.32621	79.67379
20	0.85	413.8	577.4	163.6	8.110654	28.43686	71.56314
30	0.6	577.9	837.1	259.2	12.85013	41.287	58.713
40	0.425	575.4	1015	439.6	21.79366	63.08066	36.91934
50	0.3	448.9	708.3	259.4	12.86005	75.94071	24.05929
100	0.15	341.6	695.8	354.2	17.55986	93.50057	6.49943
200	0.075	334	422.7	88.7	4.397402	97.89797	2.102028
pan		412.6	455	42.4	2.102028	100	0

Σ

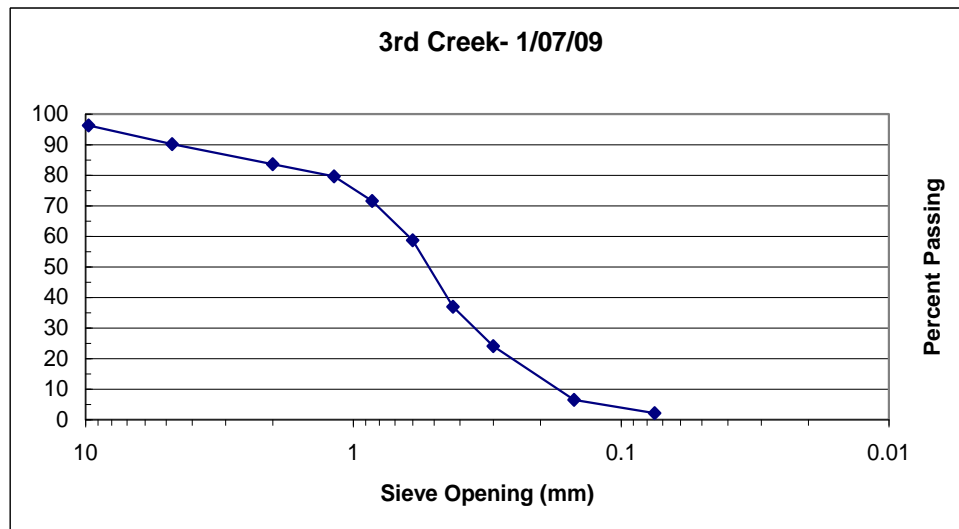


Table 21: Beaver Creek Sample 12/10/2009

Sample Location Beaver Creek
Storm Date 12/10/2008
Trap Type dhj
Total Sample Mass 1611.3

ASTM Sieve #	Sieve Opening (mm)	Sieve Mass (g)	Sieve and Soil Mass (g)	Mass Retained (g)	Percent Retained	Cumm. % Retained	Percent Passing
3/8"	9.75	813.7	813.7	0	0	0	100
4	4.75	526.1	532.2	6.1	0.378576	0.378576	99.62142
10	2	562.1	637.3	75.2	4.667039	5.045615	94.95438
16	1.18	428.3	559	130.7	8.111463	13.15708	86.84292
20	0.85	413.1	692.1	279	17.31521	30.47229	69.52771
30	0.6	577.4	871.2	293.8	18.23372	48.70601	51.29399
40	0.425	575.1	783.5	208.4	12.93366	61.63967	38.36033
50	0.3	448.7	594.4	145.7	9.042388	70.68206	29.31794
100	0.15	341.5	557.1	215.6	13.3805	84.06256	15.93744
200	0.075	333.9	495.1	161.2	10.00434	94.0669	5.933097
pan		412.5	508.1	95.6	5.933097	100	0
Σ							

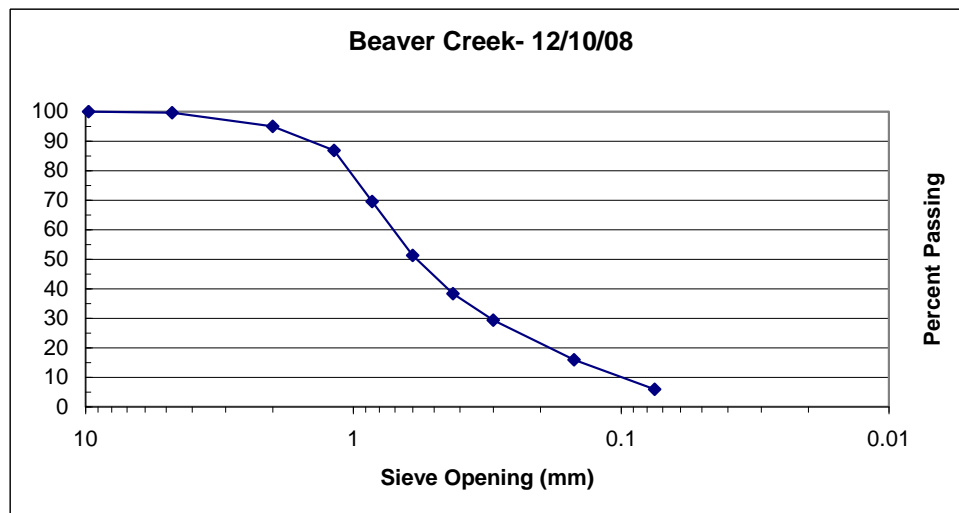


Table 22: Beaver Creek Sample 1/7/2009

Sample Location Beaver Creek
Storm Date 1/7/2009
Trap Type wrc
Total Sample Mass 1580.8

ASTM Sieve #	Sieve Opening (mm)	Sieve Mass (g)	Sieve and Soil Mass (g)	Mass Retained (g)	Percent Retained	Cumm. % Retained	Percent Passing
4	4.75	526.1	535	8.9	0.563006	0.563006	99.43699
10	2	562	597.1	35.1	2.220395	2.783401	97.2166
16	1.18	428.6	507.7	79.1	5.003796	7.787196	92.2128
20	0.85	413.4	863.3	449.9	28.46027	36.24747	63.75253
30	0.6	577.6	941.6	364	23.02632	59.27379	40.72621
40	0.425	575.7	755.2	179.5	11.35501	70.6288	29.3712
50	0.3	448.8	561.2	112.4	7.110324	77.73912	22.26088
100	0.15	341.6	509.1	167.5	10.5959	88.33502	11.66498
200	0.075	334	452.9	118.9	7.521508	95.85653	4.143472
pan		412.6	478.1	65.5	4.143472	100	0

Σ

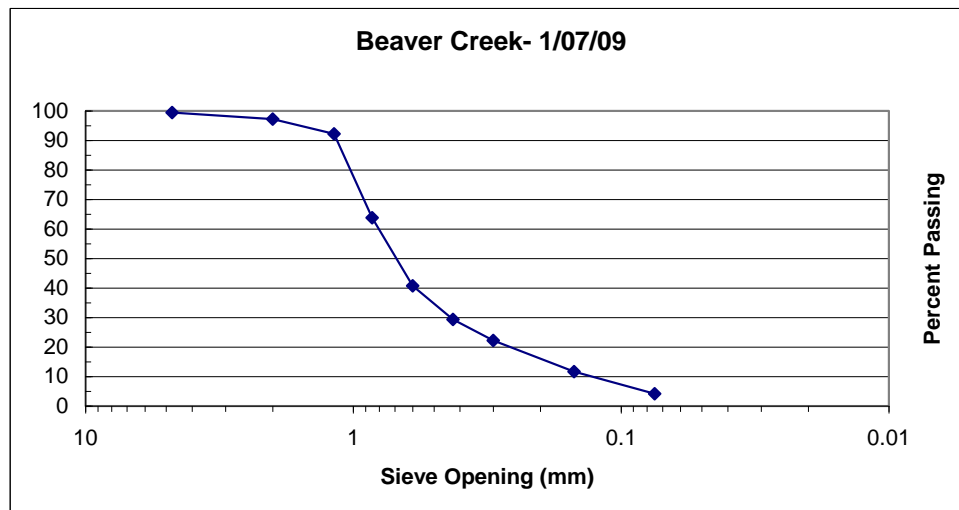


Table 23: Willow Fork Sample 12/10/2008

Sample Location Willow Fork
 Storm Date 12/10/2008
 Trap Type dhj
 Total Sample Mass 575.4

ASTM Sieve #	Sieve Opening (mm)	Sieve Mass (g)	Sieve and Soil Mass (g)	Mass Retained (g)	Percent Retained	Cumm. % Retained	Percent Passing
4	4.75	526.4	554.7	28.3	4.918318	4.918318	95.08168
10	2	561.9	604	42.1	7.316649	12.23497	87.76503
16	1.18	428.6	472.1	43.5	7.559958	19.79493	80.20507
20	0.85	413.3	452.1	38.8	6.743135	26.53806	73.46194
30	0.6	578	631.4	53.4	9.280501	35.81856	64.18144
40	0.425	575.3	650.6	75.3	13.08655	48.90511	51.09489
50	0.3	492.2	580.8	88.6	15.39798	64.30309	35.69691
100	0.15	341.4	500.4	159	27.63295	91.93604	8.063956
200	0.075	334	366.2	32.2	5.596107	97.53215	2.467848
pan		412.7	426.9	14.2	2.467848	100	0

Σ

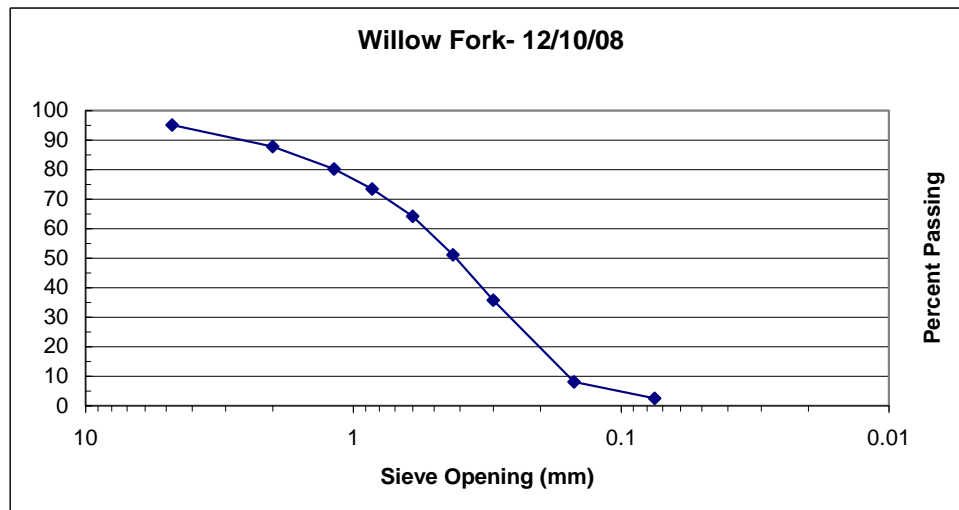


Table 24: Willow Fork Sample 1/7/2009

Sample Location Willow Fork
Storm Date 1/7/2009
Trap Type wrc
Total Sample Mass 3291

ASTM Sieve #	Sieve Opening (mm)	Sieve Mass (g)	Sieve and Soil Mass (g)	Mass Retained (g)	Percent Retained	Cumm. % Retained	Percent Passing
3/8"	9.75	813.7	887.5	73.8	2.242479	2.242479	97.75752
4	4.75	526.3	595.3	69	2.096627	4.339107	95.66089
10	2	562	647.2	85.2	2.588879	6.927985	93.07201
16	1.18	428.3	498.1	69.8	2.120936	9.048921	90.95108
20	0.85	413.6	652.3	238.7	7.253115	16.30204	83.69796
30	0.6	577.7	899.9	322.2	9.790337	26.09237	73.90763
40	0.425	575.2	1368.7	793.5	24.11121	50.20359	49.79641
50	0.3	448.8	1287.2	838.4	25.47554	75.67912	24.32088
100	0.15	341.5	972	630.5	19.15831	94.83744	5.162565
200	0.075	334	447.1	113.1	3.436645	98.27408	1.725919
pan		412.6	469.4	56.8	1.725919	100	0
Σ							

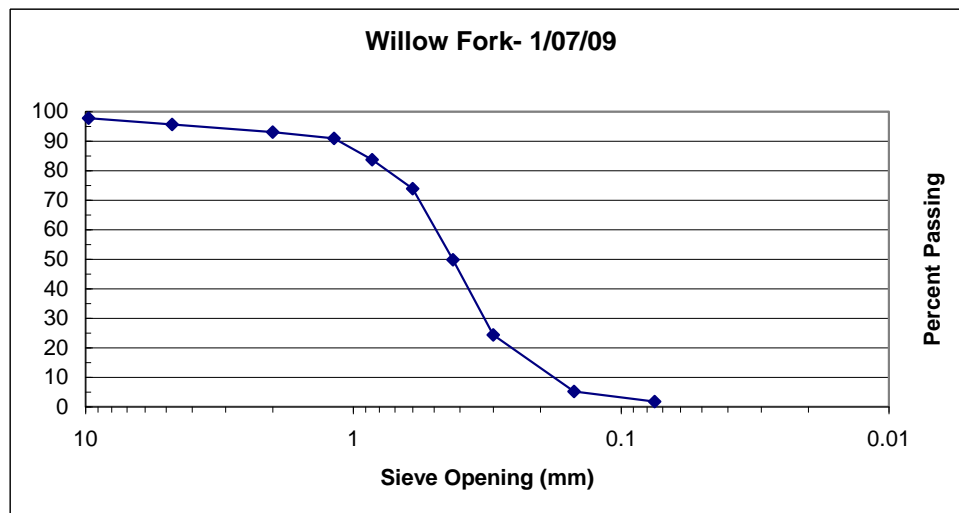


Table 25: Lammie Branch Sample 1/7/2009

Sample Location Lammie Branch
Storm Date 1/7/2009
Trap Type wrc
Total Sample Mass 294.5

ASTM Sieve #	Sieve Opening (mm)	Sieve Mass (g)	Sieve and Soil Mass (g)	Mass Retained (g)	Percent Retained	Cumm. % Retained	Percent Passing
3/8"	9.75	813.7	880.2	66.5	22.58065	22.58065	77.41935
4	4.75	526.4	563.4	37	12.56367	35.14431	64.85569
10	2	562.3	583	20.7	7.028862	42.17317	57.82683
16	1.18	428.9	441.9	13	4.414261	46.58744	53.41256
20	0.85	414	418.6	4.6	1.561969	48.14941	51.85059
30	0.6	579	585.9	6.9	2.342954	50.49236	49.50764
40	0.425	576.2	590.5	14.3	4.855688	55.34805	44.65195
50	0.3	449.7	474	24.3	8.251273	63.59932	36.40068
100	0.15	342.3	402.5	60.2	20.44143	84.04075	15.95925
200	0.075	334.5	357.4	22.9	7.775891	91.81664	8.183362
pan		413	437.1	24.1	8.183362	100	0

Σ

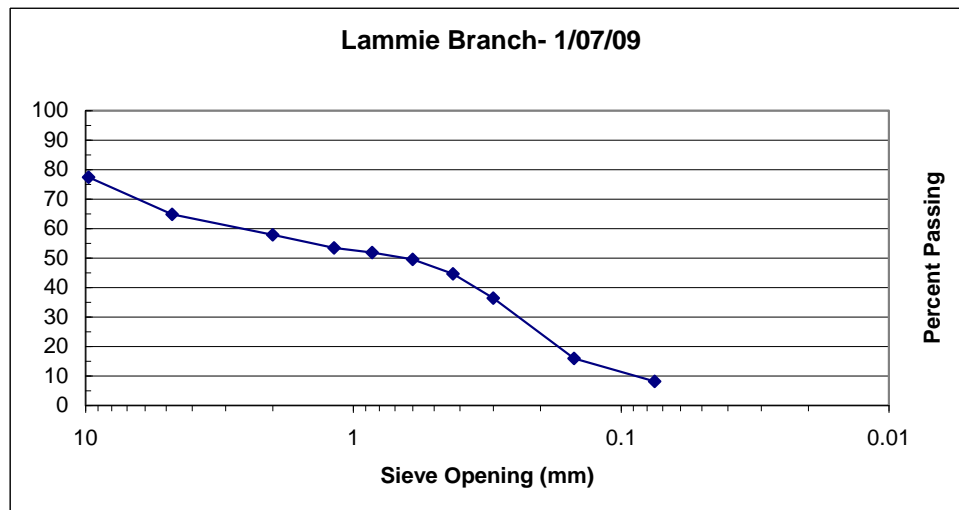


Table 26: Cox Creek Sample 12/10/2008

Sample Location Cox Creek
Storm Date 12/10/2008
Trap Type dhj
Total Sample Mass 146.2

ASTM Sieve #	Sieve Opening (mm)	Sieve Mass (g)	Sieve and Soil Mass (g)	Mass Retained (g)	Percent Retained	Cumm. % Retained	Percent Passing
3/8"	9.75	813.6	885.4	71.8	49.11081	49.11081	50.88919
4	4.75	526	542.8	16.8	11.49111	60.60192	39.39808
10	2	562	576.7	14.7	10.05472	70.65663	29.34337
16	1.18	428.3	444.4	16.1	11.01231	81.66895	18.33105
20	0.85	413.4	418.1	4.7	3.214774	84.88372	15.11628
30	0.6	577.6	580.7	3.1	2.120383	87.0041	12.9959
40	0.425	575.3	577.8	2.5	1.709986	88.71409	11.28591
50	0.3	448.8	451.2	2.4	1.641587	90.35568	9.644323
100	0.15	341.4	346.6	5.2	3.556772	93.91245	6.087551
200	0.075	334	337.8	3.8	2.599179	96.51163	3.488372
pan		412.5	417.6	5.1	3.488372	100	0

Σ

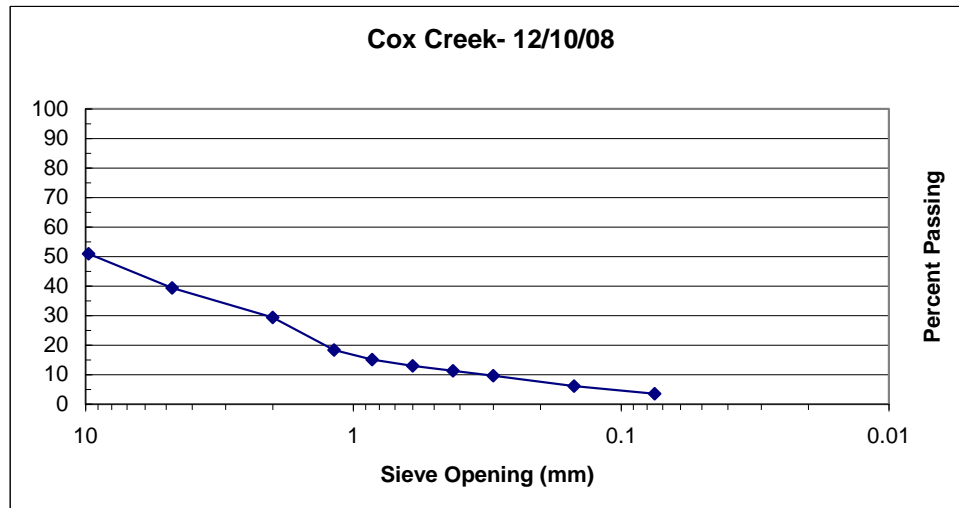


Table 27: Cox Creek Sample 1/7/2009

Sample Location Cox Creek
Storm Date 1/7/2009
Trap Type wrc
Total Sample Mass 804.8

ASTM Sieve #	Sieve Opening (mm)	Sieve Mass (g)	Sieve and Soil Mass (g)	Mass Retained (g)	Percent Retained	Cumm. % Retained	Percent Passing
4	4.75	526.9	586.4	59.5	7.393141	7.393141	92.60686
10	2	562.3	595.2	32.9	4.087972	11.48111	88.51889
16	1.18	429	477.3	48.3	6.001491	17.4826	82.5174
20	0.85	414.3	526.2	111.9	13.90408	31.38668	68.61332
30	0.6	579.4	683.6	104.2	12.94732	44.334	55.666
40	0.425	576	661.5	85.5	10.62376	54.95775	45.04225
50	0.3	449.5	515.1	65.6	8.151093	63.10885	36.89115
100	0.15	341.9	468.6	126.7	15.74304	78.85189	21.14811
200	0.075	334.4	445.5	111.1	13.80467	92.65656	7.343439
pan		412.7	471.8	59.1	7.343439	100	0

Σ

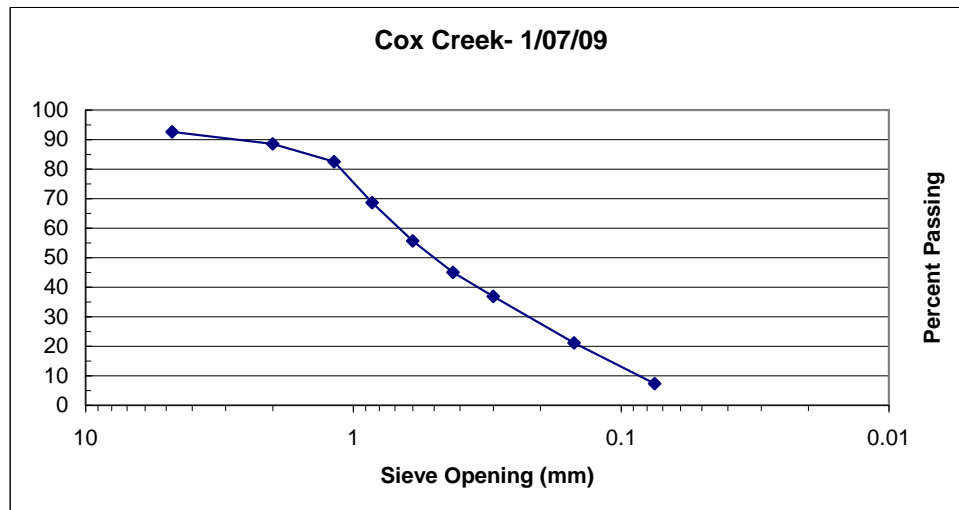


Table 28: Cox Creek Sample 1/28/2009

Sample Location Cox Creek
Storm Date 1/28/2009
Trap Type wrc
Total Sample Mass 6136.5

ASTM Sieve #	Sieve Opening (mm)	Sieve Mass (g)	Sieve and Soil Mass (g)	Mass Retained (g)	Percent Retained	Cumm. % Retained	Percent Passing
3/8"	9.75	1627	2245.3	618.3	10.07578	10.07578	89.92422
4	4.75	1051.8	2293.6	1241.8	20.23629	30.31207	69.68793
10	2	1124	2442.1	1318.1	21.47967	51.79174	48.20826
16	1.18	833.8	1589.6	755.8	12.31647	64.10821	35.89179
20	0.85	851.8	1057.9	206.1	3.358592	67.4668	32.5332
30	0.6	1154	1344.5	190.5	3.104375	70.57117	29.42883
40	0.425	769.4	947.1	177.7	2.895788	73.46696	26.53304
50	0.3	902	1043.3	141.3	2.302615	75.76958	24.23042
100	0.15	705.2	1316.8	611.6	9.966593	85.73617	14.26383
200	0.075	667	1039.1	372.1	6.063717	91.79989	8.200114
pan		759	1262.2	503.2	8.200114	100	0

Σ

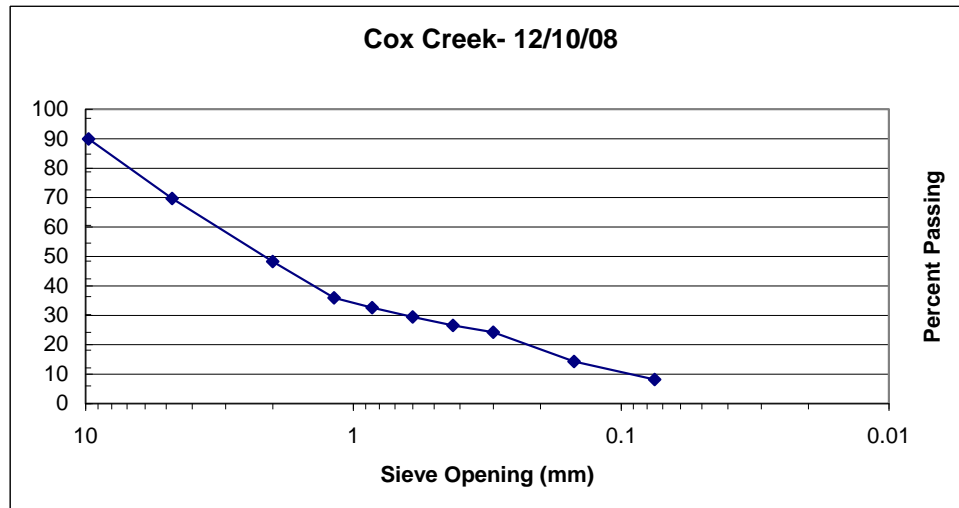


Table 29: Hines Branch Sample 1/7/2009

Sample Location Hines Branch
Storm Date 1/7/2009
Trap Type wrc
Total Sample Mass 1317.2

ASTM Sieve #	Sieve Opening (mm)	Sieve Mass (g)	Sieve and Soil Mass (g)	Mass Retained (g)	Percent Retained	Cumm. % Retained	Percent Passing
3/8"	9.75	813.6	906.3	92.7	7.037656	7.037656	92.96234
4	4.75	526.1	555.2	29.1	2.209232	9.246887	90.75311
10	2	562	601.5	39.5	2.998785	12.24567	87.75433
16	1.18	428.3	495.1	66.8	5.071363	17.31704	82.68296
20	0.85	413.4	497.7	84.3	6.399939	23.71698	76.28302
30	0.6	577.6	683.7	106.1	8.054965	31.77194	68.22806
40	0.425	575.4	712.5	137.1	10.40844	42.18038	57.81962
50	0.3	449	562.5	113.5	8.616763	50.79715	49.20285
100	0.15	341.7	566.9	225.2	17.09687	67.89402	32.10598
200	0.075	334.1	602.5	268.4	20.37656	88.27057	11.72943
pan		412.6	567.1	154.5	11.72943	100	0
Σ							

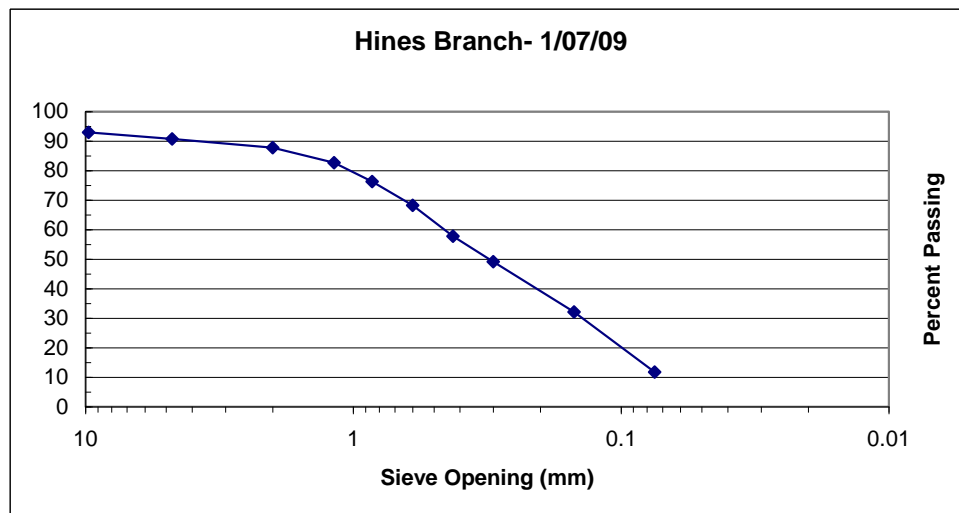
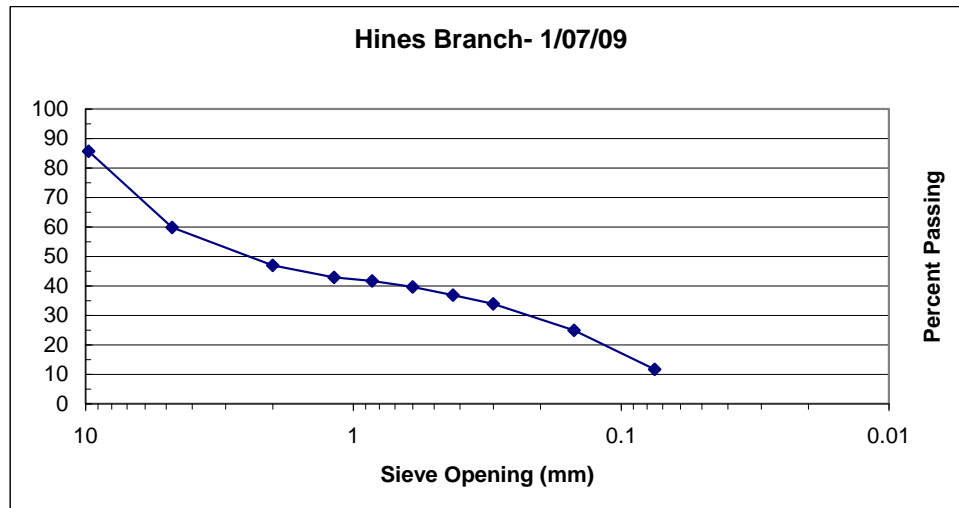


Table 30: Hines Branch Sample 1/28/2009

Sample Location Hines Branch
Storm Date 1/28/2009
Trap Type wrc
Total Sample Mass 240.7

ASTM Sieve #	Sieve Opening (mm)	Sieve Mass (g)	Sieve and Soil Mass (g)	Mass Retained (g)	Percent Retained	Cumm. % Retained	Percent Passing
3/8"	9.75	813.5	848	34.5	14.33319	14.33319	85.66681
4	4.75	525.9	588.2	62.3	25.88284	40.21604	59.78396
10	2	562	592.8	30.8	12.79601	53.01205	46.98795
16	1.18	416.9	426.9	10	4.154549	57.1666	42.8334
20	0.85	425.9	428.7	2.8	1.163274	58.32987	41.67013
30	0.6	577	582	5	2.077275	60.40715	39.59285
40	0.425	384.7	391.4	6.7	2.783548	63.19069	36.80931
50	0.3	451	458	7	2.908184	66.09888	33.90112
100	0.15	352.6	374.2	21.6	8.973826	75.0727	24.9273
200	0.075	333.5	365.4	31.9	13.25301	88.32572	11.67428
pan		379.5	407.6	28.1	11.67428	100	0

Σ



Appendix E: Crest Stage Gage and Bed-load Trap Construction/Performance

Crest-Stage Gage Construction

In preparing to gather data, USGS Type A and C Crest-Stage Gages were investigated. The simplicity in measuring the crest stage on the staff was an advantage; however the complexity of constructing these gages led to the design of a simpler device operating with similar principles. Instead of a galvanized steel or polyvinyl chloride (PVC) pipe housing a staff to which granulated cork adheres a clear, hard, impact resistant plastic pipe was used. The granulated cork adhered to the inside of the pipe in a similar manner as it did to the staff in the USGS gage and could be marked and surveyed to the cross section benchmark following the flow events. The pipe used was 1 inch inner diameter with a wall thickness of 1/8 inch. A screen was attached with worm screw type clamps to the bottom to hold the granulated cork if the stage fell below the bottom of the pipe. A tight fitting, removable plastic cap was fitted to the top to ensure that rain did not wash the granulated cork from the peak stage mark. Finally, a small vent hole was drilled just below the cap. Twenty four of these recorders were assembled and installed during the course of the data collection. A new crest stage can be seen in the following figure. This is represented by the ring of granulated cork near the top of the photograph. A previous peak stage is also marked in the photograph.



Figure 23: New Peak Stage (top of photo) on Peak Stage Gage

Portable Bed-Load Trap Construction

With the number of research sites and samples required in the course of this research, a bed-load sampling method that did not require personnel on site through the sampling event was required. With bedrock at shallow depths at some sites, portable bed-load traps after Bunte (2004) were chosen over pit-traps similar to Wilcock (2001). The general concept of the portable bed-load traps is a frame that can be affixed to the bed with a net trailing downstream to capture material moving along the bed. The traps were constructed in the Civil and Environmental Machine Shop at the University of Tennessee Knoxville. The frame was constructed of 5/16" by 3 1/2" aluminum bar stock and the screen retaining bars were 1/8" by 1" aluminum bar stock. The netting was a nylon type with .05" square openings and was reinforced with a more coarse and substantial outer net. After the materials were cut to length, holes were drilled and tapped where appropriate on a vertical end mill. Frames were assembled using gas tungsten arc welding (GTAW) and netting was attached with the screen retaining bars. Nine bed-load traps were constructed for this project. An assembled bed-load trap can be seen in Figure 2 in the body of the text.

Portable Bed-load Trap Performance

Since the portable bed-load trap design that was used as a basis for the design of traps used in this project was developed for use in high gradient, gravel and cobble bed streams in the West, performance of the traps in lower gradient, sand and gravel bed streams in the predominantly deciduous East was of interest. Trap installation is easily accomplished, being attached to the bed with #8 rebar with a 3/4" washer welded to the end. The traps were able to sample through the duration of the runoff events, with the nets being four feet long with a circumference of 30". During the Fall, when large amounts of leaf litter were present in the streams, processing of the samples was very time intensive. Methods for removing organic matter from the sediment samples discussed in section 2.2.3, ranged from 2.5 to 5 hours per sample when organic matter was present. In the late winter samples, when much of the leaf litter had dissipated, sample processing time dropped dramatically. A further effect of the leaf litter was a corresponding increase in percent fine material present in samples with high levels of organics. Further study of the interaction between saturated organics and fine bed-load transport may be of interest in the future. Information gathered in this study was insufficient to determine if there were physical processes on the bed leading to the increase of fines in the samples, or if the leaf litter merely provided a source of storage for the fines in the bed-load traps.

Appendix F: GIS Procedures and Site Watershed Maps

GIS Procedures

The following section outlines the procedures followed to compile watershed characteristics for the watershed above each research site. Table 1 in the body of the text shows the data sources used in this process. All terms used are appropriate for ESRI's ArcMAP software, version 9.3 and commands are referenced as they would be found through the Arc Toolbox interface.

Watershed Delineation:

- Load the National Elevation Dataset digital elevation model (DEM), National Landcover Database Impervious layer, and the National Atlas roads.
- Fill depressions in the DEM with Spatial Analyst Tools → Hydrology → Fill
- Produce flow direction raster from DEM using Spatial Analyst Tools → Hydrology → Flow Direction
- Produce flow accumulation raster from flow direction raster using Spatial Analyst Tools → Hydrology → Flow Accumulation
- Delineate watersheds using site location points and flow accumulation raster with Spatial Analyst Tools → Hydrology → Watershed
- Convert watershed rasters to shapefiles for ease of manipulation of watershed scale data using Conversion Tools → From Raster → Raster to Polygon

Determination of Impervious Area:

The following processes were performed for each watershed.

- Reduce Impervious raster to only what is included in watershed using watershed polygon and impervious raster with Analysis Tools → Extract → Clip

- Export value and count data from watershed impervious raster. These represent, respectively, percentages from 0 to 100 impervious and the number of cells for each percentage.
- In Microsoft Excel, the cell count for each class was multiplied by percent impervious and by size (30m x 30m) and summed to provide total impervious area for the watershed. This value was converted to acres.
- The total number of cells was multiplied by cell size (30m x 30m) and converted to acres.
- Total percent impervious for the watershed was calculated from Total impervious area and total area.

Roads in 50ft Buffer:

The following processes were performed for each watershed.

- A 50ft buffer was placed around roads using National Atlas Roads shapefile by Analysis Tools → Proximity → Buffer
- National Atlas Roads shapefile transformed to contain only roads within the buffer using the Roads shapefile and buffer shapefile from previous step by Analysis Tools → Extract → Clip
- Roads in buffer shapefile reduced to those found in the watershed using Roads in buffer shapefile and watershed shapefile by Analysis Tools → Extract → Clip
- Length attributes for Roads in buffer for watershed were exported to Microsoft Excel and summed.

Mapping for Display

The following processes were performed for each watershed.

- Flow accumulation raster was reclassified so that contributing area above 16385 cells have a value of 1 and below 16385 have a value of 0. This is based on field observations in the headwaters of the watershed where the streams first exhibit baseflow.
- The reclassified flow accumulation raster was converted to a shapefile for ease of displaying in watershed maps using Conversion Tools → From Raster → Raster to Polyline
- Watershed boundaries, flow accumulation shapefiles, and impervious rasters were used to produce final watershed maps.

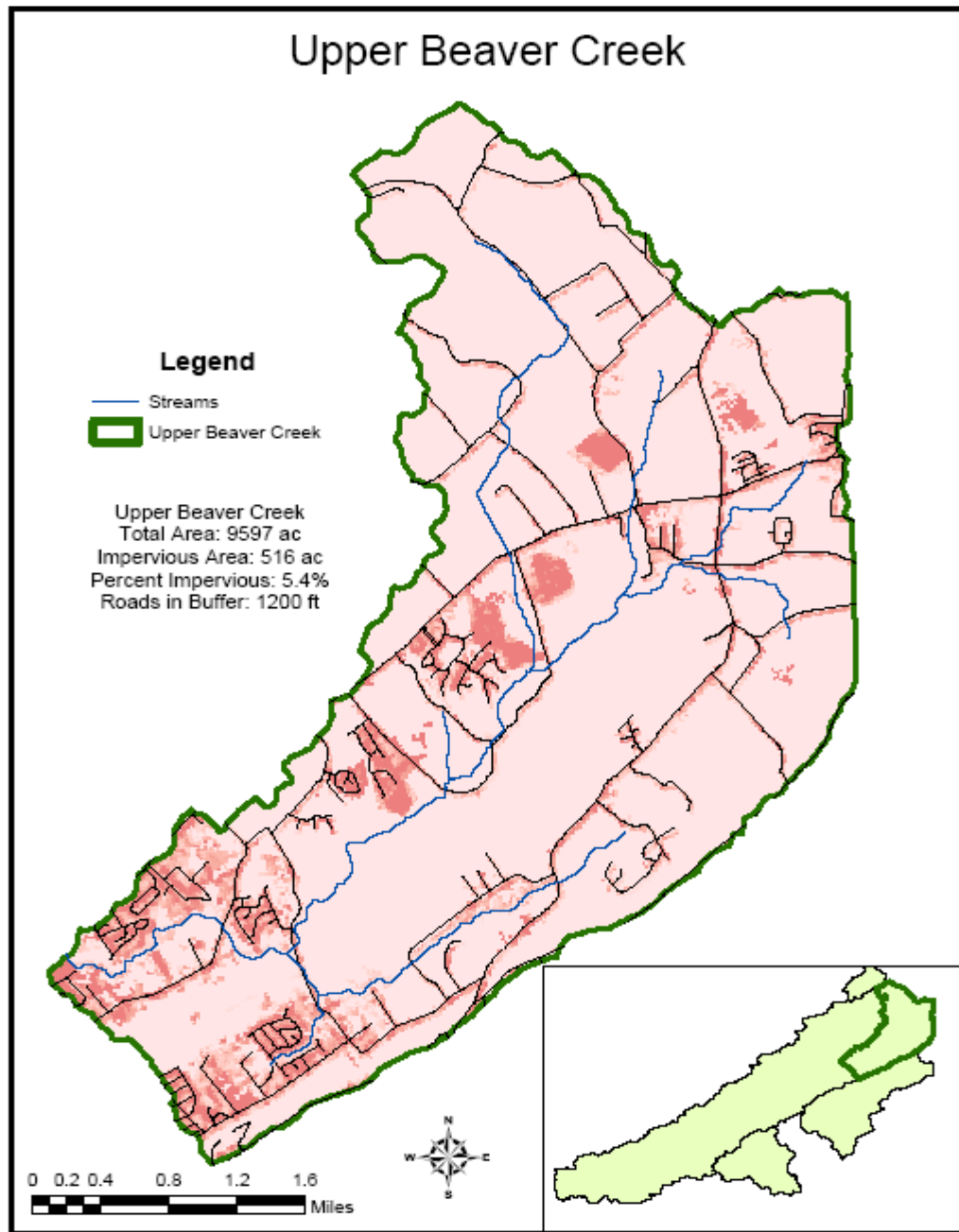


Figure 24: Upper Beaver Creek Watershed Map

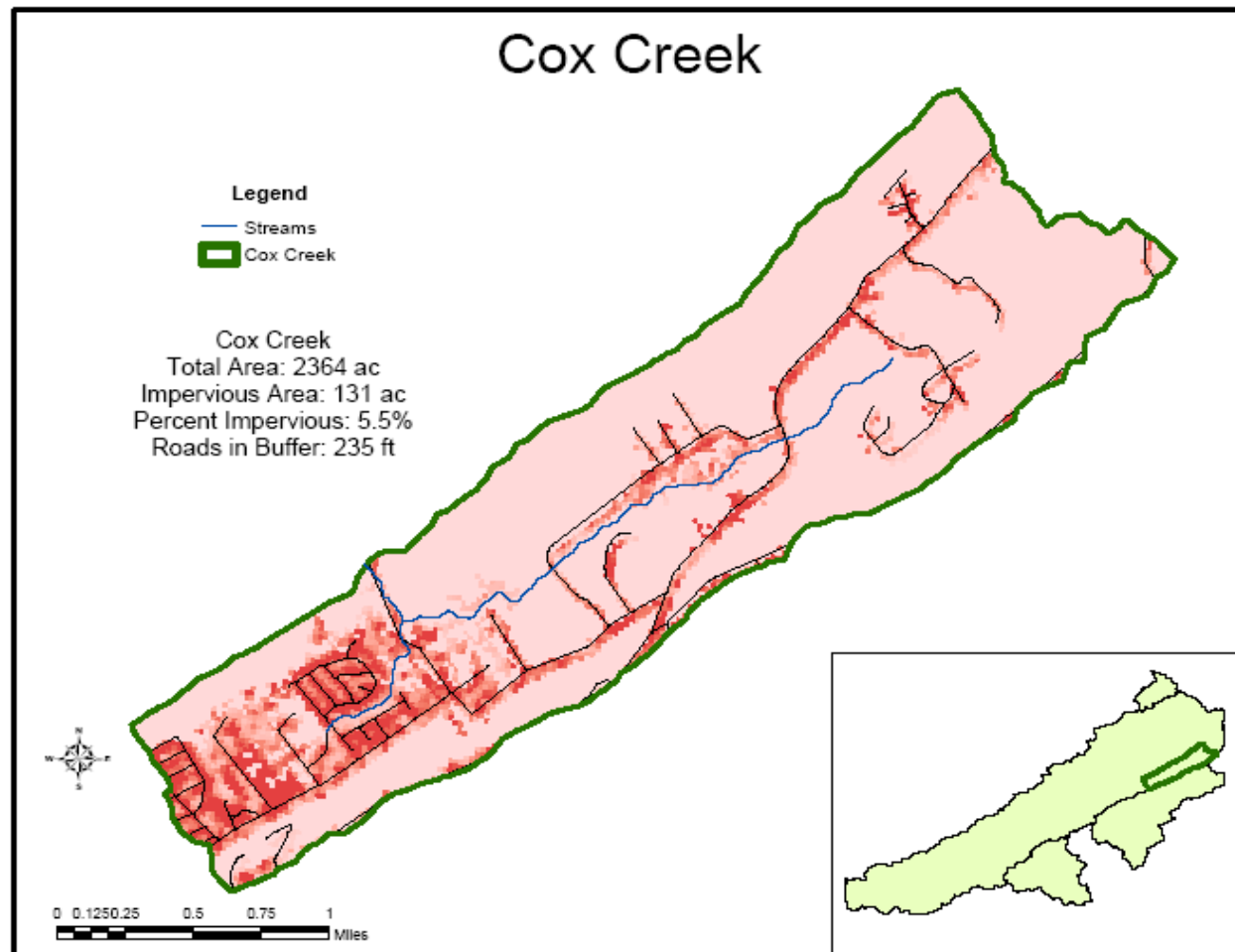


Figure 25: Cox Creek Watershed Map

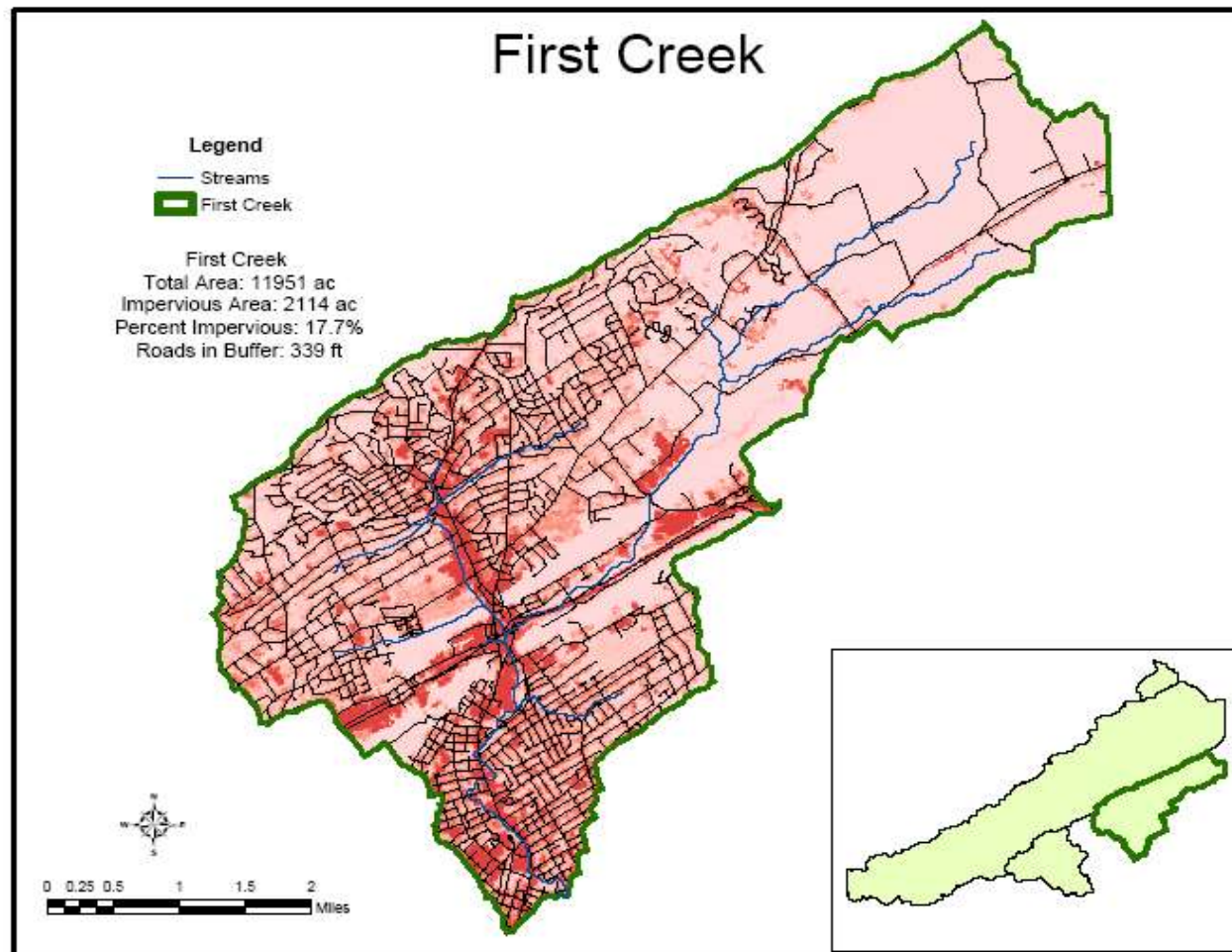


Figure 26: First Creek Watershed Map

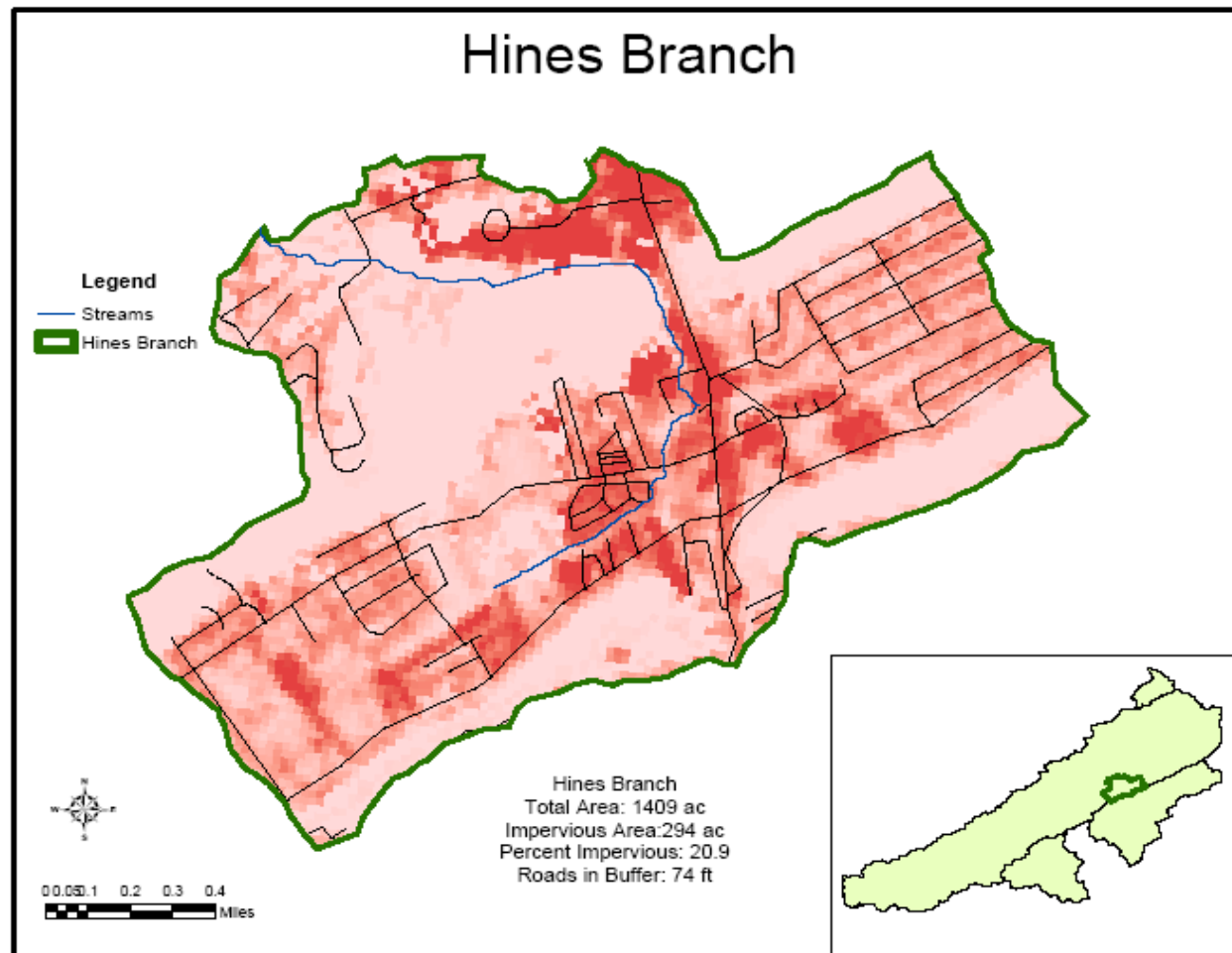


Figure 27: Hines Branch Watershed Map

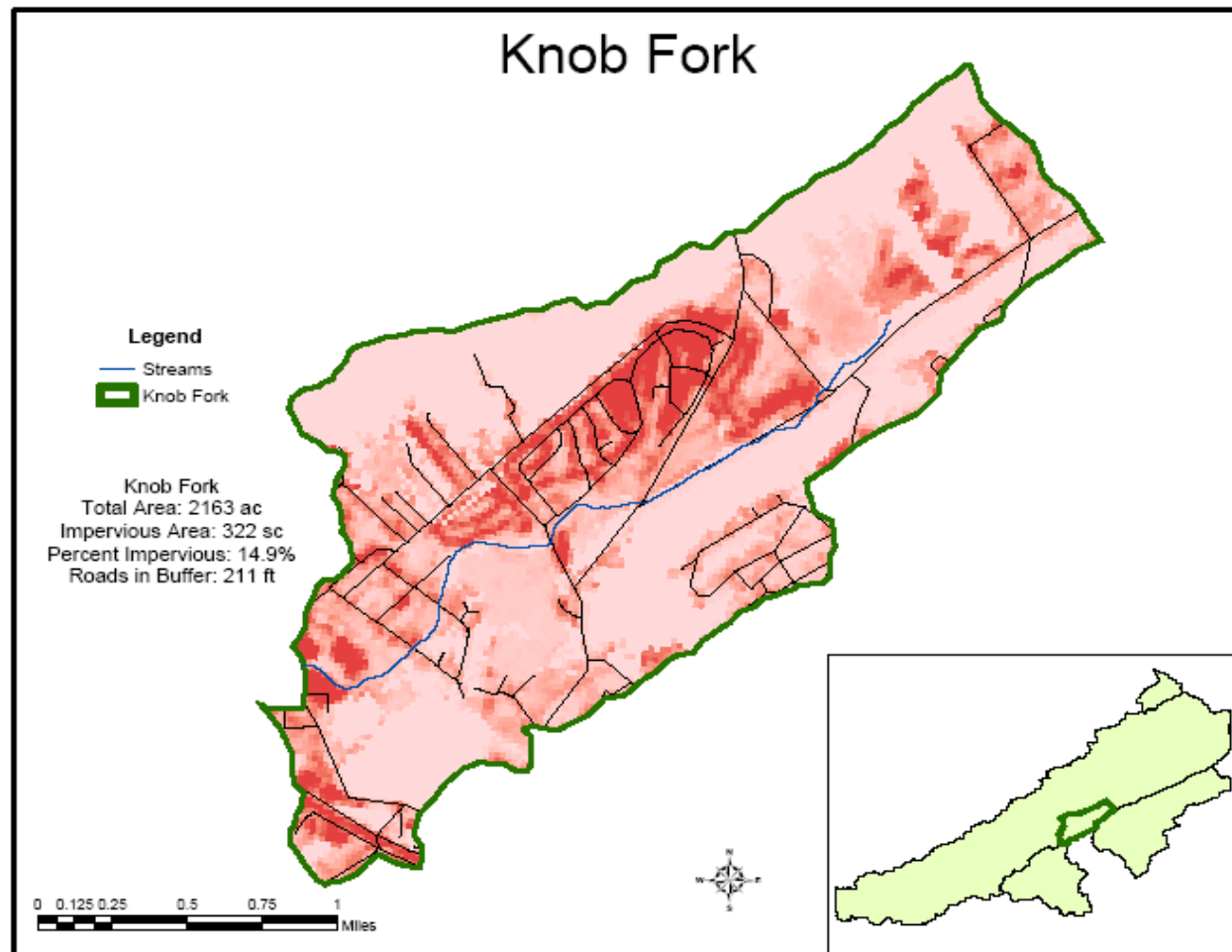


Figure 28: Knob Fork Watershed Map

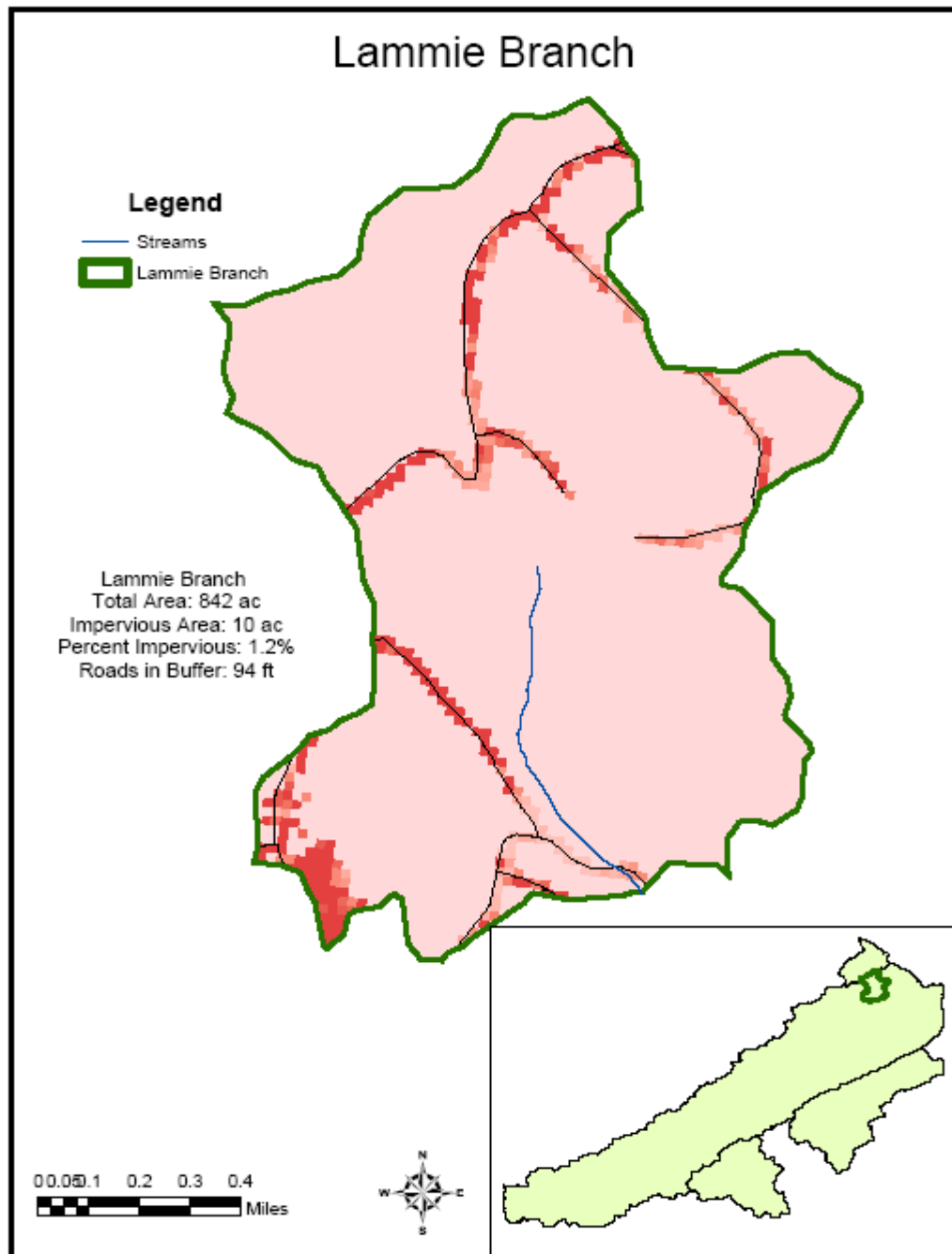


Figure 29: Lammie Branch Watershed Map

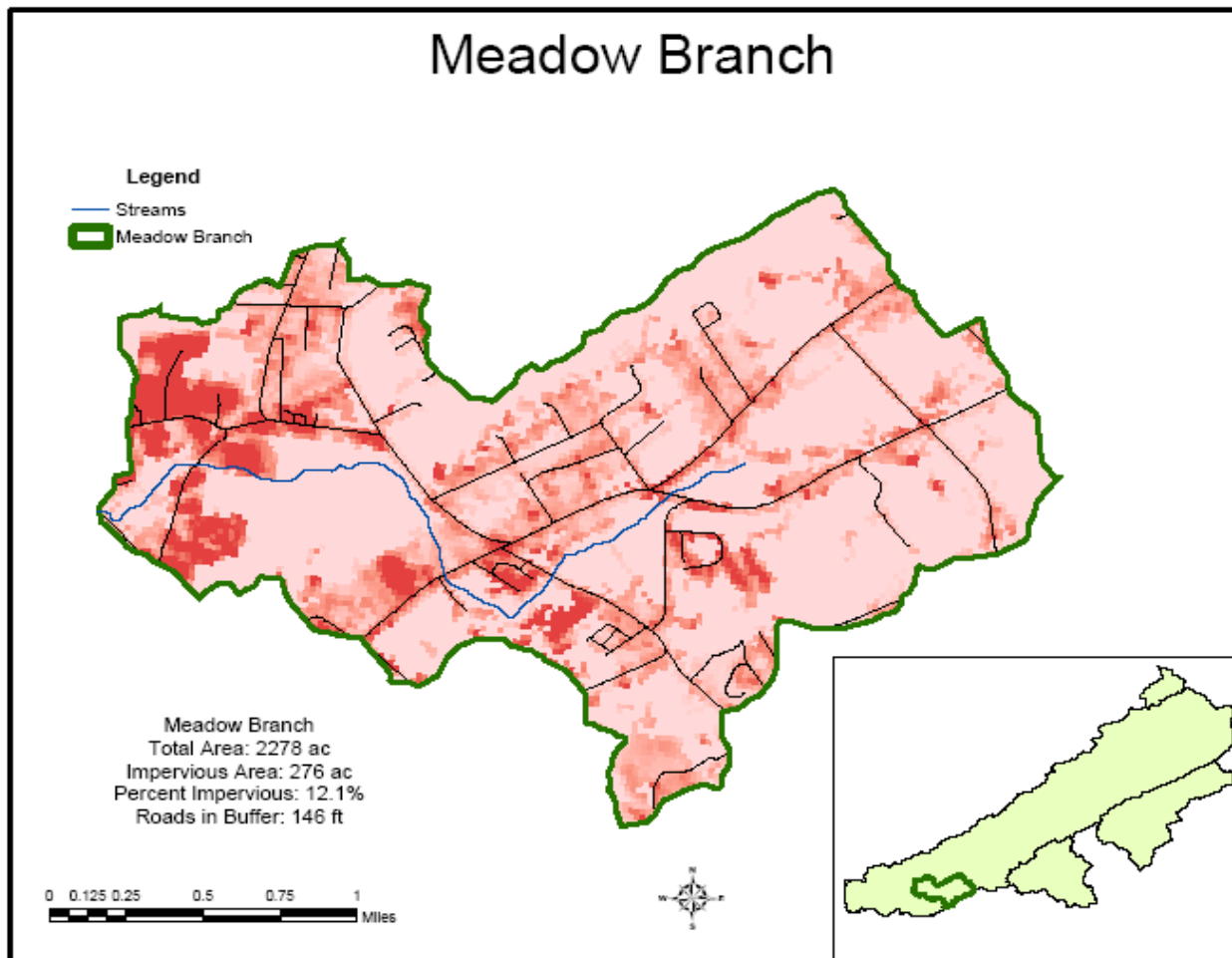


Figure 30: Meadow Branch Watershed Map

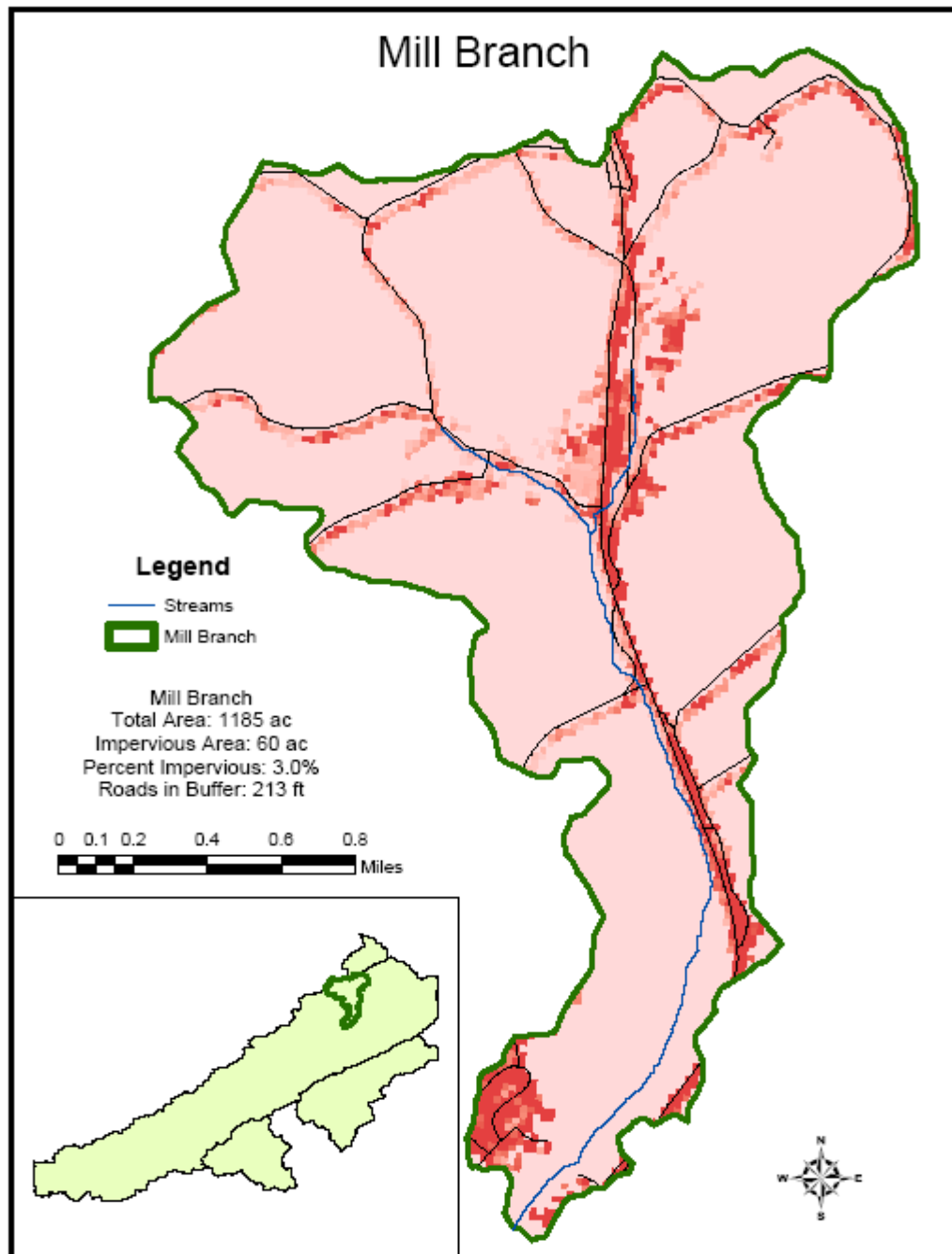


Figure 31: Mill Branch Watershed Map

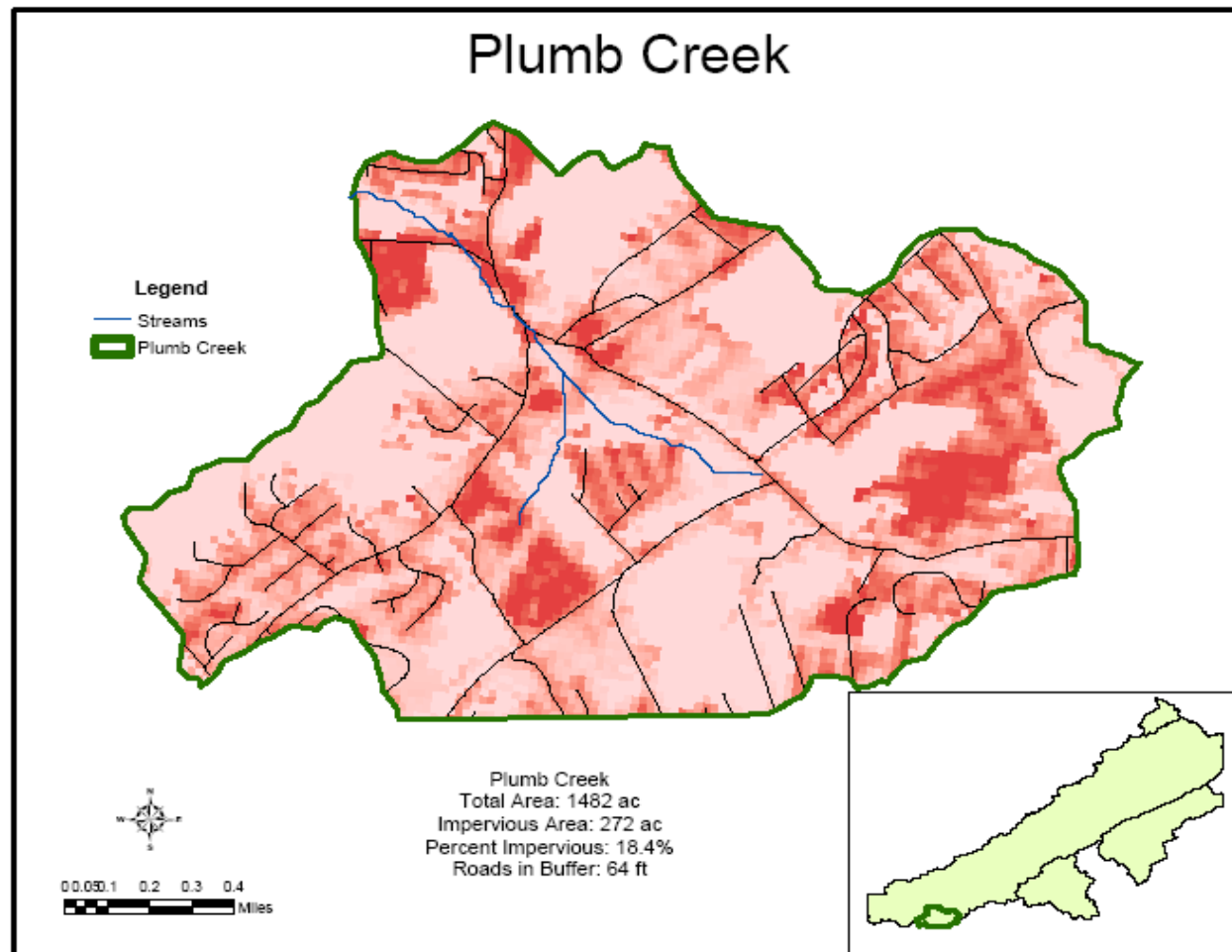


Figure 32: Plumb Creek Watershed Map

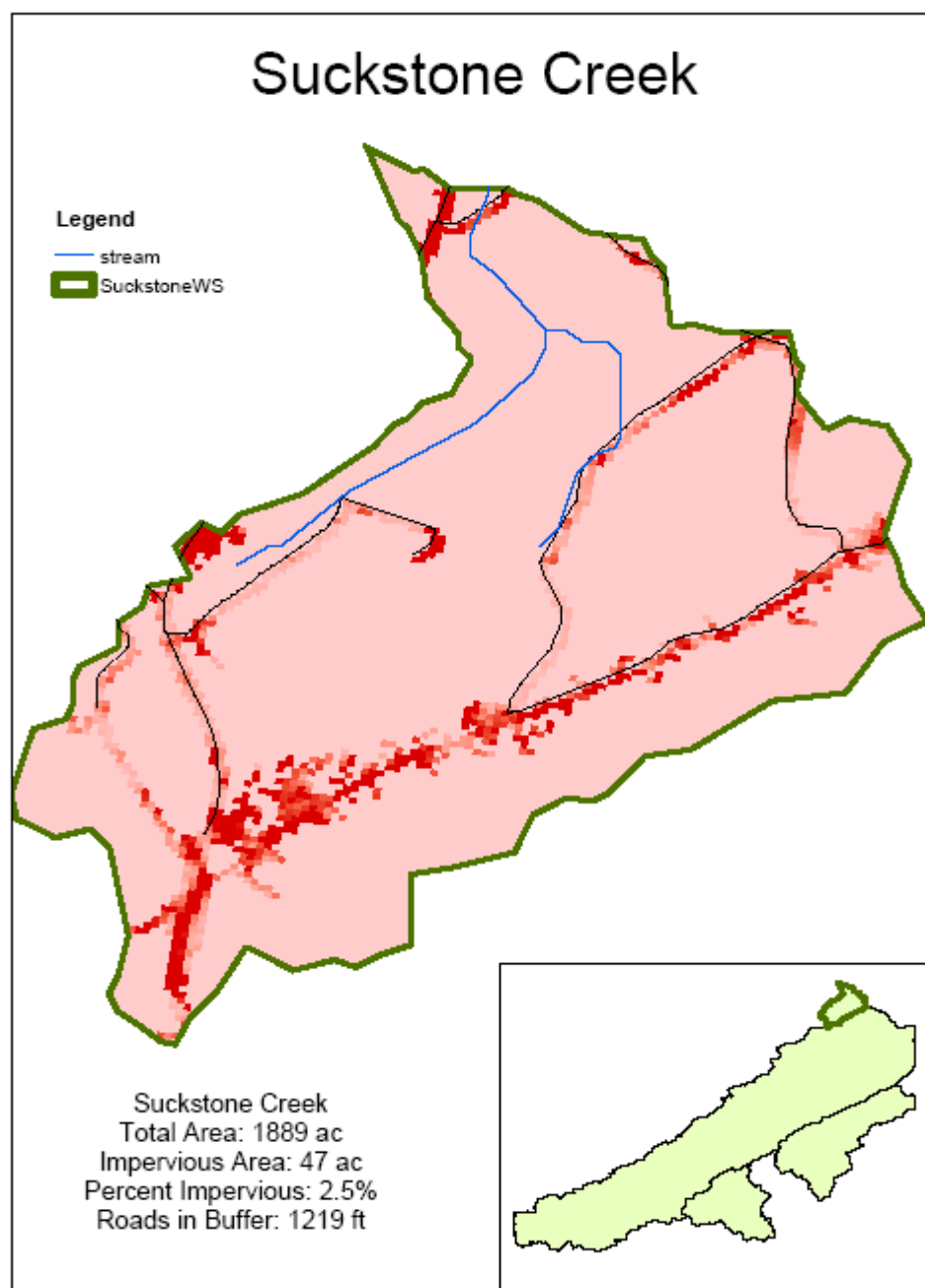


Figure 33: Suckstone Creek Watershed Map

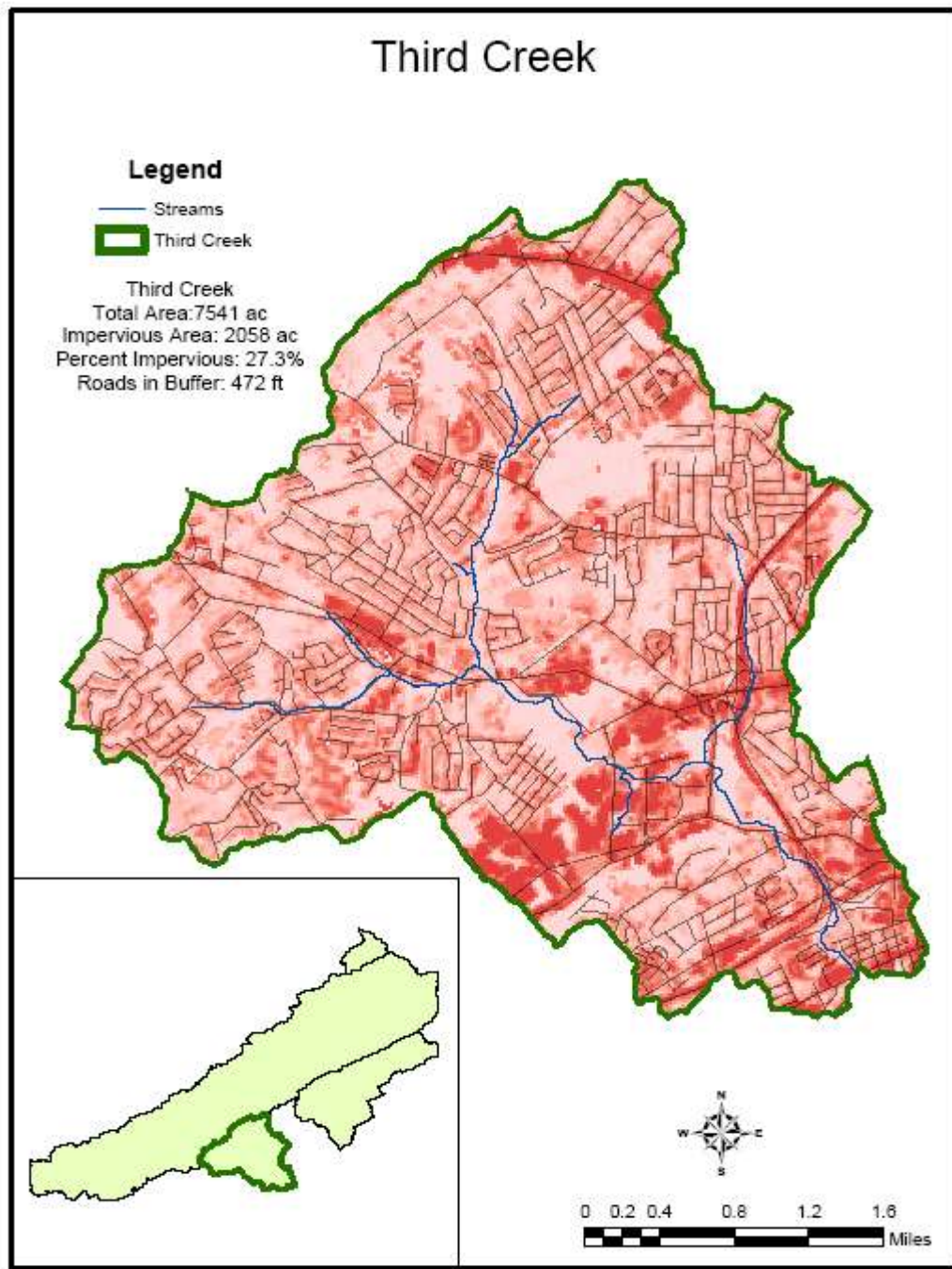


Figure 34: Third Creek Watershed Map

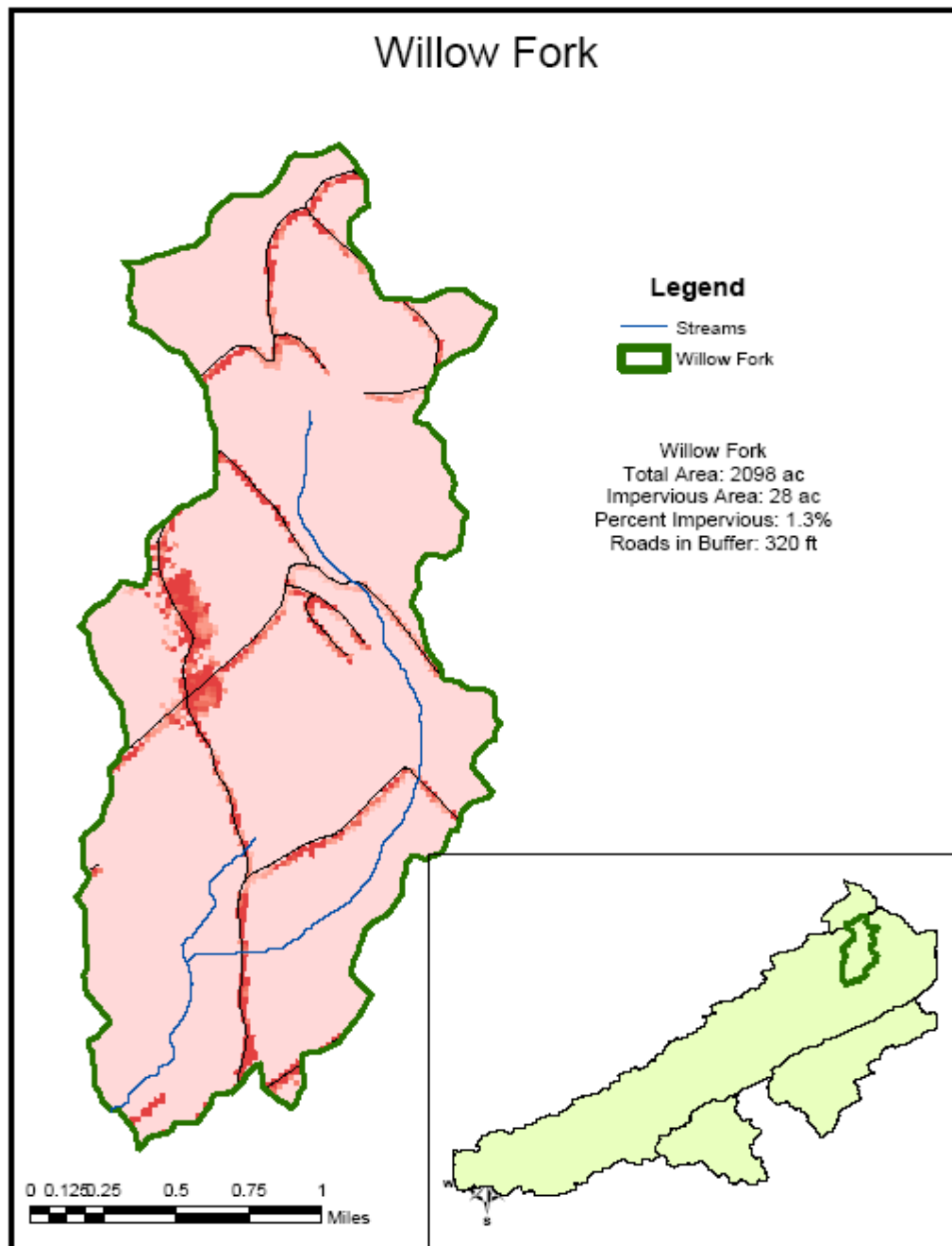


Figure 35: Willow Fork Watershed Map

Appendix G: Scatterplot Matrices

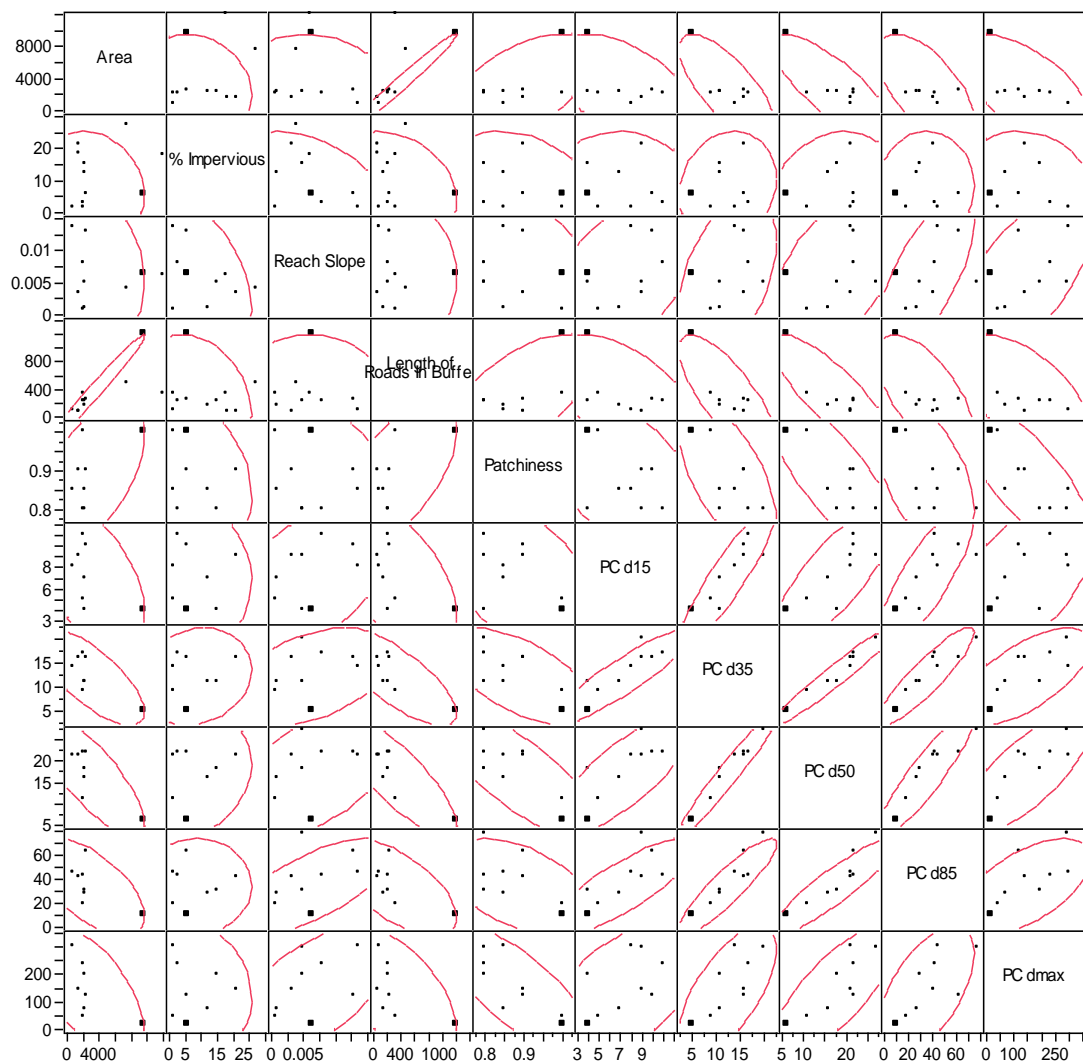


Figure 36: Watershed Characteristics with Pebble Count Data Scatterplot Matrix

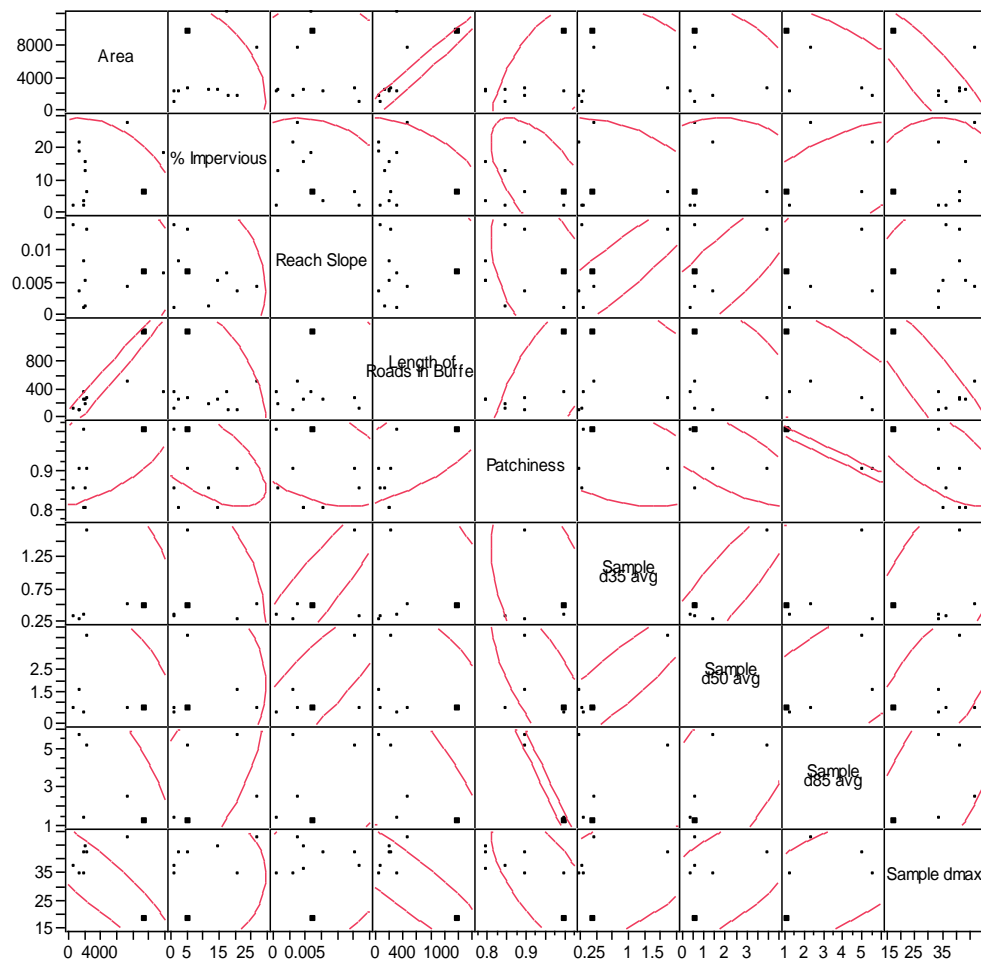


Figure 37: Watershed Characteristics with Bed-load Sample Data Scatterplot Matrix

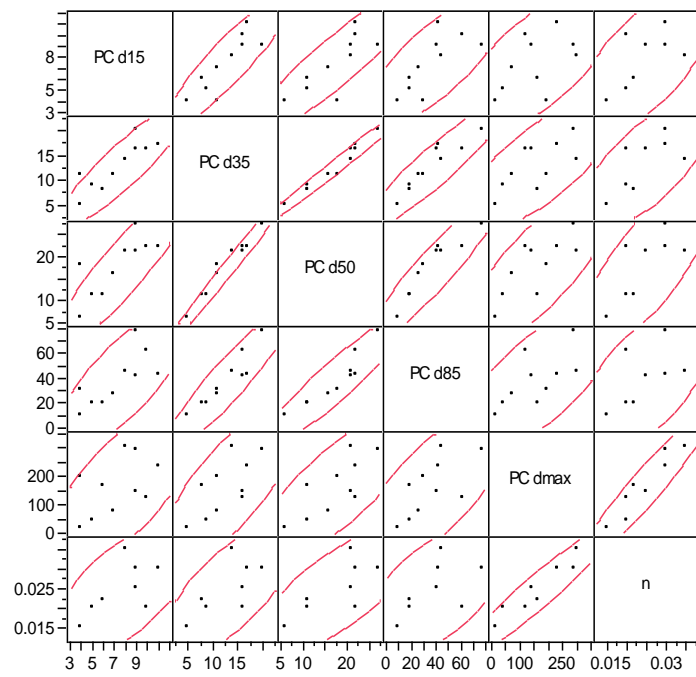


Figure 38: n^* with Pebble Count Data Scatterplot Matrix

Vita

William Cantrell was born and raised in Knoxville, TN where he attended Carter High School. Graduating in 1998, he received a Bicentennial Scholarship from the University of Tennessee and began studying music. After moving to the Art Department to study photography and sculpture, he gained an interest in structures and moved to the Civil and Environmental Engineering department from which he graduated in 2006. Having worked for a summer at S&ME Inc. during school, he worked for them again in the Environmental Department for nearly a year before returning to pursue a Master's Degree in Environmental Engineering with a focus in Water Resources Engineering. His research, sponsored by S&ME, Inc., developed an empirical relationship between bed characteristics and an effective Manning's n value, that will accurately predict bed shear values. William graduated with a Master's of Science in Environmental Engineering in the Summer of 2009.